CANADIAN THESES

THÈSES CANADIENNES

NOTICE

The quality of this microfiche is heavily dependent upon the quality of the original thesis submitted for microfilming. Every effort has been made to ensure the highest quality of reproduction possible.

If pages are missing, contact the university which granted the degree.

Some pages may have indistinct print especially if the original pages were typed with a poor typewriter ribbon or if the university sent us an inferior photocopy.

Previously copyrighted materials (journal articles, published tests, etc.) are not filmed.

Reproduction in full or in part of this film is governed by the Canadian Copyright Act, R.S.C. 1970, c. C-30.

AVIS

La qualité de cette microfiche dépend grandement de la qualité de la thèse soumise au microfilmage. Nous avons tout fait pour assurer une qualité supérieure de reproduction.

S'il manque des pages, veuillez communiquer avec l'université qui a conféré le grade.

La qualité d'impression de certaines pages peut laisser à désirer, surtout si les pages originales ont été dactylographiées à l'aide d'un ruban usé ou si l'université nous a fait parvenir une photocopie de qualité inférieure.

Les documents qui font déjà l'objet d'un droit d'auteur (articles de revue, examens publiés, etc.) ne sont pas microfilmés.

La reproduction, même partielle, de ce microfilm est soumise à la Loi canadienne sur le droit d'auteur, SRC 1970, c. C-30.

THIS DISSERTATION HAS BEEN MICROFILMED EXACTLY AS RECEIVED

LA THÈSE A ÉTÉ MICROFILMÉE TELLE QUE NOUS L'AVONS REÇUE

NL-339 (r 86/06)

Canada

DISCHARGE CHARACTERISTICS OF SOME DIVERGING LATERAL FLOWS

Mysore G. Satish

A Thesis

In

The Department

of

Civil Engineering

Presented in Partial Fulfillment of the Requirements
for the Degree of Doctor of Philosophy at
Concordia University
Montréal, Québec, Canada

September 1986

ISBN 0-315-32230-6

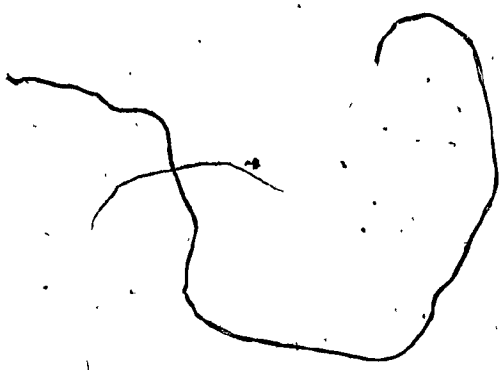

ABSTRACT

ABSTRACT

The present investigation deals with the discharge characteristics of diverging lateral flows. The study considers some aspects of division of flows in both open channels and closed conduits.

The first part of the thesis deals with the study of the discharge characteristics of flow past transverse floor outlets located in an open channel floor. For such systems, used in diverting open channel flows, the outlet width and the characteristics of flow in the approach channel are the most important parameters that determine the outlet discharge . To determine the relationship that governs the outlet discharge, an existing model of the lateral efflux from a two-dimensional channel is used as the basis. Experimental results are presented to validate the proposed relationship. Experiments were also conducted to study the interference effects due to the outlet spacings on the discharge characteristics of flow.

The second part of the present investigation deals with the division of flow in branch channels. For the division of flow in a branch channel set at right angles to a main channel ,a theoretical model is presented for various width ratios of the branch channel to the main channel. The model is developed using the principles of momentum , energy and continuity and is based on the existence of free flow conditions in the branch channel. The analysis makes use of the similarity of flow configuration between the division of flow in a branch channel and in a two-dimensional lateral conduit outlet fitted with a barrier. This similarity of flow is used to estimate the global contraction coefficient of the converging jet entering the branch channel. The ratio of the branch channel flow to the main channel flow is related to the Froude numbers in the main channel upstream and downstream of the junction. Theoretical lower limits for the upstream Froude numbers in the main channel are established. Data from the present experimental study and the available data from earlier investigators are presented to validate the proposed model.

The third part of the investigation deals with the study of diverging lateral flows in open channels. Here, the governing equations for spatially varied diverging lateral flows in open channels are proposed using momentum principles. Such flows are normally encountered in open channel manifold systems consisting of series of branch channel outlets , batteries of side weirs or flow diversion works such as floor outlets. To account for the uncertainty in the axial momentum transported across the lateral area, a pressure recovery factor is introduced in the formulation of the governing equations. A Limited number of experiments were conducted to estimate the pressure recovery factors for the particular case of a discrete branch channel junction and the results are presented.

The final part of the thesis deals with the internal hydraulics of multiport diffusers for which the lateral momentum distribution is uniform. Multiport diffuser systems consisting of lateral outlets located in closed conduits are generally found suitable for mixing chemicals and for disposing large quantities of industrial effluents. Effective dilution of the effluent may be obtained by discharging it as a counter jet opposing the main flow. The length scale characteristics of the counter jet flow is determined by the main flow velocity and the kinematic momentum of the counter jet. For a given cross-section of the main pipe, it is important to maintain a uniform lateral momentum distribution along the length of the main pipe. This part of the study deals with the internal hydraulics of a multiport diffuser which ensures uniform lateral momentum distribution along the span of the main pipe. Experiments were conducted to verify the proposed model and the results are presented.

ACKNOWLEDGEMENT

ACKNOWLEDGEMENT

The author wishes to express his appreciation to Dr. A. S. Ramamurthy for his guidance in the course of this investigation.

The financial assistance from Concordia university in the form of a Concordia Fellowship is also greatly appreciated.

TABLE OF CONTENTS

TABLE OF CONTENTS

NOTATIONS

NOTATIONS

a	=	Main flow area (Eq. 4. 4)
a_l	=	Area of a single lateral
a_r	=	Lateral area per unit length along the diffuser
$a_r(x^*)$	=	Lateral area per unit length at x^* (Eq. 5. 14)
a_r^*	=	$a_r(x^*)$ = normalised lateral area per unit length (Eq. 5. 15)
a_1	=	Area of flow at section 1
a_2	=	Area of flow at section 2
a_3	=	Lateral area of flow
A_f	=	B L = area of the floor outlet
A_m	=	Area of the manifold pipe
A_r	=	Ratio of the area of the laterals to the area of the main pipe (Eq. 5. 2)
A_{ro}	=	Area ratio factor (Eq. 4. 3)
b	=	Width of the open channel in Eq. 4. 13
B	=	Width of the 2D - Conduit or the width of the main open channel
C	=	a Constant in Eq. 5. 4
C_c	=	Branch channel Contraction coefficient or the Contraction coefficient of a jet through a lateral outlet fitted with a barrier and set in the side of a 2D - conduit

C_d = Discharge coefficient of a single lateral

C_L = Lateral discharge coefficient in Eq. 4. 10

C_{co} = Contraction coefficient of the jet through a lateral outlet in a 2D-Conduit

C_{df} = Discharge coefficient for the floor outlet

C_1 = Coefficient in Eqs. 2. 1 and 2. 6

C_2 = Coefficient in Eqs. 2.1 and 2. 6

C_3 = Coefficient in Eqs. 2. 1 and 2. 6

d_c = Critical depth of flow in the main channel upstream of the floor outlet

d_l = Diameter of the laterals

d_1 = Depth of flow in the section upstream of the single floor outlet or the approach depth of flow for the upstream floor outlet

d_2 = Approach depth of flow for the downstream floor outlet

d_p = Pressure head against the outlet in the main conduit

dA_o = Elemental area

da_1 = An elemental area within the area a_1

da_2 = An elemental area within the area a_2

da_3 = An elemental area within the area a_3

D_f = Distance between the floor outlets (Fig. 1. c)

D_m = Diameter of the manifold pipe

E = Total energy head in the section upstream of the floor outlet

f = Friction factor

f_x = Component in the direction of the main flow of the pressure force acting on the stream surface MN

f_y = Component in the direction perpendicular to the main flow of the pressure force acting on the stream surface MN

f_r = Resultant pressure force on the stream surface MN

F_f = Froude number of the main flow upstream of the floor outlet

F_1 = Froude number of the main flow upstream of the branch

F_2 = Froude number of the main flow downstream of the branch

F_b = Frode number of the flow in the downstream section of the branch

g = Acceleration due to gravity

h_1 = Depth of flow upstream of the branch

h_2 = Depth of flow downstream of the branch

h_3 = Depth of flow at the section of minimum contraction in the branch [Section (3. 5. 1), Fig. 13]

h_b = Depth of flow in the downstream section of the branch channel

h_c	=	Critical depth of flow in the approach section of the main channel
J	=	Kinematic momentum of the counter jet
K	=	Pressure correction coefficient in Eqs. 2.9 and 4.5
K_i	=	Interference factor for floor outlets (Eq. 2. 11)
K_i	=	Floor outlet interference factor when $S_f = 10$
K_1	=	Pressure correction factor at section 1
K_2	=	Pressure correction factor at section 2
ι	=	Length of the laterals
L	=	Width of the lateral outlets or the width of the branch channel
L_m	=	Length of the manifold pipe
L_o	=	Total length of the open channel lateral outlet system
M	=	Momentum ratio (Eq. 5.10)
M_t	=	Momentum through each lateral
M_L	=	Lateral momentum per unit length
M_{av}	=	Average lateral momentum per unit length
N	=	Number of laterals
n_o	=	number of outlets in the open channel lateral flow system
p	=	pressure intensity on elemental area da
$\overline{p}$	=	Average pressure in the control volume
$\overline{p}(x^*)$	=	Average pressure in the manifold pipe at a distance x^*
p_o	=	Pressure intensity on the elemental area dA_o

p_2 = Pressure intensity on the elemental area a_2

p_A = Ambient pressure

P_d = Pressure force downstream of the control volume (Fig. 30)

P_u = Pressure force upstream of the control volume (Fig. 30)

P_{o1} = Pressure force on section 1

P_{o2} = Pressure force on section 2

P_e = Wetted perimeter

P_{AB} = Net pressure force on the branch channel wall AB

P_{CD} = Net pressure force on the branch channel wall CD

q = Main flow discharge (Eq. 4. 4*)

q_1 = Main flow discharge at section 1

q_2 = Main flow discharge at section 2

q_3 = Lateral discharge

$q(x^*)$ = discharge at a distance x^*

q^* = $q^*(x^*)$ = Normalised discharge

Q_s = Main discharge in the manifold

Q_d = Discharge in the manifold downstream of the lateral

Q_l = Discharge through a single lateral

Q_u = Discharge in the manifold upstream of the lateral

Q_L = Lateral discharge per unit length (Eq. 5. 5)

Q_{fd} = Discharge through the downstream floor outlet

Q_{fu} = Discharge through the upstream floor outlet

Q_{f1} = Discharge of the main flow upstream of the floor outlet or the main discharge in the approach section of the upstream floor outlet

Q_{f2} = Discharge of the main flow downstream of the floor outlet or the main discharge in the approach section of the downstream floor outlet

Q_1 = Discharge in the main channel upstream of the branch

Q_2 = Discharge in the main channel downstream of the branch

Q_3 = Discharge in the branch channel

Q^* = $Q^*(x^*)$ = Normalised main discharge in the manifold [$Q(x^*)/Q(0)$]

Q_L^* = Normalised lateral discharge per unit length ($- dQ^*/dx^*$)

R = Pressure recovery factor in closed conduits

R_o = Pressure recovery factor in open channel

Re = Re (x^*) = Reynolds number

Re (0) = Inlet Reynolds number

s = s(x) = The width of the lateral area segments (Fig. 40)

S_f = Outlet spacing coefficient [$= (D_f + L)/L$]

s_l = Spacing between the laterals

S_p = Stagnation point

S_o = Slope of the open channel

t = Width of individual lateral opening (Eq. 4.3)

T_1 = Coefficient in Eq. 5.7

T_2 = Coefficient in Eqs. 5.7 and 5.19

T_3 = Coefficient in Eq. 5.19

U = Velocity of the main stream

U_1 = Velocity of the main flow upstream of the floor outlet or the velocity upstream of the lateral outlet in the conduit

U_2 = Velocity of the main flow downstream of the floor outlet or velocity of the main flow downstream of the lateral outlet in the conduit

U_x = Local velocity in the direction of the main flow (Eq. 2.10)

V_1 = Average velocity of the main flow at section (1)

V_2 = Average velocity of the main flow at section (2)

V_3 = Average velocity of the branch channel jet at section (3)

V_d = Velocity downstream of the control volume (Fig. 30)

V_u = Velocity upstream of the control volume (Fig. 30)

V_x = Velocity component along the manifold in the control volume(Fig. 30)

V_y = Velocity component normal to the manifold (Fig. 30)

V_{jc}	=	Velocity of the jet through the lateral outlet (Fig. 1b)
V_{jf}	=	Velocity of the jet through the floor outlet(Fig. 1b)
V	=	Average velocity in the control volume (Fig. 30)
V (x*)	=	Average velocity along the manifold at a distance x*
w_1	=	Velocity of flow at section 1
w_2	=	Velocity of flow at section 2
w_x	=	Velocity in the axial direction X of the main flow
w_y	=	Velocity of the flow in the direction normal to the main flow
w	=	Average velocity of the main flow
w (x*)	=	Average flow velocity at a distance x*
x	=	Distance along the axial direction or the direction of the main flow
x*	=	Normalised distance x/L_m or x/L_o
X	=	Direction of the main flow or the axial direction
y	=	Depth of main flow (Eq. 4.4)
y_1	=	Depth of flow at section 1
y_2	=	Depth of flow at section 2
y	=	Depth of flow
Y	=	Direction normal to the main flow
z	=	Height of the elemental area dA_o above the channel floor(Eq. 2.10)
α	=	Exponent in Eq. 5.19
β	=	Momentum correction factor (Eq. 4.6)

β_1 = Momentum correction factor at section 1

β_2 = Momentum correction factor at section 2

γ = Specific weight of water

δ = Depth of corrugation (Ref. 67)

θ = Angle of inclination of the open channel floor with the horizontal

ρ = Mass density of water

η = Ratio of velocity head to the total head (Eq. 5. 24)

η_c = Velocity parameter ($= U_1 / V_{jc}$)

η_f = Velocity parameter for floor outlets ($= U_1 / V_{jf}$)

η_1 = Velocity parameter for the branch channel flow ($= V_1 / V_3$)

η_{fd} = Velocity parameter for the downstream floor outlet

η_{fu} = Velocity parameter for the upstream floor outlet

λ = Porosity of the manifold Eq. 5. 1

ν = Kinematic viscosity of water

τ = Boundary shear stress

SUPERSCRIPTS

$\bar{}$ = Average value

* = Non - dimensional Value

$'$ = First derivative [d / dx^*]

$''$ = Second derivative [d^2 / dx^{*2}]

LIST OF FIGURES

LIST OF FIGURES

LIST OF FIGURES

LIST OF FIGURES

LIST OF FIGURES

LIST OF FIGURES

LIST OF FIGURES

LIST OF TABLES

LIST OF TABLES

CHAPTER I

THESIS OUTLINE

CHAPTER I

THESIS OUTLINE

The division of flow from an outlet structure housed in a conduit or in an open channel is commonly found in many hydraulic systems. Familiar examples of such systems include branch channels, side weirs, floor outlets, multiport diffuser manifolds and canal locks. The present investigation deals with the study of the discharge characteristics of diverging or dividing lateral flow systems comprising of floor outlets or branch channel junctions in open channels and closed conduit multiport diffuser systems. A brief schematic layout of the present study is outlined below.

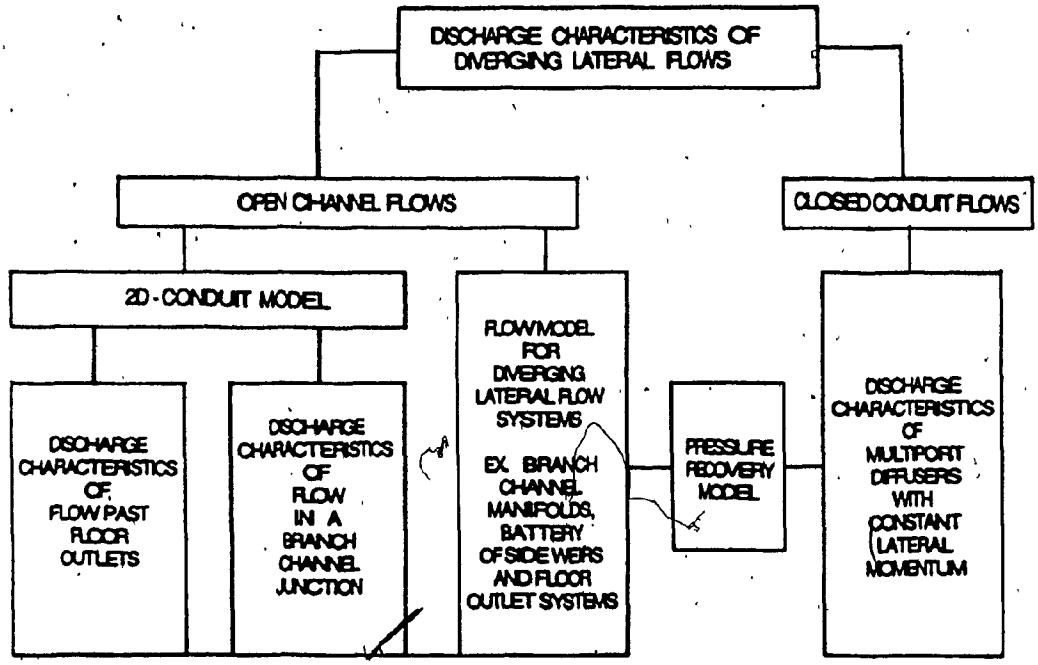

In order to understand the behaviour of a diverging lateral flow system, it is essential to study the behaviour of flow past individual lateral outlets. Hence, the study related to the discharge characteristics of diverging lateral flows in open channels was divided into three primary parts. The first and the second parts deal with the study of the discharge characteristics of flow past floor outlets and branch channel junctions respectively. To this end, existing solutions for lateral efflux from a two dimensional conduit were adopted in the development of the models for division of flows in branch channel junctions and floor outlets. Experimental results from the present study and the available data from earlier investigations were used to verify the validity of the proposed models.

The third part of the open channel study deals with the development of generalised expressions for diverging lateral flow systems using momentum principles. To account for the uncertainities in axial momentum transported due to the turning of the flow, a pressure recovery coefficient is introduced in the development of the governing equations. The theoretical evaluation of this pressure recovery factor is very complex. However, the pressure recovery factors for various lateral flow systems can be estimated by means of laboratory experiments. An experimental procedure for estimating the pressure recovery factors for the specific case of a discrete branch channel junction is proposed and the results are presented.

The final part of the thesis deals with dividing lateral flows in closed conduit multiport diffuser systems with constant lateral momentum distribution. These multiport diffuser systems consisting of a series of lateral outlets housed in the side

of a main pipe are found suitable for mixing of chemicals and for the disposal of large quantities of industrial effluents. The pressure recovery model which was used earlier for lateral flow systems in open channels was extended for the case of multiport diffuser systems with constant lateral momentum distribution along the span of the main pipe. Experiments were also conducted to verify the proposed model and the results are presented.

CHAPTER II

DISCHARGE CHARACTERISTICS OF TRANSVERSE FLOOR OUTLETS IN AN OPEN CHANNEL

CHAPTER II

DISCHARGE CHARACTERISTICS OF TRANSVERSE FLOOR OUTLETS IN AN OPEN CHANNEL

2.1 GENERAL REMARKS

This chapter deals with the study of discharge characteristics of flow past transverse floor outlets located in an open channel floor (Fig. 1a). An analytical model based on the lateral efflux from a two-dimensional channel (Fig. 1b) is proposed. Experimental results are presented to validate the model. Preliminary experimental results regarding the effects of outlet spacings on the slot discharge are also presented.

2.2 INTRODUCTION

Floor outlets or bottom racks are frequently used to divert flow from one stream to another. Applications also include their use as horizontal trash-racks in hydro power plants and as curb outlets in streets [6, 66, 68]. An understanding of the flow behaviour over bottom or floor outlets is very important for the proper design and performance of such flow diversion works. Number of studies have been conducted to analyse the behaviour of flow in such outlets [33, 34, 40, 63, 65]. These studies generally assume conservation of specific energy of the flow along the rack. Based on experimental results, design charts for multiple outlets oriented in the flow direction have been developed [30, 63].

In order to predict the behaviour of flow over a system of floor outlets (Fig. 1c), it is essential to understand the characteristics of flow past a single floor outlet (Fig.1a) The performance of such a system may be expected to be essentially dependent on the ratio of the main discharge to the diverted discharge, the state of the approaching flow (subcritical or supercritical) and the geometry of the system.

Recently, an expression for the discharge through a single transverse floor outlet located in an open channel has been proposed [36]. However, in this simplified model, the effect of the ratio of the outlet width L to the flow depth d_1 on the outlet discharge was not considered. The present investigation specifically includes the effect of the outlet width to the flow depth ratio L / d_1 on the floor outlet discharge. For this purpose, the results from the existing hydrodynamic model [28, 32] for the lateral efflux from a two dimensional conduit (Fig. 1b) have been adopted [47,56]. Experiments were conducted to verify the validity of the model.

In a floor outlet system composed of multiple outlets, the interference effects of adjacent outlets on the outlet discharge can be considerable. As such, the data related to the discharge characterstics of a single outlet should be supplemented with information concerning outlet interference effects. Preliminary experiments were conducted to study the effects of outlet spacing on the outlet discharge and the results are presented.

2. 3 THEORETICAL CONSIDERATIONS

Based on the model for the lateral efflux from a two- dimensional conduit (Fig.1b), the problem of dividing flow past a rectangular transverse outlet located in an open channel floor (Fig. 1a) is studied.

2. 3.1 LATERAL EFFLUX FROM A TWO DIMENSIONAL CONDUIT

The characteristics of lateral efflux from a two dimensional conduit (Fig. 1b) based on free stream line theory have been determined earlier [28, 32]. For the flow through a lateral outlet of width L in a two dimensional channel of width B, the dependence of the contraction coefficient C_{co} on the velocity parameter η_c ($= U_1 / V_{jc}$) with L / B as the group parameter is shown in Fig. 2. Here, U_1 and V_{jc} refer to the velocity of the main flow upstream of the outlet and the velocity of the lateral efflux respectively.

For $0 < L/B \leq 1.0$ and $0 < \eta_c \leq 1.0$, the relationship between C_{co} and η_c can be approximated [45] by the following polynomial.

$$C_{co} = 0.611 + C_1 \eta_c^2 + C_2 \eta_c^4 + C_3 \eta_c^6 \qquad (2.1)$$

where,

$$C_1 = -0.538 + 0.254\,(L/B) \quad ;$$

$$C_2 = 0.058 + 0.234\,(L/B) \quad ;$$

$$C_3 = -0.129 - 0.489\,(L/B) \qquad (2.2)$$

2. 3. 2 FLOOR OUTLET IN AN OPEN CHANNEL

Fig.1.b denotes the flow past a transverse rectangular floor outlet of width L located in an open channel of width B. The main variables that characterise the lateral outlet flow are the discharge coefficient C_{df} , the velocity parameter η_f and the parameter L / d_1. Here, d_1 denotes the depth of flow in the approach section and η_f denotes the ratio of the velocity U_1 in the approach section to the resultant velocity V_{jf} of the jet emerging from the slot (Fig. 1a). The discharge coefficient for the floor outlet C_{df} may then be defined as,

$$C_{df} = \frac{\text{Discharge through the floor outlet}}{B\ L\ V_{jf}} \qquad (2.3)$$

Here,

$$V_{jf} = \sqrt{2\,g\,E} \qquad (2.4)$$

and

$$E = \left[\frac{U_1^2}{2g} + K\,d_1 \right] \qquad (2.5)$$

In Eq. 2.5, K denotes the pressure correction factor for curvilinear flows. A note related to the estimation of K is given in section 2. 3. 3.

The following assumptions are made in relating the parameters C_{df}, η_f and L/d_1 for flow through the floor outlet.

1. The channel is rectangular and horizontal.
2. The flow is essentially two dimensional.
3. The contraction coefficient C_{co} of the lateral efflux from a two dimensional conduit model closely approximates the coefficient of contraction of the jet emerging from the open channel floor slot. For this to be valid, the width B of the two dimensional conduit model should correspond to the depth d_1 of the open channel model.

Based on the above assumptions, the relationship between C_{df} and η_f with L/d_1 as the group parameter for the floor slot in an open channel can now be expressed as,

$$C_{df} = 0.611 + C_1 \eta_f^2 + C_2 \eta_f^4 + C_3 \eta_f^6 \qquad (2.6)$$

where, for $0 < L/d_1 \leq 1.0$; $0 \leq \eta_f \leq 1.0$

$$C_1 = -0.538 + 0.254 (L/d_1) ;$$

$$C_2 = 0.058 + 0.234 (L/d_1)$$

and

$$C_3 = -0.129 - 0.489 (L/d_1) \qquad (2.7)$$

The relationship between C_{df} and η_f denoted by Eq. 2.6 is plotted in Figures 6 to 10 for specific values of L/d_1.

Further, it may be noted that the Froude Number of the approach flow F_f (Eq. 2.8) is related to η_f as shown in Eq. 2.9 .

$$F_f = \frac{U_1}{\sqrt{g\, d_1}} \qquad (2.8)$$

$$\eta_f = \frac{1}{\sqrt{1 + \frac{2K}{F_f^2}}} \qquad (2.9)$$

2. 3. 3 CORRECTION FOR FLOW CURVATURE

Significant curvature of stream lines may be expected in flows dealing with floor outlets due to the continuous removal of water through the lateral outlet. Hence, in evaluating the total energy head E (Eq. 2.5) in the approach section of the main channel, a conventional pressure correction coefficient K as shown in Eq. 2. 10 will have to be employed to account for the deviation from the hydrostatic pressure distribution .

$$K\, \gamma\, Q_{f1}\, d_1 = \int [(p_o/\gamma) + z]\, \gamma\, U_x\, dA_o \qquad (2.10)$$

In Eq. 2.10 , Q_{fl} is the discharge in the main channel upstream of the floor outlet, U_x is the local velocity in the direction of the main flow, p_o the pressure intensity on an elemental area dA_o located at a height z above the channel bed.

2. 3. 4 INTERFERENCE EFFECTS DUE TO OUTLET SPACING

In earlier studies related to interference effects in conduit flows [29], the number of outlets were limited to two. Increasing the number of outlets did not produce any significant change in the characterstics of the outlet flow. Hence, the present study on interference effects were confined to a two outlet system.

For the floor outlet configuration shown in Fig. 1c , the lateral discharge Q_{fd} may be obtained from Eq. 2.11 .

$$Q_{fd} = K_i C_{d2} A_f \sqrt{2gE} \qquad (2.11)$$

Here,

C_{d2} = discharge coefficient for the downstream floor outlet

A_f = B L = area of the floor outlet

E = total energy head in the approach section

In Eq. 2.11 , K_i is a coefficient which accounts for the interference effect of the upstream outlet on the outlet downstream. Experiments were conducted to study the variation of the interference factor K_i with the outlet spacing coefficient S_f [= $(D_f + L) / L$].

2. 4 EXPERIMENTAL SET-UP : FLOOR OUTLETS

The experimental arrangement used is shown in Fig. 3. The main channel rectangular in cross section, 25.4 cm wide and 12 m long was made out of polished stainless steel plates. Transverse rectangular slots fixed in the channel floor were obtained from machined plexiglass sheets. A gradual channel transition along with screens at the channel entrance ensured stable and smooth flow in the approach section. The discharges through the slot and the main channel were measured by previously calibrated V-notches. Very small discharges through the slots were measured by gravimetric measurement. The depth of flow in the V-notches were measured using point gauges accurate to 0.001 ft (0.3 mm). The depth d_1 was measured at a section just upstream of the floor outlet (Fig. 5a). The velocity and pressure distributions across the channel section were recorded at regular intervals. A 3 mm diameter pitot tube was used to obtain the total head and a screw driver static probe with a flattened end section was used to get the static pressure. The pressure along the channel bed was recorded by means of piezometers.

2. 5 DISCUSSION OF RESULTS

2. 5. 1 SINGLE FLOOR OUTLET

2.5.1.1 CURVATURE CORRECTION

The experimental results for the variation of pressure correction factor K [Eq. 2.10] with the slot width L and the conditions of flow in the main channel approach are shown in Fig. 4. The results include the data from the present study and the data available from earlier investigators[37]. A polynomial fit such as Eq. 2.12 was used to obtain the value of K for purposes of computing the total energy head in the approach section of the main channel.

$$K = 1.00 - 0.35 \left(L / d_c \right) - 0.95 \left(L / d_c \right)^2 + 0.90 \left(L / d_c \right)^3 \quad (2.12)$$

where, d_c is the critical depth of flow in the approach section.

2. 5. 1. 2 DISCHARGE - η_1 - L/d_1 RELATION

Fig. 5b shows the velocity and pressure profiles at various sections of the main flow along the open channel. The floor pressure recorded at section 3 (Fig. 5a) just upstream of the floor outlet approaches that of the atmospheric pressure. The floor pressure at a section downstream of the floor outlet at section 4 corresponds to the total head of the flow due to the occurence of the stagnation point at a location near the downstream end of the outlet [4, 8]. The theoretical relationship between the

discharge coefficient C_{df} and η_f is shown in Figs. 6 to 10 with L/d_1 as the group parameter. The experimental results from the present and previous investigations [66] are shown in these figures. It is seen that the experimental results agree fairly well with the theoretical relationship and support the choice of L/d_1 as the group parameter. The theoretical lower bounds of η_f for given values of L/d_1 are also shown in these figures. However, it should be noted that in the subcritical range, for $L/d_1 < 0.2$., the flow in the vicinity of the floor outlet was generally characterised by the formation of large scale undulations and vortices and hence reliable data could not be obtained in this range.

The Froude number F_f in the approach channel is related to the velocity parameter η_f through Eq. 2.9. The latter has a finite upper bound of one and hence facilitates the presentation of experimental data. Knowing the discharge and depth in the approach channel, L/d_1 and η_f can be determined. This in turn enables one to obtain the discharge through the outlet using Eq. 2. 6. When there is a rapid change in the flow profile caused by a hydraulic jump, a hydraulic drop or vortices, the proposed relationship between C_{df} and η_f (Eq. 2.6) will not be valid.

2. 5. 2 INTERFERENCE EFFECTS IN A TWO-OUTLET SYSTEM

Fig. 11a shows a typical run for a two floor outlet system. The velocity and pressure profiles at various sections along the flow in the main channel are shown in Fig. 11b.

The dependence of K_f on the outlet spacing S_f with η_f as the group parameter is shown in Fig. 12 . From Fig. 12, it can be seen that the interference effect on the downstream outlet diminishes as the outlet spacing S_f is increased. For practical considerations , the interference effects on the downstream outlet due to the outlet upstream may be deemed negligible when the outlet spacing S_f exceeds a value of 7. Further, when the outlet spacing S_f is decreased, the interference effects become significant and appear to reach a maximum value around $S_f = 2$. The interference effects in this range can be considerable and must be taken into account in designing floor outlet systems. Further reduction in the outlet spacing tends to reduce the interference effects on the downstream outlet and finally the two outlets behave as a single unit when the spacing is very small ($S_f < 1.25$).

CHAPTER III

DICHARGE CHARACTERISTICS OE FLOW IN OPEN CHANNEL BRANCHES

CHAPTER III

DISCHARGE CHARACTERISTICS OF FLOW IN OPEN CHANNEL BRANCHES

3.1 GENERAL REMARKS

This chapter deals with division of open channel flows in a branch channel junction. To this end, an analytical model based on existing solutions for flow past a barrier set in the side of a two-dimensional channel is proposed. Experimental results from the present study and the data from previous investigators are presented to validate the proposed model.

3.2 INTRODUCTION

A comprehensive experimental study to determine the characteristics of dividing flows in an open channel junction is difficult because, the flow at the junction is characterised by features like separation, recirculation in the branch and wave formation in both the main channel and the branch channel. Further, depending on the control conditions in the main channel and the branch channel, the flow in the junction may be subcritical or supercritical. At present, comprehensive analytical studies related to the division of flow in open channels do not seem to exist.

The first detailed experimental study of dividing flows in an open channel was done by Taylor (62). In this study, the main channel and the branch channel were of the same width. The branch off-take was at right angles to the main channel. Using the experimental results, Taylor proposed a graphical solution which included a trial and error procedure. Grace (18) presented experimental results for different width ratios of the branch channel orientation with the main channel on the division of flow and classified the division of flow into two

regimes based on the existence of surface waves. The regime without waves corresponded to the cases where the Froude numbers were relatively small. The regime with waves corresponded to free over-fall conditions at sections downstream of the junction. Experimental studies for other Froude number ranges covering the intermediate flow conditions were not made by Grace (18).

Milne-Thomson (31), Tanaka (61) and Murotta (35) have solved the problem of branch channels analytically using conformal transformation. However, the assumption of flow depth being constant in all the channels makes it unrealistic for use in practice.

Division of flows with subcritical flow in the main horizontal channel and supercritical flow in sloping branch channels have also been studied by earlier investigators (22,41,42,43). In these studies, the branch channel flow was treated as flow through a side weir of zero sill height to obtain an experimental coefficient. Hager (19) has recently proposed a simplified model for evaluating loss coefficients for flow through branches by neglecting the transverse variations perpendicular to the channel floor.

Both analytical and experimental investigations of the problem of dividing flows for right angled channel junctions have been made by Law and Reynolds (25). Their experiments were confined to subcritical flows in the main channel. The flow in the main channel and the branch channel, was controlled by means of tail gates. The width of the main channel B and the width of the branch channel L was 8". The measurement of depth in the main channel upstream and downstream of the junction as well as in the branch channel were made at a fixed distance of 34" from the centre of the junction. The momentum equation was applied to the main channel and the branch channel separately. Because of the existence of flow separation and the return flow separation and the return flow in the branch a contraction coefficient C_c was introduced to account for the effective width of the branch channel. However, the mean depth of flow in the branch channel was always measured at the centre

line of the channel and at a fixed location. This leads to considerable errors in the estimation of the contraction coefficient C_c since the complete contraction of the jet (Fig. 13) and subsequent reattachment of the flow to the branch channel walls might have already occurred ahead of the depth measuring section in the branch. This seems to be the case for a large range of values reported by Law and Reynolds for which C_c is indicated as unity. It should be noted that separation and hence considerable contraction of the flow entering the branch increases generally with the increase in the upstream Froude number F_1 in the main channel. Further, the section of maximum contraction shifts downstream with the increase in the value of F_1. This observation has also been made by Rao and Sridharan (23).

Systematic experimental studies have been carried out by Rao et al (23,24,59,60) for dividing flows in a branch channel. They have analysed the division of flow based on continuity, energy and momentum principles using the Froude numbers F_1 and F_2 as reference parameters. Here, F_2 denotes the Froude number at the downstream section of the main channel. They have experimentally determined the dependence of Q_3/Q_1 on F_1 and F_2 for various values of L/B. They further attempted to correlate the width of the return flow zone in the branch channel with the Froude number F_2 and the branch channel Froude number F_b based on visual observations. The observed value of C_c was always considerably less than unity for all flow conditions. Although, their data displays considerable scatter, the results related to C_c provide useful qualitative information.

Branching of flow finds application in flow distribution systems in plants which treat water and waste water (4). In such systems, feeder channels set in groups and linked to mixing tanks of treatment plants are often short and the existence of free over fall conditions at the end of the branches generally ensure unsubmerged conditions near the branch channel entrance. Even in irrigation systems, unsubmerged flow conditions in the branch channel may be found when the branch channel is very short and the Froude number F_b in the downstream section of the branch channel is greater than a threshold value (24,26). The present study deals with the formulation of a simple theoretical model for division of flow in short branch channels when the flow in the branch channel is not submerged due to downstream controls.

For computing the branch channel discharge, it is essential to estimate the value of the contraction coefficient C_c of the separated flow entering the branch. To this end, the present model makes use of the similarity of flow configuration between the division of flow in a branch channel and a two-dimensional lateral conduit outlet fitted with a barrier (inset - Fig. 14). This enables one to estimate the contraction coefficient C_c from the corresponding conduit outlet model. Due to the complex nature of the flow in the branch channel, only global values of C_c are sought for the branch channel model. Based on this analysis, the discharge ratio Q_3/Q_1 is related to the downstream Froude number F_2, for given values of L / B. Existing results from earlier studies (22,26,60) and the results of the present investigation are both used to validate the proposed model.In this context it should be noted that the data used from Law (26) were restricted to the cases in which the section of maximum contraction in the branch was not submerged due to the downstream control in the branch channel. Based on earlier investigations[24,26], the flow conditions at the entrance to the branch were generally not submerged when the Froude number F_b in the branch was greater than a threshold value. This threshold value was observed to be close to 0.3. The results of the present tests indicate that this threshold value is close to 0.35(section 3. 3. 7).

3.3 THEORETICAL CONSIDERATIONS

3.3.1 FLOW CONFIGURATION

The general configuration of the flow entering a branch channel (Fig. 13) closely resembles the pattern of lateral flow past a two-dimensional conduit outlet fitted with a barrier (inset - Fig. 14). Here, L denotes the width of the outlet and B the width of the conduit. In both configurations, the flow approaching the branch separates from the main channel and begins to contract and eventually attains a width C_cL at the section of maximum contraction. In the conduit model, the contracting jet assumes the terminal width C_cL at a location far away from the outlet. However, for all practical purposes, almost all of the jet contraction essentially occurs within a short distance from the conduit exit. In the case of the branch channel, the maximum contraction of the separated flow also occurs within a short distance from the main channel exit. This distance is generally of the order of the branch channel width L (23,60). Further, following the contraction, the jet expands to the width of the branch channel leading to the formation of a cavity (Fig. 13). The similarity of the two flow configurations as far as the contraction of the separated flow is concerned, enables one to estimate the contraction coefficient for the branch channel flow using the model of a lateral conduit outlet fitted with a barrier (inset- Fig. 14).

3.3.2 MAIN VARIABLES

Let (V_1, V_2, V_3) and (h_1, h_2, h_3) denote the mean velocities and depths of flow at sections 1, 2 and 3 respectively (Fig. 13). The Froude numbers $F_1 = V_1/\sqrt{gh_1}$ and $F_2 = V_2/\sqrt{gh_2}$ of the main channel and the discharge ratio Q_3/Q_1 are the main variables.

Determining the dependence of Q_3/Q_1 on F_1 and F_2 for given values of L/B constitutes the branch channel flow problem. In the development of the solution, a relationship between the contraction coefficient C_c of the separated flow in the branch channel and the velocity parameter $\eta_1 = V_1/V_3$ is required. Such a relationship is extremely difficult to establish in view of the complexities associated with free surface flows. However, as stated earlier, a close approximation for C_c of the branch channel flow is obtained using the corresponding conduit model.

3.3.3 ASSUMPTIONS

The following assumptions are made in the development of the branch channel flow analysis:

(1) The main and branch channels are rectangular and horizontal. The width of the branch channel L is restricted to a width less than or equal to the width of the main channel B and the flow in the main channel is subcritical.

(2) Energy loss is negligible between sections 1 and 3.

(3) The pressure distribution is hydrostatic at sections 1 and 2. The average pressure head acting along the dividing stream surface MN (Fig. 13) is assumed to be the average of the pressure heads at M and N.

(4) The friction loss is negligible in the short reach 1 to 2.

(5) The branch channel is short and the Froude number of flow in the branch is greater than 0.35. Hence, the flow conditions are approximately critical at section 3 where the maximum contraction occurs (see section 3.3.7).

(6) The contraction coefficient C_c for the two dimensional conduit outlet fitted with a barrier provides a good estimate for the global contraction coefficient in the branch channel when the values of L/B and h_1 are the same for both cases.

3.3.4 GOVERNING EQUATIONS

From energy considerations between sections 1 and 3 (Fig. 13),

$$V_3 = [V_1^2 + 2g(h_1 - h_3)]^{1/2} \quad ...(3.1)$$

where,

$$V_3 = Q_3 / C_c L h_3 \quad ...(3.2)$$

From continuity considerations,

$$Q_1 = Q_2 + Q_3 \quad ...(3.3)$$

Substituting for Q_1, Q_2 and Q_3 in Eq. 3.3 we have,

$$Bh_1V_1 = Bh_2V_2 + C_cL\,h_3V_3 \quad ...(3.4)$$

From the assumption of critical flow at section (3)

$$V_3^2 = gh_3 \quad ...(3.5)$$

From Eqs. (3.1), (3.4) and (3.5), one can obtain the following expression for the discharge ratio Q_3/Q_1.

$$\frac{Q_3}{Q_1} = \frac{1}{3\sqrt{3}} C_c \left[\frac{L}{B}\right] F_1^2 \left[1 + \frac{2}{F_1^2}\right]^{3/2} \quad (3.6)$$

Further, from the definitions of F_1 ($= V_1/\sqrt{gh_1}$) and η_1 ($= V_1/V_3$) and Eq. (3.5) we have,

$$F_1^2 = \frac{2}{\left[\frac{3}{\eta_1^2} - 1\right]} \quad (3.7)$$

Substituting Eq. 3.7 in Eq. 3.6,

$$\frac{Q_3}{Q_1} = \frac{2\left(\frac{L}{B}\right) C_c}{(3\eta_1 - \eta_1^3)} \quad ...(3.8)$$

From momentum considerations in the direction of the main flow between sections SM and RN in Fig. 13,

$$\rho Q_2 (V_2 - V_1) = \frac{1}{2} \gamma h_1^2 \left[B \left(1 - \frac{Q_3}{Q_1}\right)\right] - \frac{1}{2} \gamma B h_2^2 + f_x \quad (3.9)$$

In the preceding equations, Q_2 = discharge in the main channel after the branch

ρ = mass density of water

γ = specific weight of water

f_x = component of the pressure force acting along the dividing surface MN (Fig. 1) in the direction of the main flow.

The average pressure head acting along MN (Fig. 13) is taken as the average of the pressure heads at M and N.

Hence,

$$f_x = \frac{1}{2}\gamma B \left(\frac{h_1 + h_2}{2}\right)^2 \left(\frac{Q_3}{Q_1}\right) \qquad ...(3.10)$$

substituting Eqs. (3.4) and (3.10) in Eq. (3.9) and simplifying, one gets,

$$\left[\frac{h_2}{h_1}\right]^3 - \frac{1}{4}\left[1+\frac{h_2}{h_1}\right]^2 \frac{h_2}{h_1}\frac{Q_3}{Q_1} - (2F_1^2+1)\left[1-\frac{Q_3}{Q_1}\right]\frac{h_2}{h_1}$$

$$+ 2F_1^2\left[1-\frac{Q_3}{Q_1}\right] = 0 \qquad (3.11)$$

Using the definitions of F_1 and F_2 together with Eq. (3.4), one can obtain

$$F_2 = \frac{F_1\left[1 - \frac{Q_3}{Q_1}\right]}{\left(\frac{h_2}{h_1}\right)^{3/2}} \qquad (3.12)$$

3. 3. 5. CONTRACTION COEFFICIENT

The hydrodynamic model to determine the characteristics of flow past a two dimensional jet issuing out of a conduit outlet fitted with a barrier (inset - Fig. 14) has been investigated earlier (28). The solution relates the parameters C_c, L/B and $(1 - Q_3/Q_1)$. With the help of the continuity equation for the two dimensional conduit model denoted by Eq. 3.13, a relationship between C_c, η_1 and L / B is obtained [48] and is shown in Fig. 14.

2-D lateral outlet:

$$\frac{Q_3}{Q_1} = \frac{\left(\frac{L}{B}\right)}{\eta_1} C_c \qquad (3.13)$$

For the conduit model, as the discharge ratio Q_3/Q_1 approaches unity, the parameter η_1 (Fig 14), attains a minimum value for given values of L/B. At this condition, the contraction coefficient C_c will reach a maximum value (Table 1). However, in the corresponding branch channel flow problem, the ratio Q_3/Q_1 will not have reached unity for these minimum values of η_1 according to Eq. 8. In order to extend the solution for Q_3/Q_1 up to the value of unity for the given value of L/B, the maximum value of C_c is assumed to remain constant in the extended range of Q_3/Q_1. The corresponding value of h_1 is obtained through Eq. (3.8) which is based on the branch channel continuity considerations. For values of L/B < 1, the range of η_1 over which C_c is held constant in the branch channel model is relatively short (Table 1).

3.3.6 DISCHARGE - FROUDE NUMBER RELATION

For a given value of F_1, the corresponding values of η_1 and C_c can be obtained from Eq. (3.7) and Fig. 2 for fixed values of L/B. The discharge ratio in the branch channel Q_3/Q_1 for the specified value of F_1 can be readily determined from Eq. 3.8. The value of the depth ratio (h_2/h_1) can be obtained subsequently from Eq. 3.11. The downstream Froude number F_2 can be computed using Eq. (3.12). When the value of η_1 for the conduit model (Fig. 14), C_c is held constant at its maximum value for the given value of L/B (Table 1) and the above procedure is repeated.

3.3.7 DISCHARGE - BRANCH CHANNEL FROUDE NUMBER F_b RELATION

The conditions of flow in the branch channel will affect to a great extent the discharge distribution in the branch. Hence, to check the appropriateness of assumption 5 in developing the theoretical model a limited number of experiments were also conducted to study the effect of branch channel Froude number F_b on the flow division.

3.4 EXPERIMENTAL SET-UP

Some tests were conducted to obtain a verification of the proposed theoretical model for the division of flow in the branch channels. The rectangular channels used in the tests were horizontal. They were made of stainless steel and had a smooth finish (Fig. 15). The main and branch channels were 25.4 cm wide and 43.2 cm deep. The branch channel was positioned at right angles to the main channel and the edges at the junction were sharp.

The discharge from the channels were measured with the help of standard V-notches. The point gages used to measure the water levels in the channel and the V-notch tanks could be read to the nearest 0.1 mm. for each test run floor pressures and the centre line surface profiles were recorded.

Sections J and K, 25.4 cm upstream and downstream of the junction along the centre line of the main channel were chosen to measure the upstream and downstream depths h_1 and h_2 respectively. The depth h_b in the branch channel was measured at a distance of 100 cms from the centre of the junction. This location was chosen to be essentially free from the effects of the hydraulic jump and the back water effects from the downstream control in the branch. To reduce large scale turbulence and ensure smooth flow, baffle systems were provided (Fig. 15).

3.5 ANALYSIS OF RESULTS

3.5.1 EFFECT OF F_b ON FLOW DIVISION

For dividing flows in branch channels when the Froude number F_b in the branch is greater than 0.35, the results from earlier investigations [24, 26] and the present study indicate that the flow in the branch channel in the vicinity of the junction will not generally be submerged. Such situations are normally encountered in channels with short branches or branches which have steep slopes.

Recognising that the nature of flow near the branch entrance determines the discharge ratio, a limited number of experiments were conducted to determine the effect of F_b on the main channel flow [Fig. 16].

The conditions of flow in the branch may vary depending on the nature of control in the downstream section of the branch. When the flow at the section of maximum contraction (section 3 - Fig. 16) is critical, the flow immediately downstream of this section will be expanding and supercritical. Depending on the downstream control, the flow can remain supercritical or may lead to the formation of a hydraulic jump. Further, when the section of maximum contraction corresponds to critical flow conditions, the changes in the branch channel flow at a section downstream of the throat should not significantly affect the flow in the main channel. An observation of Fig. 16 shows that the conditions of flow in the main channel were relatively unaffected by the changes in the branch channel when the branch channel Froude number F_b exceeds 0.35 and the conditions of flow in the section of maximum contraction is close to critical. Further, for F_b less than 0.35 it can be seen that the conditions of flow in the section of maximum contraction is clearly subcritical and any change in the flow conditions

in the branch affects the main channel flow drastically. This observation lends support to the assumption that the flow is close to critical in the section of maximum contraction for short branch channels in which F_b is greater than 0.35 .

3.5.2 VARIATION OF Q_3/Q_1 with F_1:

The theoretical relationship between the discharge ratio Q_3/Q_1 and the Froude number F_1 of the upstream section is shown in Figs.17, 18 and 19. for three typical values of L/B. The available data from the previous investigators [22,26,60] and from the present set of experiments are also shown in Figs. 17 to 19 for the corresponding values of L/B.

Although the experimental data follows the general trend predicted by the theoretical relationship (Eq. 3.8), there is considerable scatter in the experimental data for L / B = 1 (Fig.17). the agreement improves as the value of L / B decreases (Figs. 18 and 19). The data obtained from Krishnappa et. al [22] was for branch channels having a slope of 1 in 30. Consequently, one can expect the discharge ratio Q_3/Q_1 for such cases to be higher than the theoretically predicted value for horizontal channels.

The experimental observations indicate the formation of surface waves when the value of F_1 approaches 0.8. As such, the proposed theoretical relationships are only valid for cases where F_1 is less than 0.8. The lower bounds for F_1 as predicted by the present branch channel model when Q_3/Q_1 reaches unity is shown in Figs.17 to 19 . As may be expected, the lower bound for F_1 ($Q_3/Q_1 \rightarrow 1$) increases with the width ratio L/ B.

3.5.3 VARIATION OF Q_3/Q_1 WITH F_2

The theoretical relationship between Q_3/Q_1 and F_2 is shown in Figs. 20 to 22 for three typical values of L / B. The available experimental data from the previous investigators (22,26,60) along with the data from the present set of experiments are also shown in Figs. 20 to 22, for the corresponding values of L / B. The theoretical relationship between F_2 and Q_3/Q_1 is seen to agree well with the experimental data for all the three values of L / B chosen. Consequently, for purposes of design, the relationship between Q_3/Q_1 and F_2 is recommended. Even though, the theory predicts the values of Q_3/Q_1 for the full range of F_2 from 0 to 1, the use of the model is not recommended for values of F_2 beyond 0.7 because of the presence of the cross waves.

3.6 PRACTICAL APPLICATIONS

The analytical relationships between the discharge ratio Q_3/Q_1, the upstream Froude number F_1 and the downstream Froude number F_2 for given values of L/B ratios is shown in Figs. 17 to 22. They provide a simple proceedure to estimate the discharge ratio as a function of the upstream and the downstream flow conditions in the main channel. It is to be noted that certain conditions in the branch channel affect the flow in the junction. However, the present model is effective for cases where the section of maximum contraction of the separated flow into the branch is not submerged due to the downstream control in the branch channel. This condition is generally observed when F_b is greater than 0.35 .

In a typical field problem, the rating curves relating $Q_1 - h_1$ or $Q_2 - h_2$ and $Q_3 - h_b$ are known. For subcritical flows, downstream conditions in the main channel determine the depth of flow h_2. Knowing Q_2, h_2 and the downstream Froude number F_2, Q_3 and hence h_b can be determined from Figs. 20 to 22 for a given value of L/B . For the cases where the discharge in the section upstream of the junction and the rating curves for the main channel section downstream of the junction and the branch channel are known, a simple trial procedure to find Q_3/Q_1 is presented here.

3.6.1 FIELD EXAMPLE

The following example given by Taylor (62) readily available for branch channel flow is considered for comparison:

Data: L = B = 10 ft, Q_1 = 500 cfs,

rating curves for the branch channel and the downstream section of the main channel [Fig. 8 - Ref. (62)].

Taylor's graphical trial and error procedure based on the experimental relationship between Q_3/Q_1, h_1/h_b, h_2/h_b and $V_1/2gh_1$ yields the following solution:

Q_2 = 170 cfs, Q_3 = 330 cfs and $\underline{Q_3/Q_1 = 0.66}$

Proposed Method:

Assume a trial value of Q_2 and hence obtain Q_3 and Q_3/Q_1. In turn, obtain the trial value of F_2 from Fig. 20. Using the trial values of Q_2 and F_2 compute h_2. If the trial

values of Q_2 and h_2 do not match the rating curve for the downstream section, assume a new value of Q_2 and repeat the prodecure.

For the numerical problem stated earlier, the trial solution that satisfies the rating curve and Fig. 20 is given below.

$Q_2 = 190$ cfs, $Q_3 = 310$ cfs and $Q_3/Q_1 = \underline{0.62}$

$F_2 = 0.18$ $h_2 = 6.9$ ft and $F_b = \underline{0.4}$

(Since $F_b > 0.35$, the solution from the proposed method is valid.)

CHAPTER IV

DISCHARGE CHARACTERISTICS OF SPATIALLY VARIED DIVERGING LATERAL FLOWS IN OPEN CHANNELS

CHAPTER IV

DISCHARGE CHARACTERISTICS OF SPATIALLY VARIED DIVERGING LATERAL FLOWS IN OPEN CHANNELS

4. 1 GENERAL REMARKS

This chapter deals with the formulation of governing equations for spatially varied diverging lateral flows in open channels. A pressure recovery coefficient is introduced to account for the uncertainty in the lateral momentum transferred along the lateral due to the turning of the flow. A simple experimental procedure for the evaluation of this pressure recovery coefficient for a specific case of a discrete branch channel junction is presented.

4. 2 INTRODUCTION

Flows wherein the discharge varies in the direction of flow may be described as spatially varied flows. Further, the flow in which the discharge decreases in the direction of flow can be defined as a spatially varied diverging lateral flow. Some examples of the same include side channel spillways, open channel flows with permeable boundaries, flow into gutters, flow past floor outlets and branch channels. The flow of water from side channel spillways neglecting the frictional resistance was first studied by Hinds(20). Later, the friction loss was accounted by the addition of a friction factor by Favre(13). Camp(7) studied the case of rectangular channels with uniform lateral inflow by using the Weisbach's resistance coefficients for evaluating friction losses. The case of steady flow in a trapezoidal channel with uniform lateral inflow was investigated by Li(27) using a constant Chezy resistance coefficient. In particular, studies on flows with decreasing discharge were conducted by Engels (12) and Coleman(8). An analytical study assuming a linear profile along the spillway

crest was made by Forschheimer (14). De Marchi(10) obtained theoretically the flow profile along the spillway crest assuming the energy head along the spillway crest to be essentially constant. Other theoretical and experimental investigations include the studies of Gentillini(17), Nimmo(39), Noseda(40), Schmidt(58), Mustkow(33,34), Ackers(1), Allen(2), Collinge(9), Frazer(15) and Smith(11). In the above studies, both momentum and energy principles were used. However, studies resorting to the energy approach overlooked the energy exchange due to the lateral flow. Recently Yen and Wenzel (69) pointed out the above factor and have proposed general dynamic equations for the steady spatially varied flow problems.

The present study is related to the development of an analytical procedure for determining the performance of diverging lateral flows in open channels such as branch channel manifold systems (Fig. 23), batteries of side weirs or systems of floor outlets. To this end, the momentum principle was made use of in obtaining the equations governing the flow. To account for the uncertainity in evaluating the axial momentum transported across the lateral openings, a pressure recovery factor was introduced into the governing equations. Further, a limited number of experiments were conducted to estimate the pressure recovery factor for the particular case of a discrete open channel branch set at right angles to a main channel.

4. 3 THEORETICAL CONSIDERATIONS

4.3.1 FLOW MODEL FOR A SINGLE BRANCH

Consider the flow system for a single branch shown in Fig. 23 a. Let $(q_1, w_1, y_1, a_1,)$ and

(q_2, w_2, y_2, a_2) represent the discharge, velocity, depth of flow and the area of flow at sections 1 and 2 respectively. Let a_3 be the lateral area of flow at the entrance to the branch. The dotted lines in Fig. 23a define a control volume wherein the fluid is transported across the areas a_1, a_2, and a_3. Let w_x and w_y represent the flow velocities in the axial direction X and the normal direction Y respectively. The flow in the main channel along the lateral may decelerate or accelerate due to the gradual removal of the fluid through the lateral area a_3 depending on the flow being subcritical or supercritical.

The momentum balance in the axial direction for the control volume shown in Fig. 23a is given by,

$$\int p_1 \, da_1 - \int p_2 \, da_2 = \int \rho \, w_2 \, w_2 \, da_2 - \int \rho \, w_1 \, w_1 \, da_1 + \int \rho \, w_x \, w_y \, da_3 \qquad (4.1)$$

In Eq. 4.1, da_1, da_2 and da_3 are the elemental areas on the flow areas a_1, a_2 and a_3 respectively. p_1 and p_2 are the pressure intensities on da_1 and da_2 respectively.

Earlier investigators dealing with branching of flow in conduits (3) have shown that the assumption that the fluid does not loose any of its axial momentum on leaving the control volume is not well founded due to the turning of the flow and we can expect w_x not to be equal to w_1. To account for uncertainity in the axial momentum transported across a_3, a pressure recovery coefficient R_0 is introduced in evaluating the last integral of Eq. 4.1. Now, Eq. 4.1 can be simplified as shown in Eq. 4.2.

$$P_{o2} - P_{o1} = \rho q_1 w_1 - \rho q_2 w_2 - R_o \rho q_3 w_1 \quad (4.2)$$

Where, P_{o1} and P_{o2} are the pressure forces acting on sections 1 and 2 respectively.

The value of R_o for closed conduit flows has been estimated by Bajura (3). The value of R_o for spatially varied diverging lateral flows in open channels can be estimated using Eq. 4.2. A simplified procedure for the experimental determination of R_o in a discrete branch channel junction and the results of the experiment for the partilcular case of subcritical flows in the main channel are presented in section 4. 4.

4.3.2 MODEL FOR SPATIALLY VARIED DIVERGING LATERAL FLOW SYSTEMS

Consider the case of a steady, gradually decreasing flow in an open channel with uniform cross-section and a slope S_o with the horizontal (Fig. 24). Let q be the discharge, w the average velocity in the direction of the main flow, y the flow depth, a the flow area, and w_x and w_y the local flow velocities in X and Y directions respectively.

When the number of branches in a flow distribution system is large, it is easier to analyse the flow system by means of a set of continuous equations. If the lateral area consists of a series of outlets of each width t and the number of outlets is n_o then an area ratio factor A_{ro} may be defined such that,

$$A_{ro} = \frac{n_o t}{L_o} \quad (4.3)$$

where, L_o is the total length of the lateral diversion system:

From Fig. 24, the governing equation for the axial momentum may be written as,

$$-\frac{d(Kay)}{dx} - \frac{1}{\gamma}\tau P_e + S_o a = \left(\frac{1}{g}\right)\frac{d(\beta w q)}{dx} + \left(\frac{1}{g}\right) R_o A_{ro}(w w_y y) \qquad (4.4)$$

where,

K = pressure correction factor = $\int (p\, da)/ \{\gamma a y \cos(\theta)\}$ (4.5)

β = momentum correction factor = $\int \rho w_x^2 da / \{\rho a w^2\}$ (4.6)

w = average velocity = $\frac{1}{a}\int w_x da$ (4.7)

S_o = Sin θ (4.8)

P_e = wetted perimeter

τ = boundary sheary stress

In Eqs. 4.5 to 4.7, p denotes the local pressure intensity on the elemental area da

From continuity,

$$w_y = -\frac{1}{y A_{ro}}\left(\frac{dq}{dx}\right) \qquad (4.9)$$

The normal component of the lateral flow w_y(Fig. 2b) may be determined by means of a conventional relation such as Eq. 4.10.

$$w_y = C_L\, g^{1/2}\, y^{1/2} \qquad (4.10)$$

In Eq. 4.10, C_L represents a lateral discharge coefficient and can be generally determined depending on the flow conditions and the outlet geometry. Experimental observations have shown Eq. 4.10 to be fairly valid when the lateral outflow is not excessive (69). However, when the lateral flow is considerable the relationships developed earlier in chapters II and III for floor outlets and branch channel junctions should be used in evaluating the discharge coefficient C_L.

From Eqs. 4.9 and 4.10, we have

$$y^3 = \frac{1}{A_{ro}^2 C_L^2 g} \left(\frac{dq}{dx}\right)^2 \qquad (4.11)$$

Differentiating Eq. 11 with respect to x and simplifying we get

$$\frac{dy}{dx} = \frac{2 \left(\frac{dq}{dx}\right) \left(\frac{d^2q}{dx^2}\right)}{3 g C_L^2 A_{ro}^2 y^2} \qquad (4.12)$$

Let the flow area a be defined such that

$$a = b\,y \qquad (4.13)$$

where, the value of the width b depends on the geometry of the flow channel. For the present study, b is assumed to remain constant.

Substituting Eqs 4. 9 to 4.13 in Eq. 4.6 and simplifying we have,

$$\frac{d^2q}{dx^2}\left[\left(\frac{\beta C_L^2 A_{ro}^2}{2Kb^2}\right) q^2 - \left(\frac{dq}{dx}\right)^2\right] - \left[\frac{3A_{ro}^2 C_L^2 (2\beta - R_o)}{4Kb^2}\right] q \left(\frac{dq}{dx}\right)^2$$

$$- \left(\frac{3A_{ro}^2 C_L^2}{4K}\right)\left[\frac{\tau P_e y}{b\rho} - gS_o y^2\right]\frac{dq}{dx} = 0 \qquad (4.14)$$

Eq. 4.14 forms the required governing equation for the case of steady, spatially varied decreasing flow in an open channel.

Using the non-dimensionalised values of discharge and distance such that $q^*(x^*) = q(x^*)/q(0)$ and $x^* = x/L$, for the case of steady, spatially varied decreasing flow in a frictionless horizontal channel, Eq. 4.14 with usual notations reduces to

$$q^{*''}\left[q^{*2} - \frac{2K}{\beta C_L^2 A_{ro}^2}\left(\frac{b}{L}\right)^2 (q^{*'})^2\right] - 3\left(1 - \frac{R_o}{2\beta}\right) q^* (q^{*'})^2 = 0 \qquad (4.15)$$

In Eq. 4.15, the value of the pressure recovery coefficient R_o will have to be evaluated experimentally. Although some investigators have estimated the value of R_o in closed conduit flows, no such reports have been made previously to estimate the value of R_o for open channels. In the present investigation, a simplified model for evaluating R_o for a particular case of the division of flow in a branch channel is proposed and the experimental results are presented.

4.4 EXPERIMENTAL DETERMINATION OF R_0 IN A BRANCH CHANNEL JUNCTION

The flow configuations for a single rectangular branch of width b set in the side of a horizontal, rectangular main channel of the same width is shown in Fig.3a. Let the discharge, velocity and the depth of flow at sections 1 , 2 and 3 be denoted by (q_1, w_1, y_1), (q_2, w_2, y_2) and (q_3, w_3, y_3) respectively. Let w_x and w_y denote the velocity components of the flow in X and Y directions respectively. Section (3) in Fig. 3a is chosen just beyond the point of reattachment of the jet entering branch. Here the flow may be considered to be approximately uniform. The location of section (3) is a function of the conditions of flow in the main channel and the branch and is determined experimentally. P_{CD} and P_{AB} are the pressure forces acting on the branch channel walls CD and AB respectively(50).

The momentum balance in the X direction for the control volume shown in Fig. 25a yields

$$\rho q_3 w_1 R_0 = P_{CD} - P_{AB} \qquad (4.16)$$

or,

$$R_0 = \frac{P_{CD} - P_{AB}}{\rho q_3 w_1} \qquad (4.17)$$

An estimate of R_0 can also be independently obtained by considering the momentum balance in the axial direction of the main channel (Fig. 25b) and neglecting friction as shown in Eq.4.18.

$$\beta_2 (\rho q_2 w_2) - \beta_1 (\rho q_1 w_1) + R_o \rho q_3 w_1 = K_1 b \gamma \frac{y_1^2}{2} - K_2 b \gamma \frac{y_2^2}{2} \quad \ldots (4.18)$$

or

$$R_o = \frac{b g (K_1 y_1^2 - K_2 y_2^2) + 2 (\beta_1 q_1 w_1 - \beta_2 q_2 w_2)}{2 q_3 w_1} \quad \ldots (4.19)$$

In Eqs 4.18 and 4.19, (K_1, β_1) and (K_2, β_2) refer to the pressure correction factor(Eq. 4.5) and the momentum correction factor (Eq. 4.6) at sections 1 and 2 respectively.

Experiments were conducted to evaluate the value of R_o and the results are presented for a particular case when the ratio of the main channel width to the branch channel width is equal to one.

4.5 EXPERIMENTAL SET-UP : DIVERGING OPEN CHANNEL SYSTEMS

The rectangular channels used in the tests were horizontal and made of polished stainless steel. The main and branch channels were 25.4 cm wide and 43.2cm deep. The branch channel was positioned at right angles to the main channel and the edges at the junction were sharp. The discharge from the channels were measured with the help of standard V-notches. The point gages used to measure the water levels in the channel and the V-notch tanks could be read to the nearest 0.1 mm. For each test run floor pressures and the centre line surface profiles were recorded. The branch channel walls were divided into grids for purposes of measuring the wall pressure and the pressures were recorded by means of piezometers capable of reading to the nearest mm. Detailed traverses were made in the main and the branch channel for recording velocity and pressure measurement using standard pitot tubes. A screw driver static probe was used to eliminate the effects from curvilinear flows. To reduce large scale turbulence and ensure smooth flow, baffle systems were provided in the main channel (Fig.26).

4.6 DISCUSSION OF RESULTS:

Eq. 4.15 is a second order non-linear differential equation and can be easily solved using numerical techniques or by series approximations. Although, the choice of the boundary conditions for the flow distribution appears to depend only on the geometry of the lateral flow system, a knowledge of the behaviour of the flow in the main channel is extremely essential in selecting proper boundary conditions.

Experimental investigations in the present study to estimate the pressure recovery factor R_0 were limited to subcritical flows in the main channel. Figs. 27b to 27d indicate the typical velocity distribution at various sections in the main channel. The velocity distribution is fairly uniform in the main channel approach (section a, Fig 27a) , and at the entrance to the lateral area (section 1) the flow is beginning to turn and the regions of flow with higher velocity have started to shift towards the lateral. This concentration of high velocity regions along the lateral opening may be expected to contribute further to the uncertainity associated with the axial momentum transfer across the lateral. At the end of the lateral opening (section 2) the flow in the main channel is expanding and one can observe the formation of a region of separation along the main channel wall. The static pressure distribution along the branch channel walls CD and AB for a typical case is shown in Figs 28a and 28b. At the entrance to the branch the jet is contracting and the pressure on the downstream wall of the branch channel is very much greater than the pressure on the upstream wall. As the lateral jet continues to accelerate and reaches a section of maximum contraction, the pressure on the downstream wall of the branch continues to decrease accordingly. Beyond this section of

minimum contraction the lateral jet begins to expand and fills the entire width of the branch channel. Past this section, the flow becomes relatively uniform and the static pressures become nearly equal on either side of the branch. This section where the flow becomes uniform in the branch was determined for each experiment from the pressure readings and the net force on the branch channel was computed by integrating the pressure readings. An estimate of the pressure recovery factor R_o was then obtained using Eq. 4.17.

For few of the experiments, R_o was also independently evaluated based on velocity and pressure traverses in the main flow and using Eq. 4.19. The values of R_o obtained from Eq. 4.17 and Eq. 4.19 were in fair agreement for each of the cases tested.

Fig. 29 shows the pressure recovery factor R_o plotted as a function of the discharge ratio q_3 / q_1 for subcritical approach flows in the main channel. Reliable data could not be obtained in the range $q_3/q_1 < 0.3$ due to the formation of cross waves in the main channel along the lateral outlet. Fig. 29 indicates that for the limited range of variables tested the pressure recovery factor R_o remains fairly constant over a wide range of the discharge ratio. This also compares qualitatively with the behaviour of the pressure recovery factor reported for closed conduit flows (3).

CHAPTER V

DISCHARGE CHARACTERISTICS OF MULTIPORT DIFFUSERS WITH UNIFORM LATERAL MOMENTUM DISTRIBUTION

CHAPTER V

DISCHARGE CHARACTERISTICS OF MULTIPORT DIFFUSERS WITH UNIFORM LATERAL MOMENTUM DISTRIBUTION

5.2 GENERAL REMARKS

This chapter deals with the internal hydraulics of multiport diffusers with uniform lateral momentum distribution. An analytical model for a multiport diffuser system consisting of lateral outlets housed in a closed conduit is proposed. Experiments were conducted to validate the proposed model and the results are presented.

5. 2 INTRODUCTION

Multiport diffusers are generally used for effective dispersion of fluids in a body of water (5, 16). The applications are found in systems used for mixing chemicals and in the disposal of large quantities of industrial effluents. The multiport system (Fig. 30) normally consists of a main duct carrying the effluent and discharging it as small jets through a series of lateral outlets into a main body of water. A number of studies related to the internal hydraulics of multiport diffusers have been made in the past [29,51,64,67].

One of the effective methods of effluent dilution is to discharge the effluent as a counterjet opposing the main flow [52]. For such systems, the frequency of jet oscillation and hence the scale of turbulent mixing are determined by the main flow velocity U and the kinematic momentum of the jet J. The mixing length scale characteristic of such system is given by the parameter J/U^2. Even for two dimensional and axi-symmetric jets which are frequently encountered in fluid transport, the width of the jet and hence the scale of mixing are

determined by the momentum of the jet [57]. However, when the temperature difference between the jet and the body of water is considerable as in the disposal of cooling water, the effect of the difference in densities must be considered.

The present study is limited to the internal hydraulics of diffusers used in distribution systems where momentum considerations are important. To ensure a uniform scale of mixing along the span of the diffuser, it is important to maintain a uniform lateral momentum distribution. In the past, studies have been mainly confined to the analysis of manifolds which ensure uniform lateral discharge distribution [4, 5]. For pipes of constant area, it should be noted that uniform lateral discharge criteria implies uniform lateral momentum distribution only when the lateral area distribution is uniform. This note deals with the internal hydraulics of a multiport diffuser of constant cross-sectional area, which ensures uniform lateral momentum distribution along the span of the main pipe. Experiments were conducted to verify the proposed model.

5. 3 THEORETICAL ANALYSIS

5.3.1 FLOW MODEL FOR A POROUS MANIFOLD

When the number of branch points in a manifold flow system is large, it is easier to consider the flow distribution system as a porous conduit and analyse its performance by means of a set of equations governing the flow.

Fig. 30 shows a system of n laterals of length ℓ, diameter d_ℓ and spacing s_ℓ connected to a manifold of length L_m, diameter D_m and area of cross-section A_m. Let Q, $\bar{p}$ and $\bar{V}$ denote

respectively the discharge, the average pressure and the average velocity in the control volume shown by dotted lines in Fig. 30. The flow velocities in the X and Y directions are represented by V_x and V_y respectively.

The porosity λ and the area ratio A_r of the manifold can be defined as,

$$\lambda = \frac{a_r}{\pi D_m} \qquad (5.1)$$

and

$$A_r = \frac{n d_t^2}{D_m^2} \qquad (5.2)$$

where, a_r is the lateral area per unit length. Further, the porosity λ is varied to ensure constant lateral momentum along the span of the manifold.

For the flow system illustrated in Fig. 30, the following equations governing the flow are valid.

i) Momentum balance in the direction of main flow:

$$\frac{1}{\rho}\frac{dp}{dx} + \frac{f\bar{V}^2}{2D_m} + 2\bar{V}\frac{d\bar{V}}{dx} + R\,\bar{V}V_y\lambda\frac{\pi D_m}{A_m} = 0 \qquad .....(5.3)$$

In Eq. 5.3 , the second term accounts for the friction loss on a continuous basis along the manifold. The coefficient of friction of the manifold, the kinematic viscosity and the fluid density are denoted by f , v , and ρ respectively. Further, a static pressure regain coefficient R in Eq 5. 3 accounts for the uncertainty in the estimate of the axial momentum transported across the laterals (3). Based on earlier studies (29 , 70), the value of R has been evaluated as a function of d_l/D_m and the spacing between the laterals S_l by Bajura (3).

ii) Constant lateral momentum:

$$\rho \lambda \pi D_m V_y^2 = \text{constant} = C \qquad (5.4)$$

iii) Continuity:

$$Q_L = V_y (\lambda \pi D_m) = - \frac{dQ}{dx} \qquad (5.5)$$

iv) Lateral outflow:

$$Q_L = C_d (\lambda \pi D_m) \sqrt{\frac{2 (\bar{p} - p_A)}{\rho}} \qquad (5.6)$$

where, p_A is the ambient pressure and C_d is the discharge coefficient of the laterals. For a given set of conditions, C_d can be evaluated experimentally (see section 5.3.4).

5.3.2. GOVERNING EQUATIONS FOR HYDRAULICALLY ROUGH PIPES

Using Eqs. 5.2 to 5.6 and non-dimensionalising the main variables such that $x^* = x/L$, $Q^* = Q(x^*)/Q(0)$, the following governing equation can be obtained with the usual notations.

$$Q^{**} + T_1 (Q^*)^2 (Q^{**})^3 + T_2 Q^* (Q^{**})^4 = 0 \qquad (5.7)$$

where,

$$T_1 = - f \left(\frac{L_m}{D_m}\right) \frac{C_d^2 M^2}{2} \qquad (5.8)$$

$$T_2 = - (2 - R) C_d^2 M^2 \qquad (5.9)$$

$$M = \frac{\text{Momentum at the manifold inlet}}{\text{Total lateral momentum}} = \frac{\rho Q(0) \overline{V}(0)}{C L_m} \qquad (5.10)$$

Eq . 5.7 is a second order non-linear differential equation and can easily be solved by numerical techniques. The boundary conditions for a manifold with the downstream end closed may be formulated as follows:

$$x^* = 0 ; \quad Q^* = 1$$
$$x^* = 1 ; \quad Q^* = 0 \qquad (5.11)$$

From Eqs. 5.5 ,5. 6 and 5.10, the pressure head $\bar{p}(x^*)/\gamma$ in the manifold is given by the relationship in Eq. 5.12.

$$\frac{\frac{\bar{p}(x^*) - p_A}{\gamma}}{\frac{\bar{V}^2(0)}{2g}} = \frac{1}{M^2 C_d^2 (Q_L^*)^2} \qquad (5.12)$$

where,

$$Q_L^* = -\frac{dQ^*}{dx^*} \qquad (5.13)$$

Further, from Eqs. 5.4, 5.5 and 5.10 the lateral area distribution is given as,

$$a_r(x^*) = M \left(\frac{A_m}{L_m}\right) (Q_L^*)^2 \qquad (5.14)$$

The non-dimensional lateral area a_r^* may then be written as,

$$a_r^* = \frac{a_r(x^*)}{a_r(0)} \qquad (5.15)$$

Solutions in the form of design charts for the variation of Q_L^* and a_r^* with M for two typical values of f are shown in Figs. 31b and 32b.

5.3.3 GOVERNING EQUATIONS FOR SMOOTH PIPES

An estimate of the coefficient of friction f in the manifold may be obtained by using the Blasius relationship for turbulent flows given by Eq. 5.16 for the Reynolds number Re ($= \overline{V}(x^*)\, D_m / \nu$) $< 10^5$ and by an approximate relationship of the form given in Eq. 5.17 for $10^5 < Re \leq 10^6$.

$$f = 0.3164 \left[\frac{\overline{V}(x^*)\, D_m}{\nu} \right]^{-0.25} \qquad (5.16)$$

$$f = 0.16 \left[\frac{\overline{V}(x^*)\, D_m}{\nu} \right]^{-0.19} \qquad (5.17)$$

Eq. 5. 17 was obtained by fitting a polynomial to the implicit relationship between f and R_e for smooth pipes (Eq. 5. 18) in the range $10^5 < R_e \leq 10^6$

$$\frac{1}{\sqrt{f}} = 2 \log Re\sqrt{f} - 0.8 \qquad (5.18)$$

Using Eqs. 5.2 to 5.6, 5.16 and 5. 17 and non-dimensionalising the main variables as before, the following governing equation may be obtained

$$Q^{*''} + T_3 (Q^*)^{\alpha} (Q^{*'})^3 + T_2 Q^* (Q^{*'})^4 = 0 \qquad (5.19)$$

where, for $10^5 < Re(0) \leq 10^6$

$$T_3 = - \frac{0.08 M^2 C_d^2}{[Re(0)]^{0.19}} \left(\frac{L_m}{D_m}\right) \quad ; \quad \alpha = 1.81 \quad .. (5.20)$$

and for $Re(0) < 10^5$

$$T_3 = - \frac{0.158 M^2 C_d^2}{[Re(0)]^{0.25}} \left(\frac{L_m}{D_m}\right) \quad ; \quad \alpha = 1.75 \quad .. (5.21)$$

Here,

$$Re(0) = \frac{\bar{V}(0) D_m}{\nu} = \text{inlet Reynolds number.} \qquad (5.22)$$

A typical solution of Eq. 5.19 with the given boundary conditions (EQ. 5. 11) for the variation of Q^*, Q_L^* and a_r^* with specific values of M are shown in Fig. 33b. Since the Reynolds number Re of the main flow is continuously decreasing in the direction of flow, the

solution procedure consists of two segments. For the first segment of the diffuser where $10^5 < R_e \leq 10^6$, Eq. 5. 19 is solved with coefficients given in Eq. 5.20. When the Reynolds number in the pipe reaches 10^5, the solution procedure is continued for the second segment of the diffuser using Eq. 5. 19 with coefficients given in Eq. 5. 21. The relationships shown in Figs. 33a and 33b were used in the design of the experimental manifold for verification of Eq. 5.19.

5.3.4 THE DISCHARGE COEFFICIENT FOR THE LATERALS:

The discharge coefficient C_d for a single lateral of length ι and area a_t attached to a manifold (inset, Fig. 34) may be defined as shown in Eq. (5.23).

$$C_d = \frac{Q_t}{a_t \sqrt{2g\left(\frac{\bar{p}}{\gamma}\right)}} \qquad (5.23)$$

where, Q_t is the discharge through the lateral, a_t is area of the lateral and $\bar{p}/\gamma$ is the average pressure head across the upstream face of the lateral and γ is the specific weight of the fluid.

Experiments were conducted to evaluate the value of C_d as a function of the parameters a_t/A_m, ι/d_m and η (Eq. 5. 24).

$$\eta^2 = \frac{\left(\frac{V_u^2}{2g}\right)}{\left(\frac{\bar{p}}{\gamma} + \frac{V_u^2}{2g}\right)} \qquad (5. 24)$$

5. 4 EXPERIMENTAL SET - UP : MULTIPORT DIFFUSERS

The main manifold consisted of a 2" diameter PVC (poly vinyl chloride) pipe. A machined PVC block was glued to this pipe as shown in Fig. 35. Lateral holes 14.3 mm in diameter were drilled through the PVC block. Sufficient care was exercised to clean the inside of the main pipe and the laterals to remove all burrs. Constant values of 0.92 for the pressure recovery factor . [3] and 0.73 for the discharge coefficient C_d (section 5. 3. 4) were adopted in the design of the experimental manifold. The continuous lateral area distribution (Fig. 33b) was discretised into equal areas and the laterals were placaed in the centres of these areas. Different area ratios A_r and momentum ratios M were obtained by closing the upstream laterals by means of plugs machined to fit the inside of the main pipe.

The discharge measurements from each of the laterals were made by gravimetric measurments. To this end, a previously calibrated precision scale was used to weigh the water collected for a period of 100 seconds or more. The total discharge from all the laterals was measured by means of venturimeters made to ASME specifications. The difference between the sum of the individual discharges and the total discharge measured independently was usually within ± 3 % of the total discharge.

The pressure measurements in the main manifold were made by means of a series of pressure taps located along the main pipe. The pressure head was recorded to the nearest mm on a water manometer board.

5. 5 .DISCUSSION OF RESULTS:

5.5.1 DISCHARGE COEFFICIENT FOR A SINGLE LATERAL

The functional dependence of C_d on the parameters a_t/A_m, ι/d_t, and η is shown in Fig. 34 . When ι/d_t is very small, the jet will not reattach to the walls of the lateral and the effective head causing the flow decreases resulting in lower values of C_d. Also, when ι/d is very large, the increased lateral resistance will reduce the value of C_d. Hence, when the lateral resistance is not excessive, the ratios a_t/A_m and ι/d can be properly chosen on the basis of experimental results to obtain a fairly constant and relatively high value of C_d for the laterals over a large range of η^2. The optimum value of ι/d based on the present experimental study was between 7 and 10. This is also in agreement with earlier investigations. In the design of the test manifold, the value of a_t/A_m used was 0.1. A constant value of 0.73 was chosen for the discharge coefficient C_d of the laterals (Fig. 34).

Based on the work of Rawn et al [51], Vigander [67] has presented an empirical relationship given in Eq. 5. 25

$$C_d = 0.63 - 0.58\,\eta^2 \qquad (5.25)$$

Eq. 5. 25 is shown as a curve A in Fig. 34. It must be noted that this relationship based on two dimensional theory is only valid for small discharges from small holes ($a_t/A_m < 0.015$) and when the velocities upstream and downstream of the lateral are approximately equal. As such , the comparison of the present experimental data for sharp - edged orifices with the data of Rawn et al should be only considered as qualitative.

The results of Vigander et al [67] for orifices in the side of corrugated pipes are shown as curve B in Fig. 8. The agreement between curve B and the present data is seen to be fairly good.

For sharp edged orifices ($\iota/d_t \to 0$), from the present study, the following polynomial may be used to approximate C_d as a function of η^2

$$C_d = 0.61 - 0.4(\eta^2) + 0.8(\eta^2)^2 - (\eta^2)^3 \qquad (5.26)$$

5.5.2 LATERAL DISCHARGE AND LATERAL MOMENTUM

For specific values of f = 0.025 and 0.05, the variation of Q_L^* (0) with momentum ratio is shown in Figs. 31a and 32a respectively. The variation of the normalised values of the main discharge, the lateral discharge and the lateral area with the momentum ratio for f = 0.025 is shown in Fig. 31b . The variation of the lateral discharge and the lateral area with the momentum ratio for f = 0.05 is shown in Fig. 32b . The variation in the lateral area and the lateral discharge is observed to be considerably larger near the manifold inlet and is nearly uniform towards the end of the manifold. This is due to the compensating nature of the static pressure gain caused by the deceleration of the flow and the static pressure loss due to friction in the header pipe. It is seen from the Figures 31b and 32b that as M approaches zero, the lateral discharge distribution is nearly uniform and approaches the so called reservoir condition in the main pipe. For such a condition, the lateral area distribution will also be nearly uniform. As M increases, the lateral area distribution will no longer be uniform and the lateral discharge will vary in accordance with the constant lateral momentum requirement.

For hydraulically smooth pipes, for an inlet Reynolds number Re(0) of 10^6, the variation of $Q_L^*(0)$ with M is shown in Fig. 33a and the variation of Q^*, Q_L^* and a_r^* with specific values of M is shown in Fig. 33b. The test manifold was designed for a momentum ratio of 1.45. This value of M corresponds to the maximum value of M obtained in the laboratory during preliminary tests.

Fig. 36 shows the variation of pressure and the discharge coefficient C_d along the diffuser. The experimental pressure distribution is seen to agree fairly well with the theoretical model. The value of 0.73 used for C_d in designing the experimental manifold is also seen to be appropriate.

Figs. 37, 38, and 39 show the lateral discharge and momentum variation along the span of the diffuser for different values of M and A_r. The experimental results agree fairly well with the theoretical prediction for the 3 models tested. When the outlet spacing is very close, it may be expected to have an effect on the values of C_d and the pressure recovery factor R. This may account for the slight scatter in the data near the manifold inlet. Further the flow in the header pipe is spatially varied and not fully developed. Hence, the solution utilising the traditional friction formulae based on fully developed flows may be expected to be only approximate.

5, 5. 3 DESIGN EXAMPLE [Constant friction coefficient design - rough pipe]

A multiport diffuser is to be designed to handle a discharge of 18 cfs and the total head available is 3 ft. The friction coefficient for the commercial pipe is estimated as 0. 025.

1. Let the diameter of the main pipe be 18" and the length of the diffuser L be 75 ft. such that $D_m/L_m = 0.02$, $A_m = 1.767$ ft^2, $\overline{V}(0) = 10.2$ ft/sec.

2. The available pressure head at the entrance to the diffuser

$$\frac{\overline{p}(0)}{\gamma} = 3.0 - \frac{\overline{V}^2(0)}{2g} = 1.38 \text{ ft.}$$

3. Let C_d for the laterals be 0.73 (Fig. 34) Substituting for C_d, $\overline{p}(0)$ and $\overline{V}(0)$ in Eq. 5.12 and simplifying we have

$$M Q_L^*(0) = 1.48$$

From Fig. 31a, $M = 1.2$ and $Q_L^*(0) = 1.22$ satisfy this requirement. Choose $M = 1.2$ curve in Fig. 31b for lateral area distribution.

4. From Eq. 5.14,

$$a_r(0) = \frac{1.2 \times 1.767}{75} 1.22^2 = 0.042 \text{ ft}^2/\text{ft.}$$

$$a_r(1) = \frac{1.2 \times 1.767}{75} 0.91^2 = 0.023 \text{ ft}^2/\text{ft.}$$

The lateral area distribution along the diffuser is shown in Fig. 40.

5. Total lateral area = 2. 12 ft^2 . Choose 11 laterals of diameter 6". a_l / A_m = area of lateral /area of main pipe = 0. 11.

6. Length of the lateral /dia of lateral = say 7 (Fig. 34). Length of lateral = 42 in.

7. Dividing the lateral area distribution into 11 equal parts and placing the laterals in the centroid of these areas we have the location of the laterals given in Table 2.

CHAPTER VI

CONCLUSIONS AND SCOPE FOR FURTHER STUDY

CHAPTER VI

CONCLUSIONS AND SCOPE FOR FURTHER STUDY

6.1 CONCLUSIONS

6.1.1 OPEN CHANNEL FLOWS PAST FLOOR OUTLETS

1. Based on the two dimensional channel outlet model, a functional relationship between the discharge coefficient , C_{df} , and the velocity parameter , η_f , is proposed with L / d_1 as the group parameter for the floor outlet discharge.

2. The experimental results from the previous studies and from the present investigation agree well with the proposed functional relationship in the range $0 < L / d_1 \leq 1$.

6.1.2 DIVIDING FLOWS IN OPEN CHANNEL BRANCHES

(1) Based on the two dimensional conduit model fitted with a barrier , a functional relationship between the discharge ratio Q_3 / Q_1 , the width ratio L / B and the Froude numbers F_1 and F_2 is proposed.

(2) The theoretical relationships obtained from the present model for the flow in short branch channels is in good agreement with the experimental data.

(3) The parameters like the discharge ratio Q_3/Q_1, L/B ratio, and the upstream and the downstream Froude numbers in the main channel, required in the design of branch channels are obtained directly. However, from practical considerations, the application of the model should be limited for cases in which $L/B \leq 1$, $F_2 < 0.7$, and $F_b > 0.35$.

(4) For given values of L/ B, as the discharge ratio Q_3 / Q_1 tends to unity, the approach Froude number F_1 reaches a lower limit.

(5) For subcritical flows, the correlation of the discharge ratio Q_3/Q_1 with the downstream Froude number F_2 agrees very well with the experimental results and is recommended for use in the design procedure for values of $L/B \leq 1$, $F_2 < 0.7$, and $F_b > 0.35$.

6.1.3 SPATIALLY VARIED DIVERGING OPEN CHANNEL FLOWS

(1) Generalised governing equations for spatially varied diverging lateral flows in open channels using momentum principles and a pressure recovery factor accounting for the uncertainities in the axial momentum transferred due to the turning of the lateral flow are proposed.

(2) An experimental procedure to estimate the pressure recovery factor for open channel flows in a discreet branch channel is given and preliminary experimental results for L/B = 1 are presented.

(3) Over the range of Q_3 / Q_1 tested , the value of the pressure recovery factor R_o in open channel branches appears to be fairly constant.

6.1.4 MULTIPORT DIFFUSERS WITH UNIFORM LATERAL MOMENTUM DISTRIBUTION

(1) A procedure for maintaining uniform lateral momentum distribution along the span of a multiport diffuser fitted with a system of short laterals is proposed.

(2) Based on numerical techniques, the solution of the governing equations in the form of design charts for both hydraulically rough as well as hydraulically smooth pipes are presented.

(3) The experimental results are also presented to validate the suggested model.

6.2 SCOPE FOR FURTHER STUDY

Generalised governing equations for spatially varied diverging lateral flows has been proposed in chapter IV. The pressure recovery factor in open channel flows has been experimentally determined for a particular case of an open channel branch with the width of the main channel equal to the width of the branch. It is desirable to study the effects of the branch to the main channel width ratio on the pressure recovery factor. Further, estimation of the pressure recovery factors for floor outlets and side weirs will be helpful in using the governing equations proposed here for specific spatially varied open channel flow systems.

The present model for the division of flow in branch channels can be modified to include cases where the branch channel is set at a gradient with the parent channel. Also, the proposed model for division of flows in right angled branch channel junctions can be extended to include other angles of intersection between the main and the branch channels. For this purpose, existing two dimensional model for flow past a lateral outlet fitted with a barrier inclined at an arbitrary angle to the main conduit can be readily used.

APPENDIX I - REFERENCES

APPENDIX I. REFERENCES

1. Ackers, P., " A Theoretical Consideration of Side Weirs as Storm-Water Overflows," Proceedings, Institution of Civil Engineers, London, Vol. 6, pp. 250-269, Feb., 1957.

2. Allen, J. W., " The Discharge of Water over Side Weirs in Circular Pipes," Proceedings, Institution of Civil Engineers, London, Vol. 6, pp. 270-287, Feb. 1957.

3. Bajura, R. A., " A Model for Flow Distribution in Manifolds," ASME Journal of Engineering for Power, Vol. 93, pp. 7-12, Jan. 1971.

4. Benefield, L. D., Judkins, J. F., and Parr, A. D., " Treatment Plant Hydraulics for Environmental Engineers," Prentice-Hall, Inc., Englewood Cliffs, New Jeresy, 1984.

5. Berlamont, J., and Van der Beken, A., "Solutions for Lateral Outflows in Perforated Pipes", J. Hyd. Div., Proc. ASCE, No. HY9, Sept., 1973, pp. 1531-1549.

6. Brune, A. W., Graf, W. H., Appel, E., and Yee, P. P., " Performance of Pennsylvania Highway Drainage Inlets," J. of the Hyd. Div., Proc. ASCE, Vol. 101, No. HY 12, 1975, pp. 1519-1537.

7. Camp, T. R., " Lateral Spillway Channels," Transactions, ASCE, Vol.105, pp. 606-617, 1940.

8. Coleman, G. S., and Smith, D., "The Discharging Capacity of Side Weirs," Institution of Civil Engineers, London, Selected Engineering Papers, No. 6, 1923.

9. Collinge , V. K., " The Discharge of Water over Side Weirs in Circular Pipes," Proceedings, Institution of Civil Engineers, London, Vol. 6, 288-304, Feb. 1957.

10. De Marchi, G., " Saggio di Teoria del Funzionamento degli Stramazzi Laterali " (Essay of the Performance of Lateral Weirs), L'Energia elettrica, Milano, vol. 15, no. 9, pp. 583-595, Sep. 1983; reprinted as Istituto di Idraulica e Costruzioni Idrauliche, Milano, Memorie e studi, No. 65, 1938.

11. El- Khashab, A., and Smith, K. V. H., " Experimental Investigation of Flow over Side Weirs," Journal of Hydraulics Division, ASCE, Vol. 102, 1976.

12. Engles, H., " Mitteilungen aus dem Dresdener Flussbau-Laboratorium (Report of the Dresden Hydraulic Laboratory), Zeitschrift des Vereins Deutscher Ingenieure, Berlin, Vol. 62, no. 24, pp. 362-365, Jun. 22;, no. 26, pp. 412-416, Jun. 29, 1918, and Vol. 64, no. 5, pp. 101-106, Jan. 1920; also Forschungsarbeiten auf dem Gebiete des Ingenieurwesens, Berlin, Nos. 200 and 201, 55 pp., 1917.

13. Favre, H., " Contribution a l'etude des courants liquides," (Contribution to the Study of Flow of Liquids), Dunod, Paris, 1933.

14. Forchheimer, P., " Hydraulik" (Hydraulics), Teubner Verlagagesellschaft, Leipzig and Berlin, 3d ed., 1930, pp. 406-409.

15. Frazer, W., " The Behaviour of Side Weirs in Prismatic Rectangular Channels," Proceedings, Institution of Civil Engineers, London, Vol. 6, pp. 305-328, Feb. 1957.

16. French, J. A., " Internal Hydraulics of Multiport Diffusers," Journal of WPCF, Vol. 44, No. 5, May 1972, pp. 782-785.

17. Gentilini, B., " Riccerche sperimentali sugli sfioratori longitudinali " (Experimental Researches on Side Weirs), L'Energia eletrica, Milano, vol. 15, no. 9, pp. 583-595, Sep. 1983; reprinted as Istituto di Idraulica e Costruzioni Idrauliche, Milano, Memorie e studi No. 65, 1938.

18. Grace, J. L., and Priest, M. S., " Division of Flow in Open Channel Junctions," Engineering Experiment station, Alabama Polytechnic Institute Bulletin, No. 31, June 1958.

19. Hager, W. H., " An approximate treatment of Flow in Branches and Bends," Proc. Instn. Mech. Engrs., Vol. 198 C, No. 4, Nov. 1983.

20. Hinds, J.,"Side Channel Spillways: Hydraulic theory, Economic Factors, and Experimental Determination of Losses," Transactions, ASCE vol. 89, pp. 881-927, 1926.

21. Hudson, H. E., Jr., Uhler, R. B., and Bailey, R. W., " Dividing -Flow Manifolds with Square -Edged Laterals," Journal of the Environmental Engineering Division, ASCE, Vol. 105, 1979; pp.

22. Krishnappa, G., and Seetharamiah, K., " A new method of Predicting the Flow in a 90^{o} Branch Channel," La Houille Blanche, Assn. pour la Diffusion de la Documentation of Hydraulique, Grenoble, No. 7, Nov., 1963.

23. Lakshmana Rao, N. S., and Sridharan, K.," Dividing Flow in an Open Channel," Discussion Journal of the Hydraulics Division, ASCE, Vol. 94, No. HY6, NOV., 1966, pp. 237-239.

24. Lakshmana Rao, N. S., Sridharan, K., and Baig, M. Y. A., " Experimental study of the Division of Flow in an Open Channel," Third Australasian Conference on Hydraulics and Fluid Mechanics, Sydney, paper No. 2587, Nov., 1968.

25. Law, S. W., and Reynolds, A. J., " Dividing Flow in an Open Channel," Journal of the Hydraulics Division, ASCE, Vol. 92, No. HY2, proc. paper 4730, March, 1966.

26. Law, S. W., " Dividing Flow in an Open Channel," Thesis presented to the Faculty of Graduate Studies, McGill University, Montreal, Canada, Aug., 1965.

27. Li, W. H.,"Open Channels with Nonuniform Discharge," Transactions, ASCE, vol. 120, pp. 255-274 , 1955.

28. McNown, S. J., and HSU, E. Y., " Application of Conformal Mapping in Divided Flow," Proceedings of the Midwestern Conference on Fluid MDynamics, First Conference, State University of Iowa, Reprint No. 96, pp. 143-155, 1950.

29. McNown, J. S., " Mechanics of Manifold Flow", Transactions ASCE, Vol. 119, 1954, pp. 1103-1142.

30. Metcalf and Eddy Inc., "Waste Water Engineering," Edn. 1, McGraw-Hill, 1972.

31. Milne-Thomson, M., " Theoretical Hydrodynamics," MacMillan and Co. Ltd., 1949.

32. Mitchell, J. M., " On the Theory of Free Stream Lines," Philosophical Transactions of the Royal Society , London, Vol. A, 81, 1890, pp. 389-431.

33. Mostkow, M. A. "Handbuch der Hydraulik," (Handbook of Hydraulics), VEB Verlag Technik, Berlin, 1956, pp. 204-208 and 213-221.

34. Mostkow, M. A.," Sur le calcul des grilles de prise d'eau (Theoretical study of Bottom Type Water Intake), La Houille blanche, Grenoble, 12th yr., no.4, pp. 570-580, Sep. 1957.

35. Murota, A., "On the Flow characteristics of a channel with a Distributory", Technology Reports of the Osaka University, Vol. 6, No. 198, 1958.

36. Nasser, M. S., Venkataraman, P., and Ramamurthy, A. S., " Flow in a channel with A slot in the Bed," Journal of Hydraulic Research, No. 4, 1980.

37. Nasser, M. S., Venkataraman, P., and Ramamurthy, A. S., " Curvature corrections in Open Channel Flow," Canadian Journal of Civil Engineering, Vol. 7, Sept. 1980, pp. 421-431.

38. Nece. R. E., " Divided Flow in Channels with Bottom Openings," Discussion, Journal of Hydraulic Division, Proceedings of ASCE, Vol. 103, No. HY11, Nov. 1977.

39. Nimmo, W. H. R., " Side Spillways for Regulating Diversion Canals," Transactions, ASCE, vol. 92, pp. 1561-1584, 1928.

40. Noseda, G.," Operation and Design of Bottom Intake Racks," Proceedings of the 6th General Meeting International Association of Hydraulic Research, The Hague 1955, Vol. 3, pp. C17-1 to C17-11, 1955; reprinted as Istituto di Idraulica e Costruzioni Idrauliche, Milano, Memorie e studi No. 130, 1956.

41. Pattabhiramiah, K. R., " Some characteristics of Branch Channel Flow," Thesis presented to the Indian Institute of Science, Bangalore, India, in partial fulfillment of the requirements for the degree of Master of Science, 1960.

42. Pattabhiramiah, D. R., and Rajaratnam, N., "A new Method to predict Flow in a Branch Channel," Journal of the Central Board of Irrigation and Power, Vol. 17, No. 1, Jan., 1960, pp 48.

43. Rajaratnam, N., " Constant Velocity concept for supercritical Branch Channel Flow," Journal of the Central Board of Irrigation and power, Vol. 19, No. 1, Jan. 1967, p. 17.

44. Ramamurthy, A. S., and Carballada, L., " Two Dimensional Lateral Flow Past a Barrier, " Journal of the Fluids Engineering, ASME, Vol. 101, No. 4, Mar., 1979, pp 449 - 452.

45. Ramamurthy, A. S., and Carballada, L., " Lateral Weir Flow Model," Journal of the Irrigation and Drainage, Proceedings, ASCE, March 1980. pp. 9-25

46. Ramamurthy, A. S., Satish, M. G., " On the Design of Multiport Diffusers; " Canadian Society of Civil Engineers Annual Conference, Montreal, Canada, 1979.

47. Ramamurthy, A. S., and Satish, M. G., " Discharge Characteristics of Flow past a Transverse Floor Slot," Journal of Irrigation and Drainage Engineering, ASCE, Vol. 112, No. 1, Feb, 1986, pp. 20 - 27.

48. Ramamurthy, A. S., and Satish, M. G., " Division of Flow in Open Channel Branches," Journal of Hydraulics, ASCE, 1985 (sent for publication).

49. Ramamurthy, A. S., and Satish, M. G., " Multiport Diffusers with Constant Lateral Momentum Distribution," Journal of Environmental Engineering, ASCE, 1985 (sent with minor revisions for publication).

50. Ramamurthy , A.,S., and Tran, D.,V., " Studies on Combining Flows in Branch Channels" Internal Report, In5 , , Department of Civil Engineering, Concordia University, Montreal, Canada, 1976.

51. Rawn, A: M., Bowerman, F. R., and Brooks, N. H., " Diffusers for Disposal of Sewage in Sea Water," Journal of the Sanitary Engineering Division, ASCE, Vol. 86, SA2, March, 1960, pp. 65-105.

52. Robillard, L., and Ramamurthy, A. S., " Experimental Investigation of the Vortex Street Generated by a Plane Jet in a Counter Flow," J. Fluids Engg. ASME, (96,1), March, 1974, pp. 43-48.

53. Satish, M. G., and Ramamurthy, A. S., " Multiport Discharge Diffusers- an Experimental Study," Fifteenth Canadian Symposium on Water Pollution Research, C.S.C.E. Sherbrooke, Canada, Dec. 1979.

54. Satish, M. G., and Ramamurthy, A. S., " A Note on Multiport Diffusers," XIX International Association of Hydraulic Research Congress. New Delhi, India, Feb. 19

55. Satish, M. G., and Ramamurthy, A. S., " Spatially Varied Diverging Flows in Open Channels," Journal of Environmental Engineering, ASCE, 1986 (sent for publication).

56. Satish, M. G., Ramamurthy, A. S., and Vo Diep, " Characteristics of Flow Past a Transverse Floor Slot in an Open Channel Floor," Canadian Society of Civil Engineers Annual Conference, Toronto, Canada, May 1986.

57. Schlichting, H., " Boundary Layer Theory," 7th ed. New York, McGraw-Hill, 1979.

58. Schmidt, M.," Gerinnehydraulik" (Open channel Hydraulics), VEB Verag Technik, Berlin and Bauverlag GMBH, Weisbaden, 1957, pp. 188-196.

59. Sridharan, K., and Lakshmana Rao, N. S., " Division and Combination of Flow in Open Channels," Journal of the Institute of Engineers, India, Civil Engineering Division, Vol. 46, No. 7, March 1966, p. 337.

60. Sridharan, K., " Division of Flow in Open Channels," Thesis presented to the Indian Institute of Science, Bangalore, India, in partial fulfillment of the requirements for the degree of Master of Science, Nov., 1966.

61. Tanaka, K., " The improvement of the Inlet of the Power Canal," Transactions of the Seventh General Meeting of I.A.H.R., Lisbon, Vol. 1, 1957, Jan. 1967, p. 17.

62. Taylor, E., " Flow characteristics at Rectangular Open Channel Junctions," Transactions, ASCE, Vol. 109, 1944.

63. Townsend, R. D., " Laboratory Tests on the Influence of Grating Pattern on Street Inlet Hydraulics," Proceedings of C.S.C.E., Annual Conference, Halifax, Canada, Vol. 11, May, 1984, pp. 685-693.

64. Tsakonas, S., " Divided Flow through a Divergent Inlet Conduilt," Journal of the Hydraulics Division, ASCE, Vol. 83, No. HY6, Dec., 1957, pp. 148-174.

65. Venkataraman, P., " Divided Flow in Channels with Bottom Openings," Journal of Hydraulics Division, Proceedings of ASCE, Vol. 103, No. HY2, Feb. 1977, pp. 190-194.

66. Venkataraman, P., " Spatially varied Flow in Open Channels," Ph.D Thesis, Dept. of Civil Engineering, Venkateshwara University, Tirupati, India, 1978.

67. Vigander, S., Elder, R. A., and Brooks, N. H., " Internal Hydraulics of Thermal Diffusers," J. Hyd. Div., ASCE, HY2, Feb. 1970, pp. 509-527.

68. White, J. K., Charlton, J. A., and Ramsay, C. A. W., " On the Design of Bottom Intakes for Diverting Stream Flows, " Proc. Institution of Civil Engineers, London, Vol. 51, 1972, pp. 337-345.

69. Yen, B. C., and Wenzel, H. G.," Dynamic Equations For Spatially Varied Flow," Journal of Hydraulics Division, ASCE, Vol. 96, 1970.

70. Zeisser, M. H., " Summary Report of Single-Tube Branch and Multi-Tube Branch Water Flow Tests Conducted by the University of Connecticut," Pratt and Whitney Aircraft Division, United Aircraft Corporation; Report No. PWAC-231 USAEC Contract AT(11-1) -229 May, 1963.

APPENDIX II - FIGURES

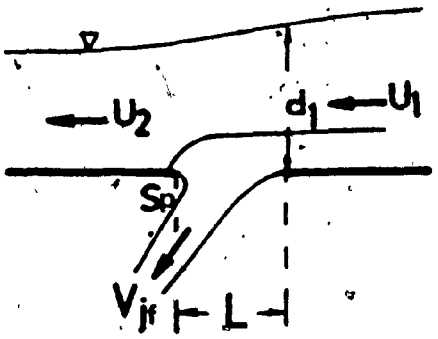

Fig.1(a) Open Channel Flow Past A Floor Outlet

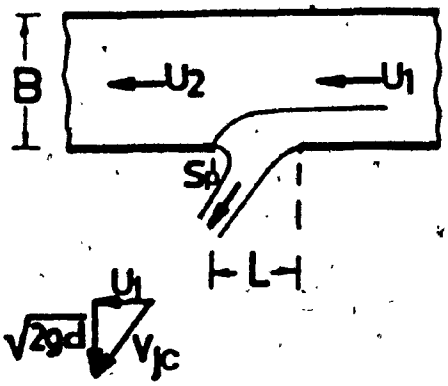

Fig.1(b) Efflux through a Lateral Outlet in a 2D- Conduit

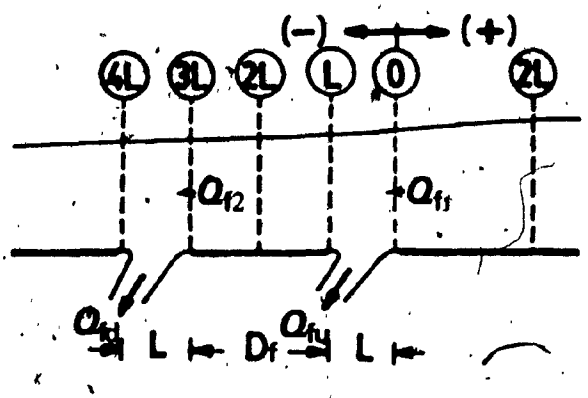

Fig.1(c) Open Channel Flow Past a Multiple Floor Outlet System

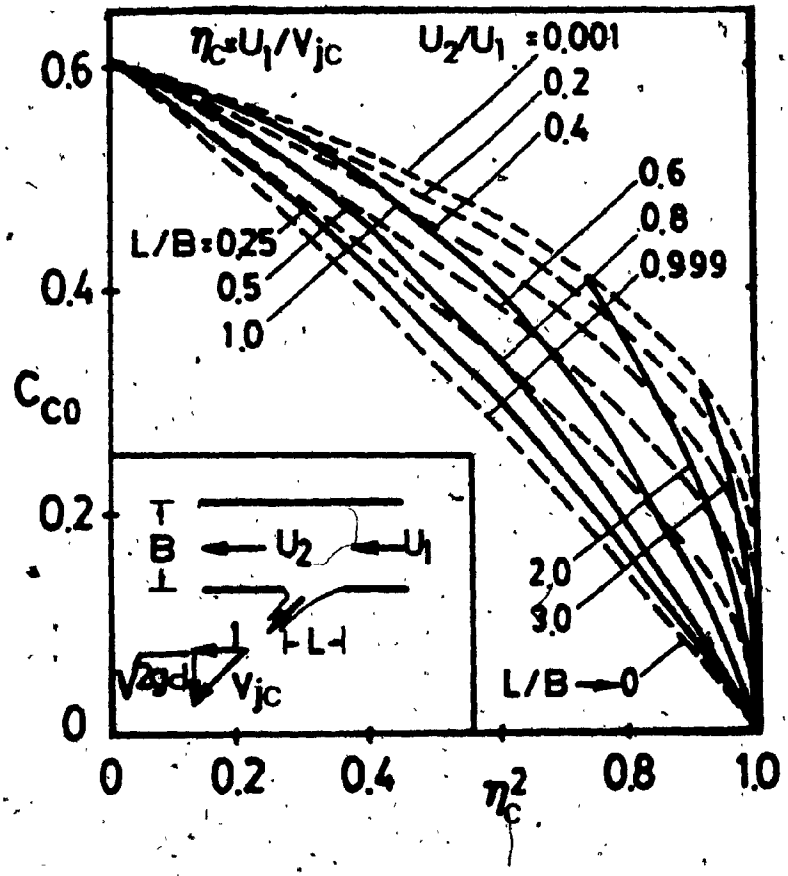

Fig.2. Variation of the contraction coefficient C_{co} as a function of η_c^2, L / B and U_2 / U_1 for an outlet in a 2D- conduit

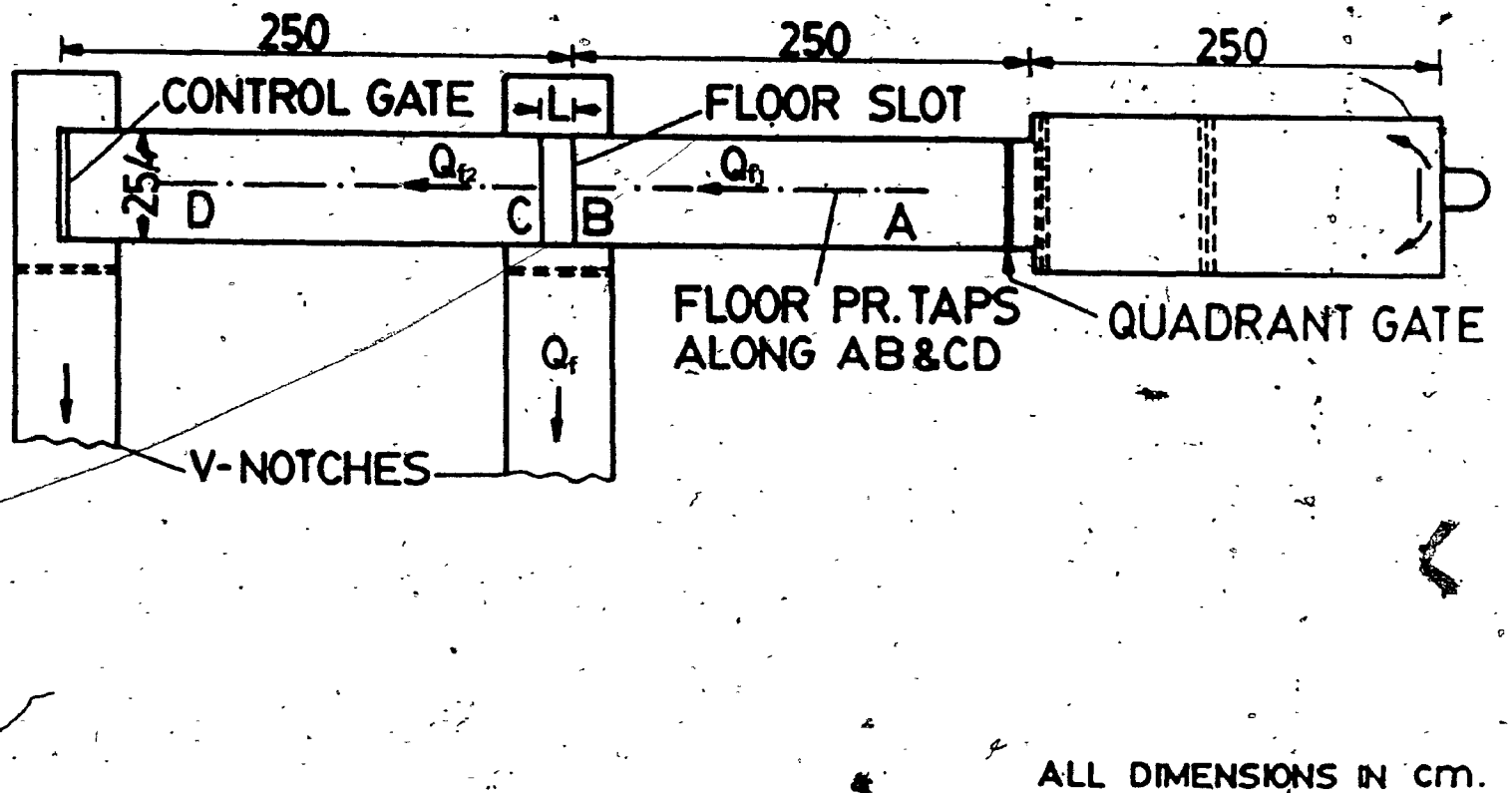

Fig.3. Experimental Set-up: Open Channel Flow Past Floor outlets

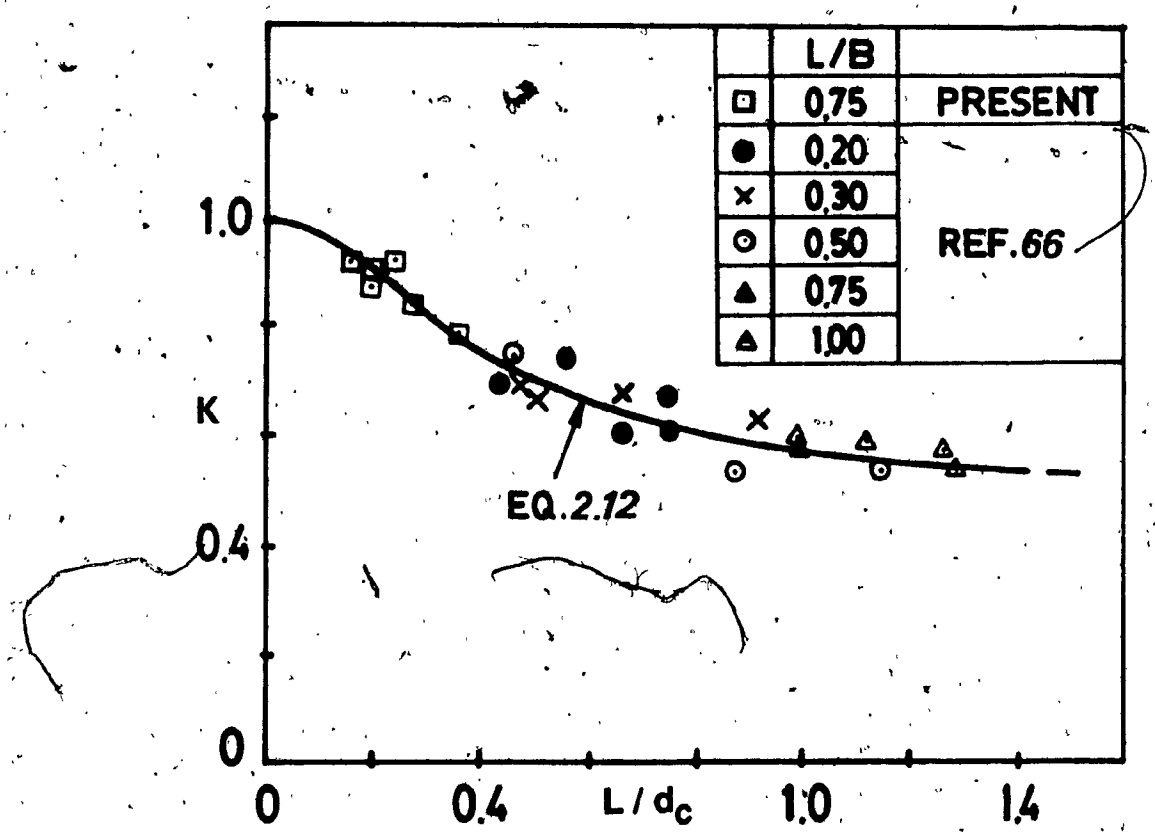

Fig.4 Variation of pressure correction coefficient K and L / d_c with L / B as the group parameter.

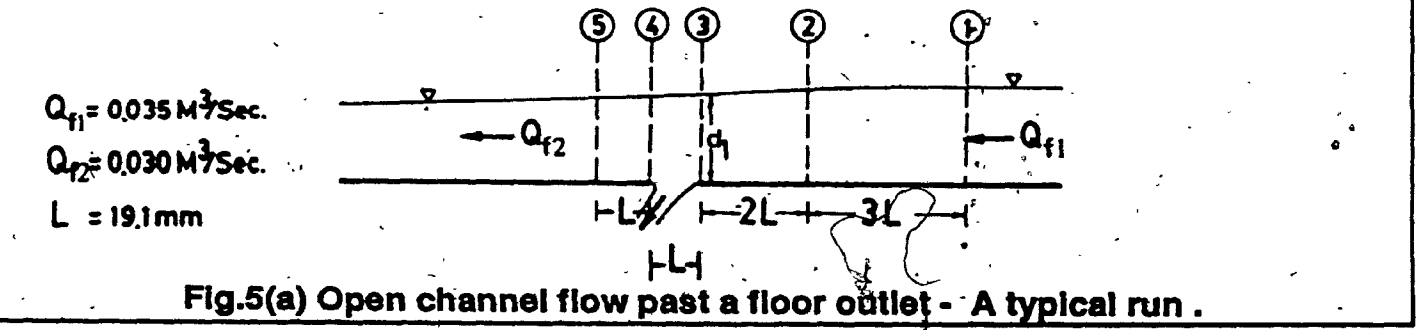

Fig.5(a) Open channel flow past a floor outlet - A typical run .

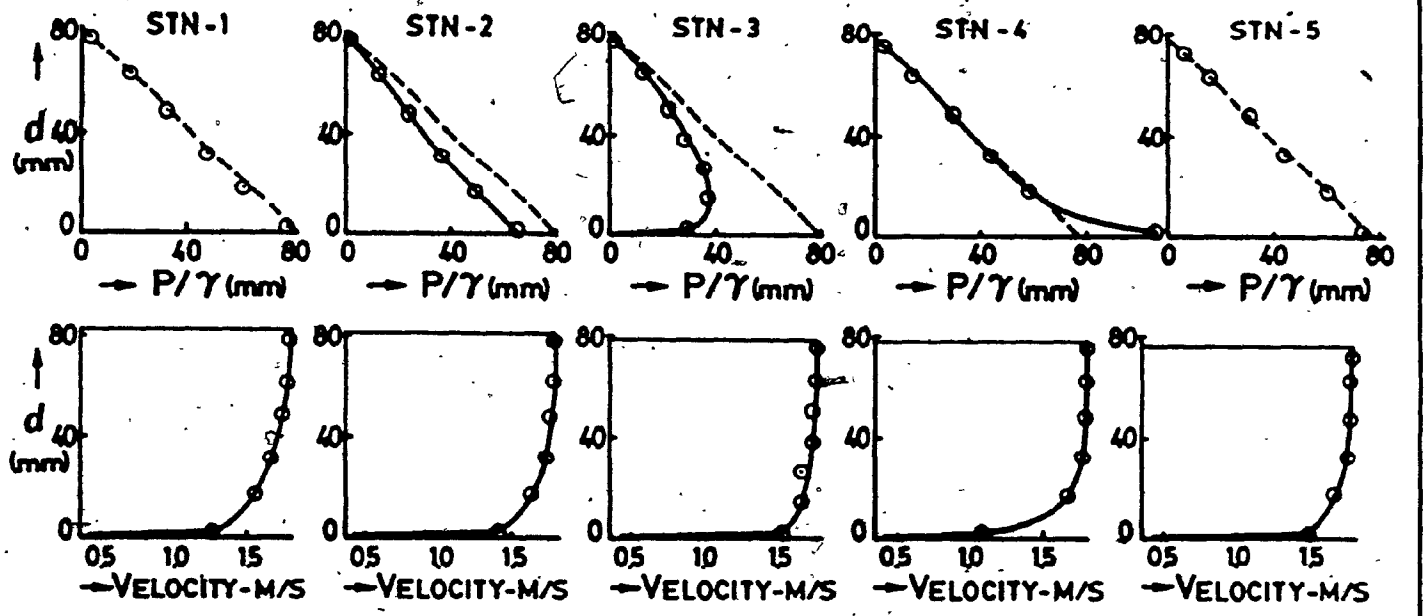

Fig.5(b) Typical Velocity and pressure profiles along the main flow shown in Fig. 5(a)

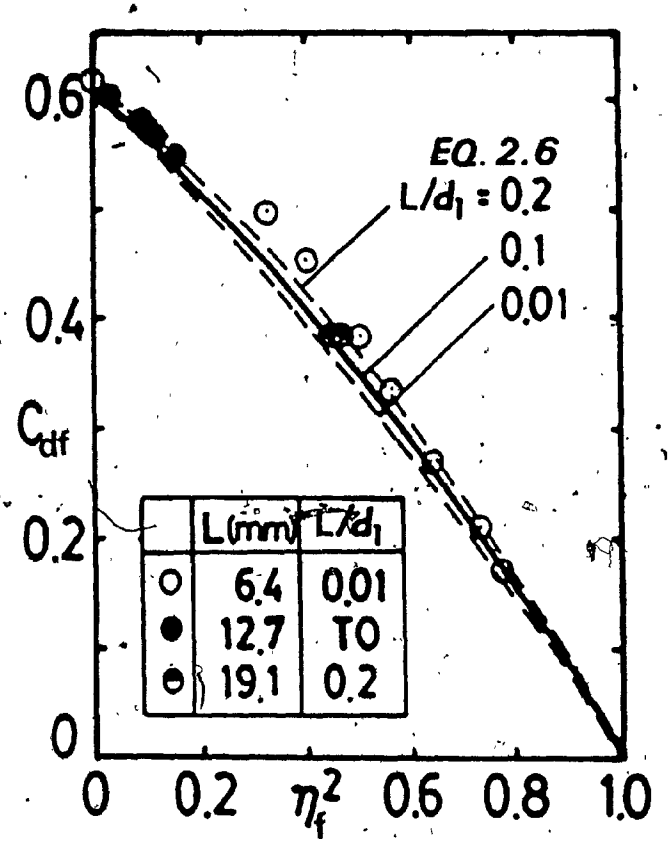

Fig.6 Relationship between Floor outlet discharge coefficient C_{df} and η_f^2 for L / d_1 = 0.01 to 0.2.

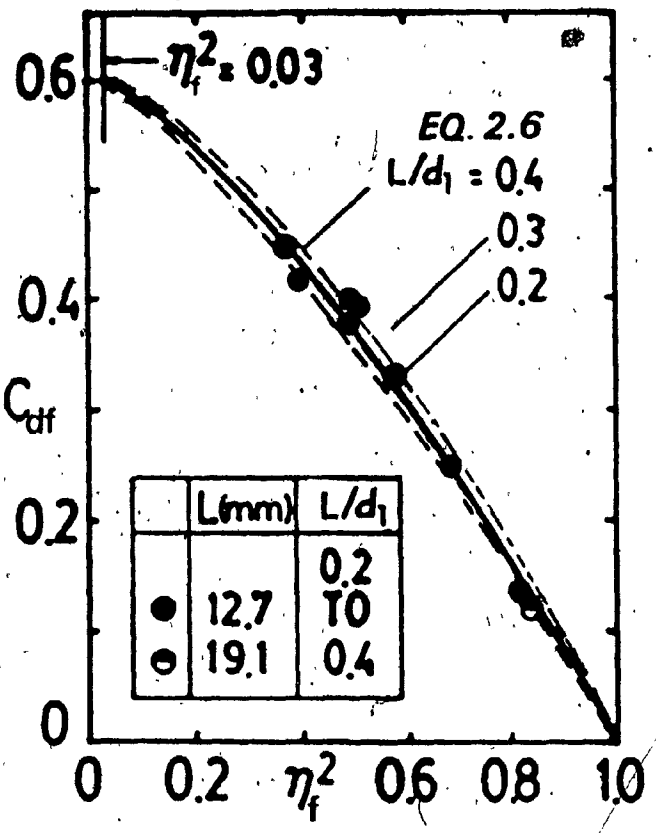

Fig.7 Relationship between Floor outlet discharge coefficient C_{df} and η_f^2 for L / d_1 = 0.2 to 0.4.

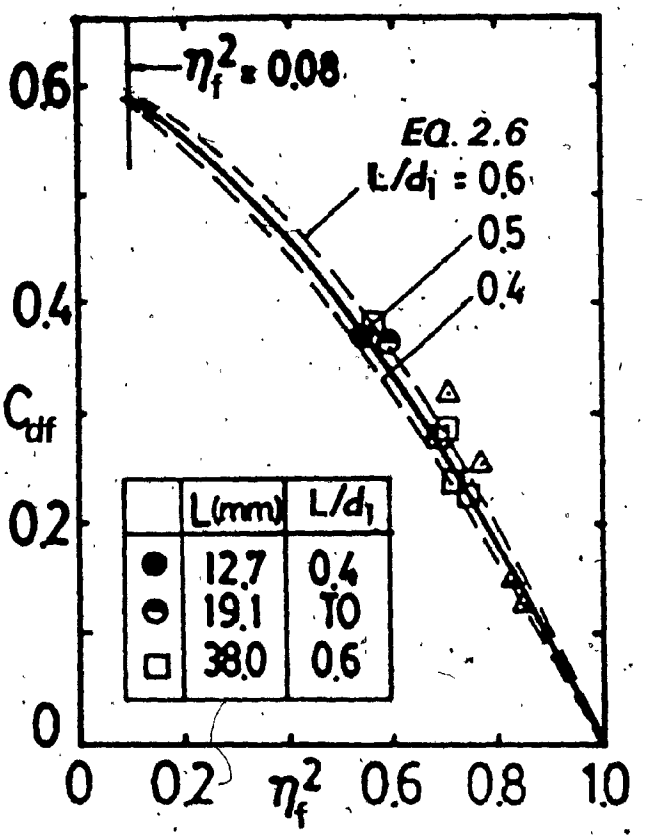

Fig.8 Relationship between Floor outlet discharge coefficient C_{df} and η_f^2 for $L / d_1 = 0.4$ to 0.6.

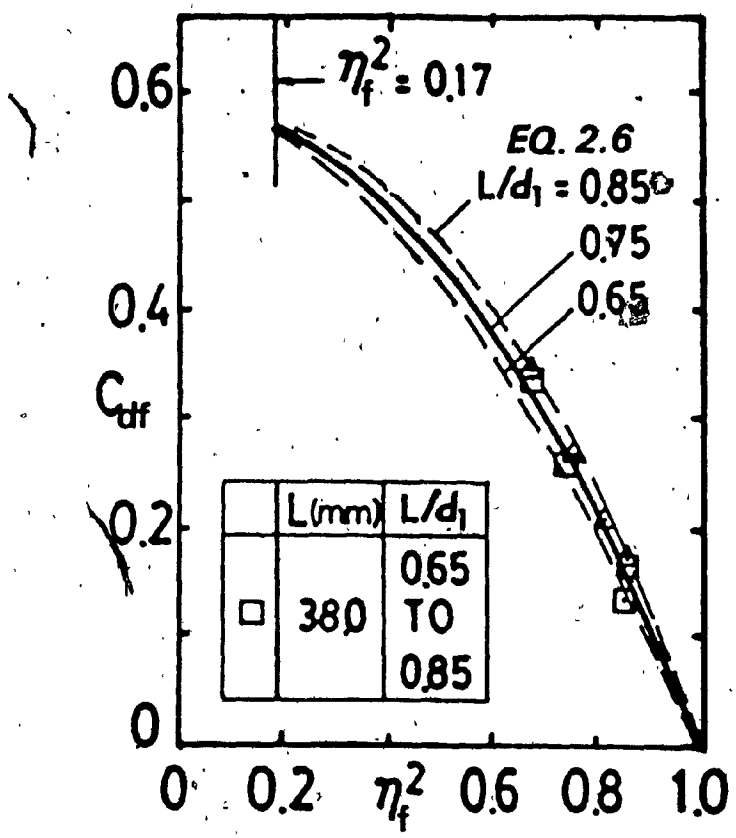

Fig.9 Relationship between Floor outlet discharge coefficient C_{df} and η_f^2 for $L / d_1 = 0.65$ to 0.85

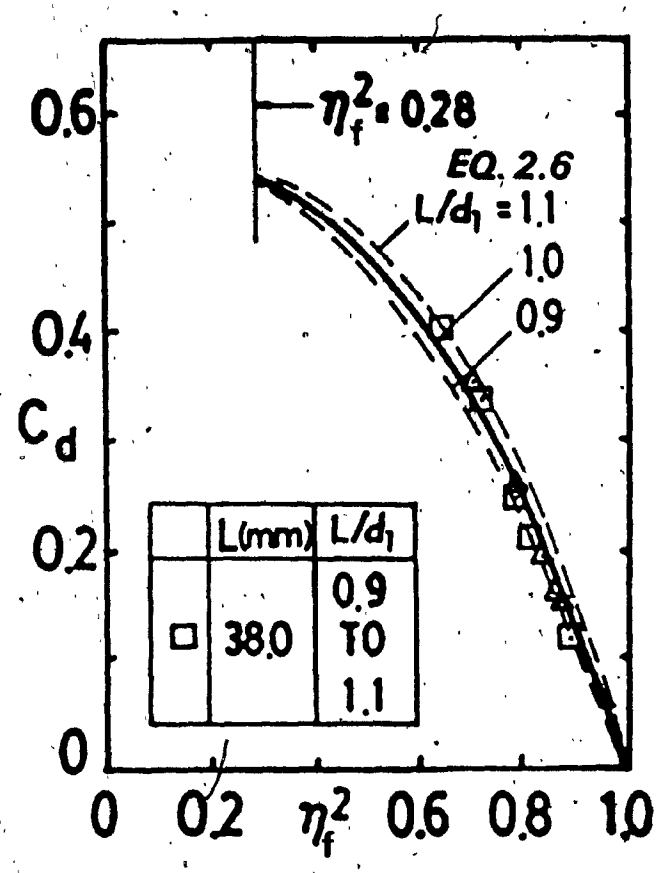

Fig.10 Relationship between Floor outlet discharge coefficient C_{df} and η_f^2 for L / d_1 = 0.90 to1.10

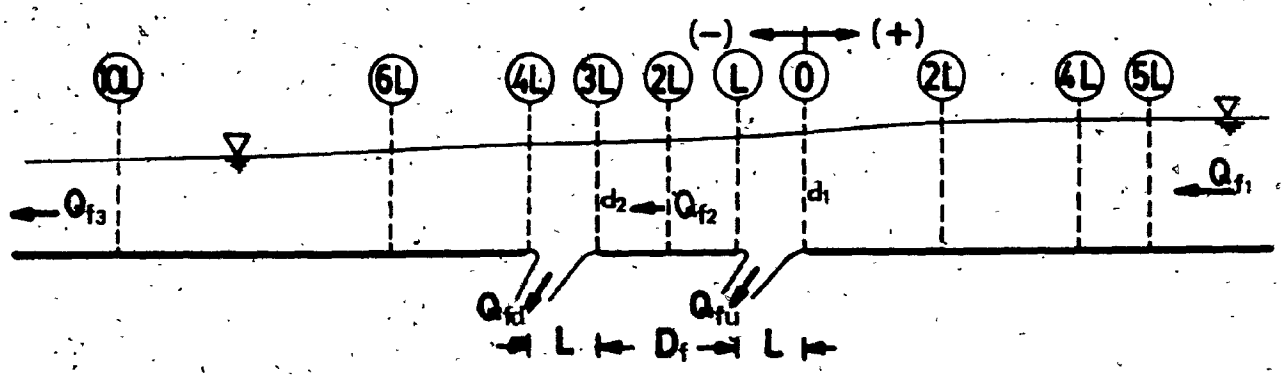

Fig.11(a) **Open channel flow past a two floor outlet system - a typical run .**

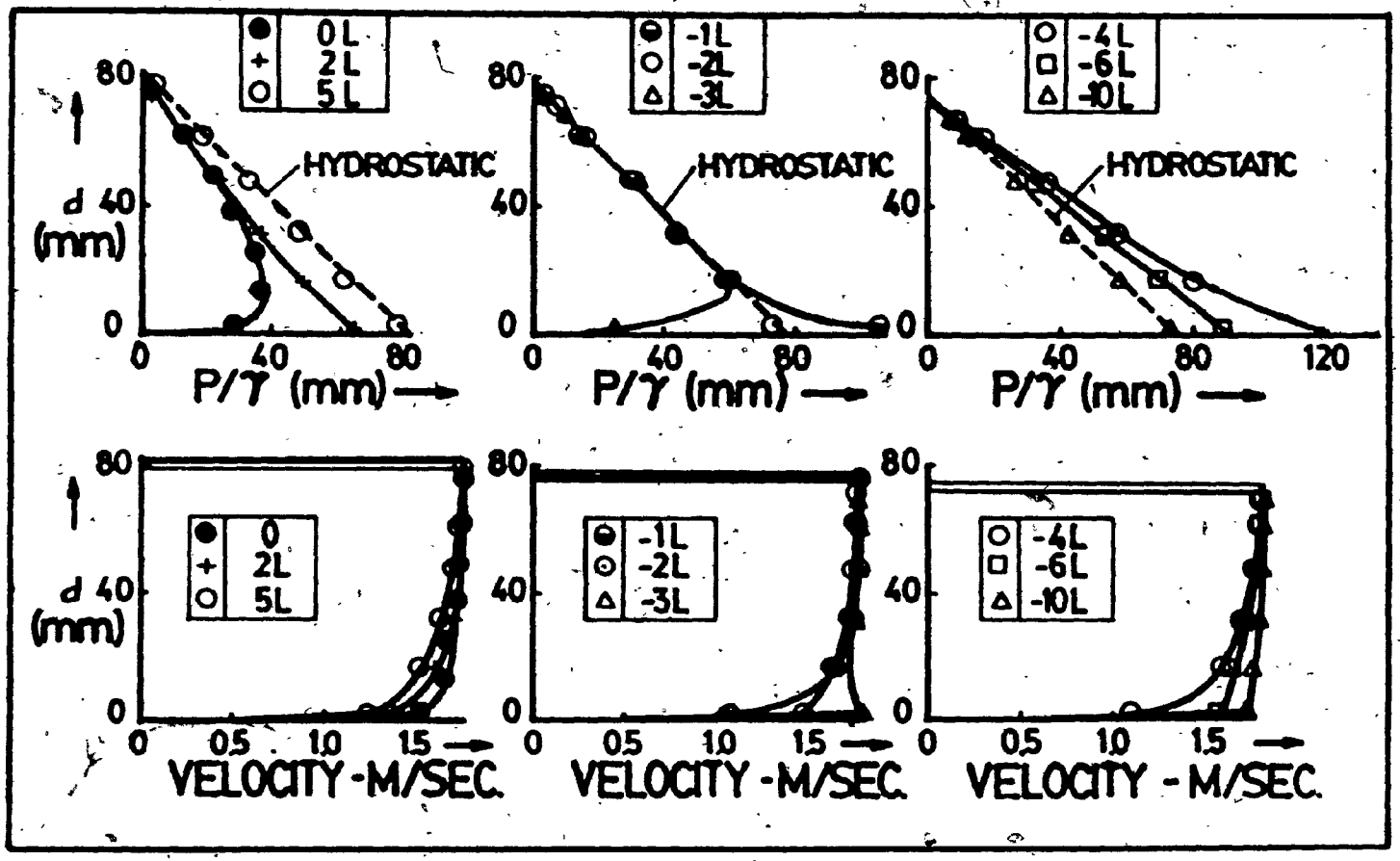

Fig.11(b) Typical velocity and pressure profiles for the flow system in Fig. 11(a) .

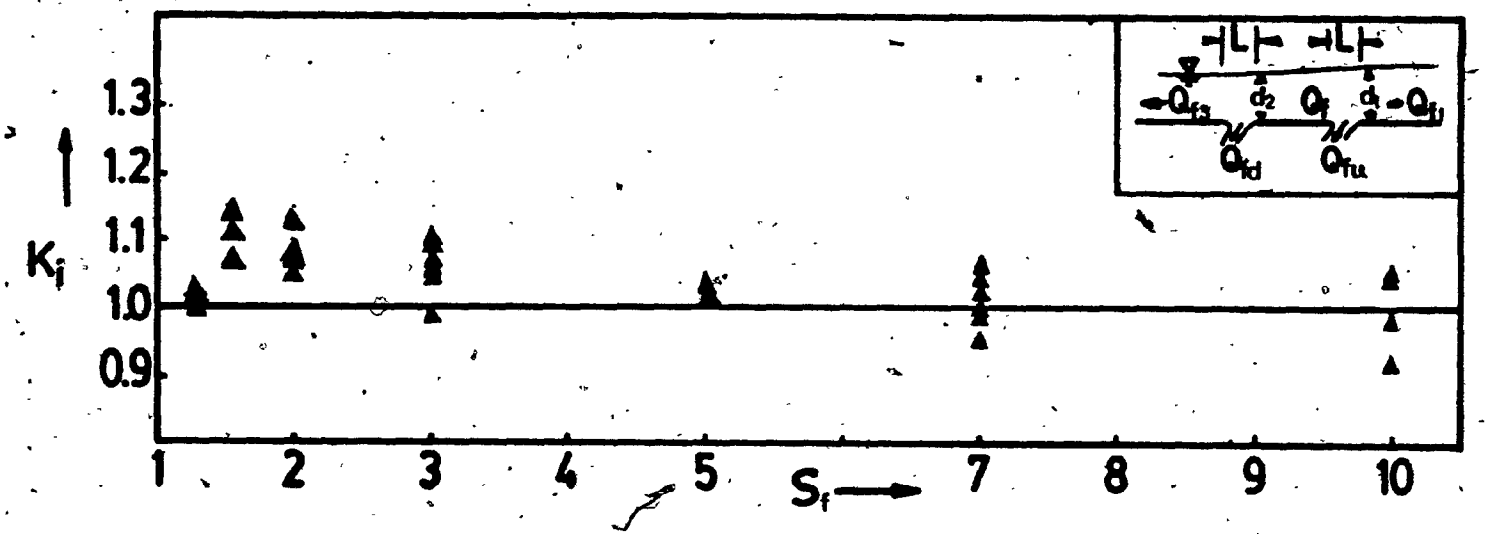

Fig.12 Variation of interference factor K_i with the outlet spacing coefficient S_f.

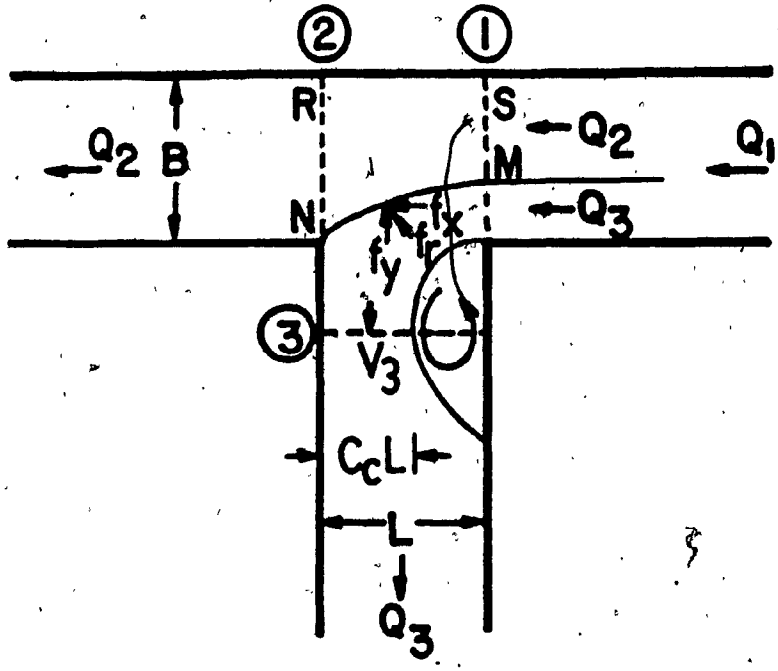

Fig.13 Definition sketch - Division of flow in a branch channel

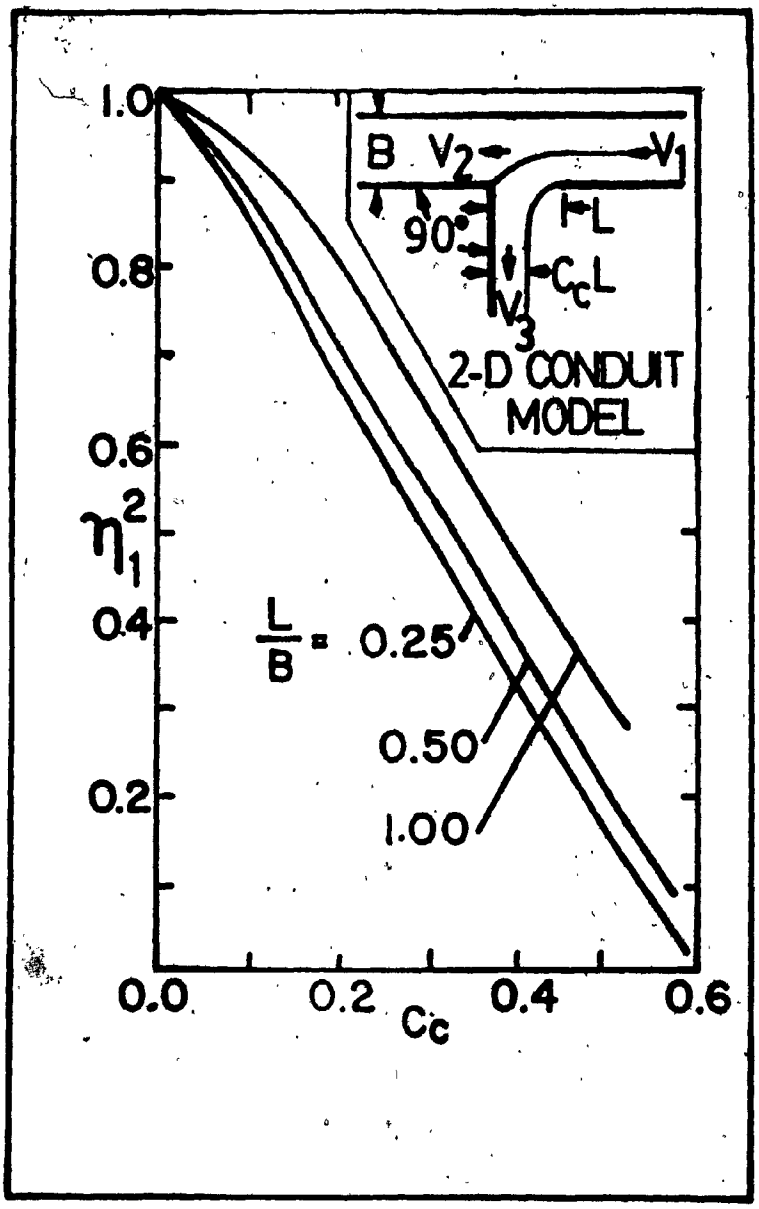

Fig.14 Variation of branch channel contraction coefficient C_c with η_1^2 and L/B for a 2D - Conduit fitted with a barrier.

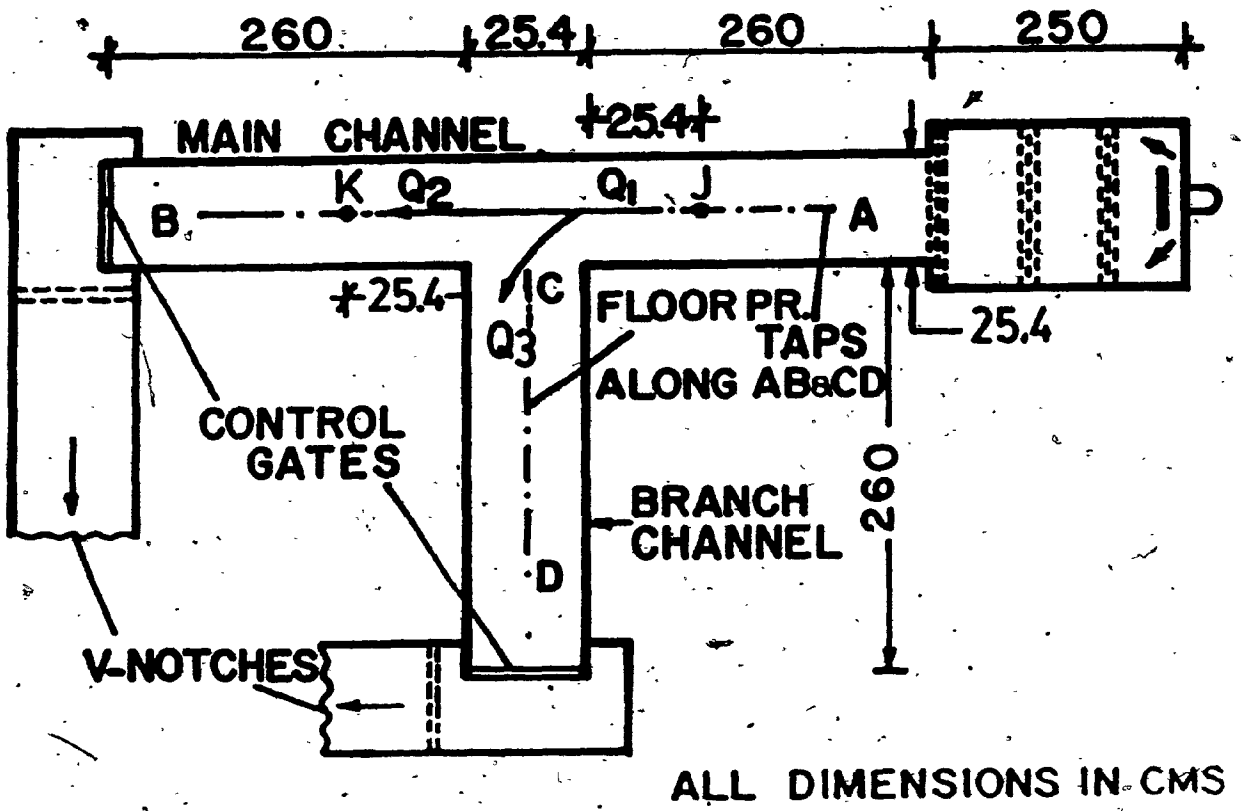

Fig.15 Experimental Set-Up : Division of flow in a branch channel

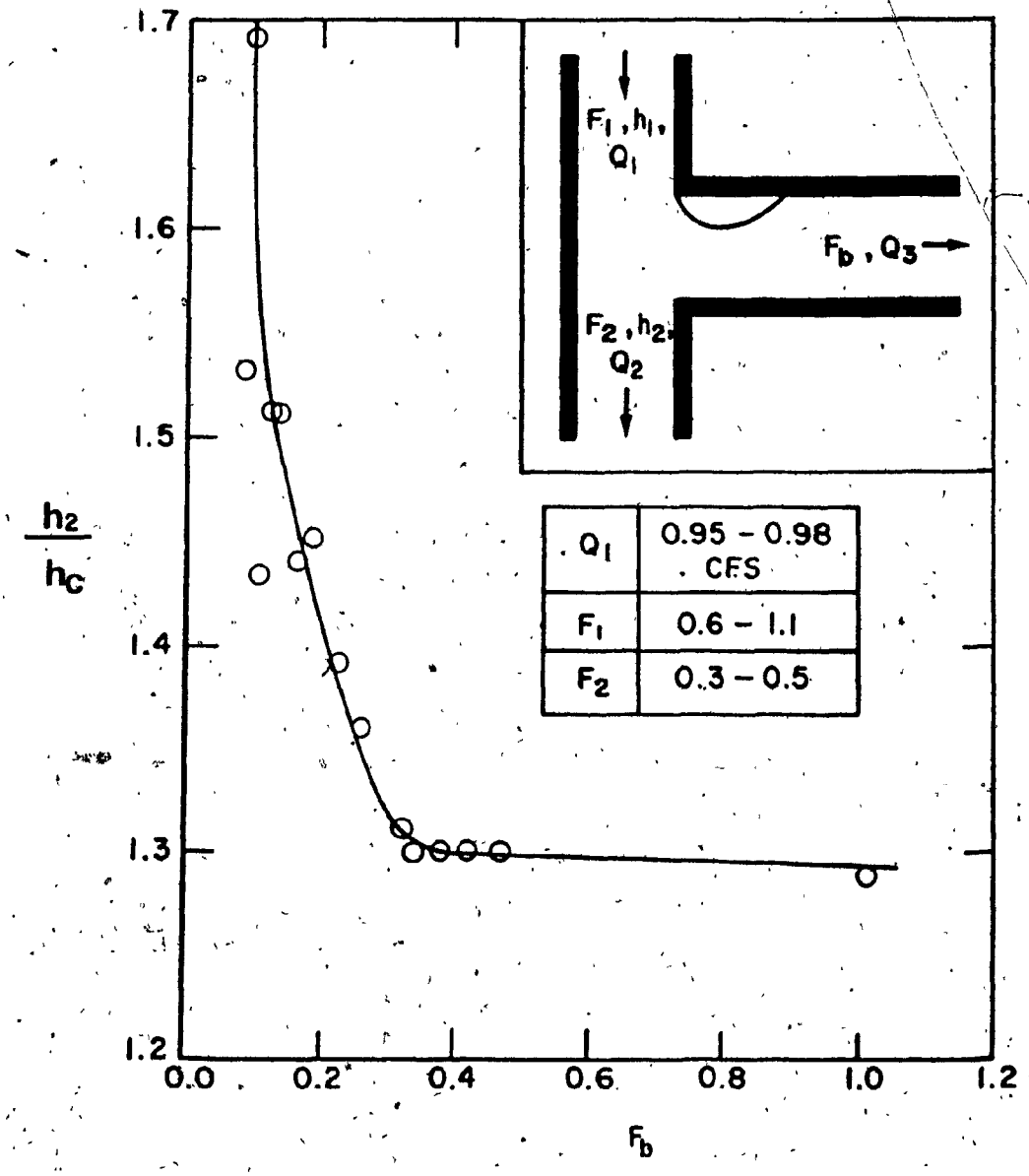

Fig.16 Variation of h_2/h_c with the branch channel Froude number F_b

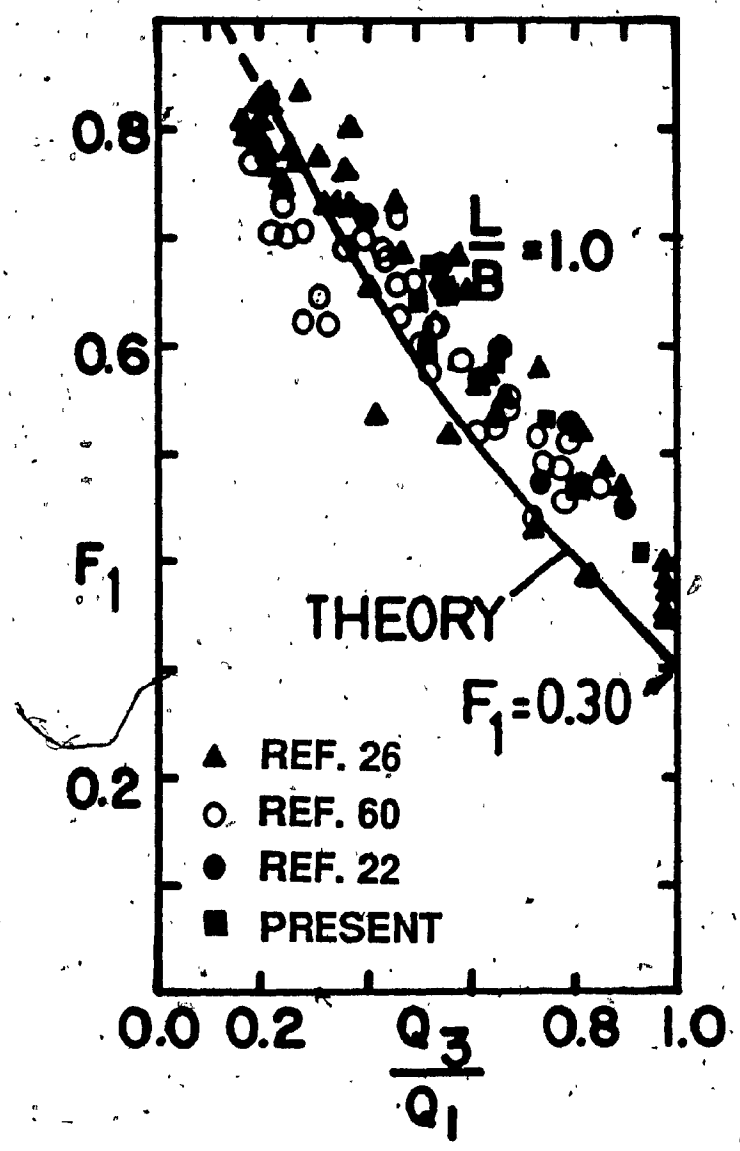

Fig.17 Analytical and experimental variation of the discharge ratio Q_3/Q_1 with the upstream Froude number F_1 for $L/B = 1.0$

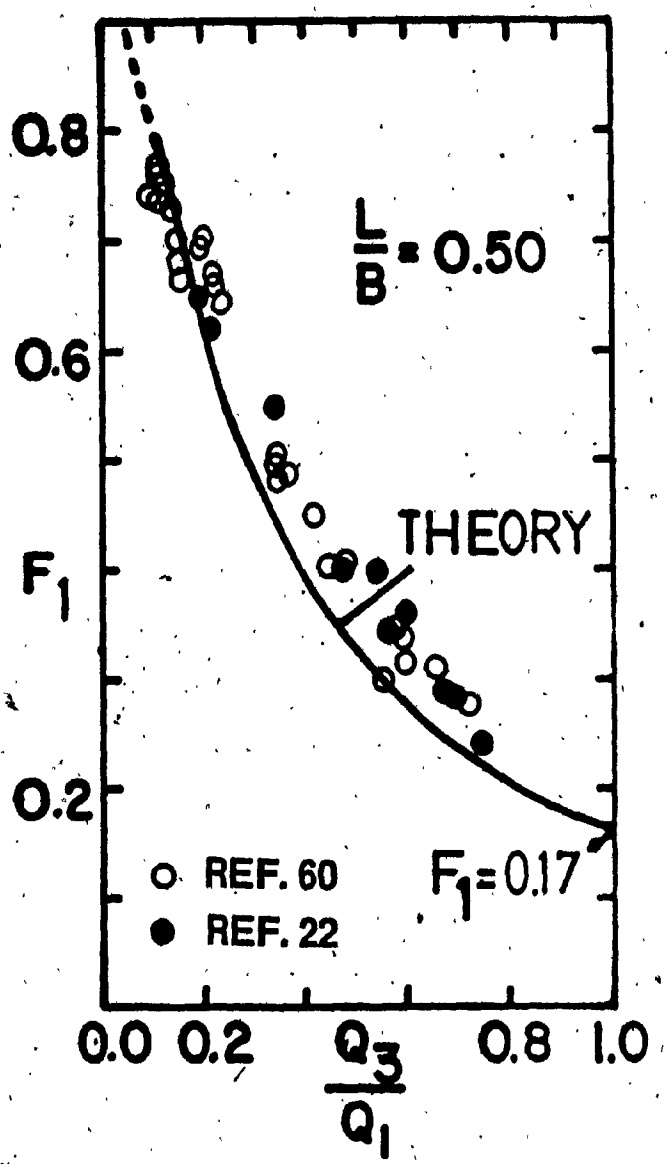

Fig.18 Analytical and experimental variation of the discharge ratio Q_3/Q_1 with the upstream Froude number F_1 for L / B = 0.50

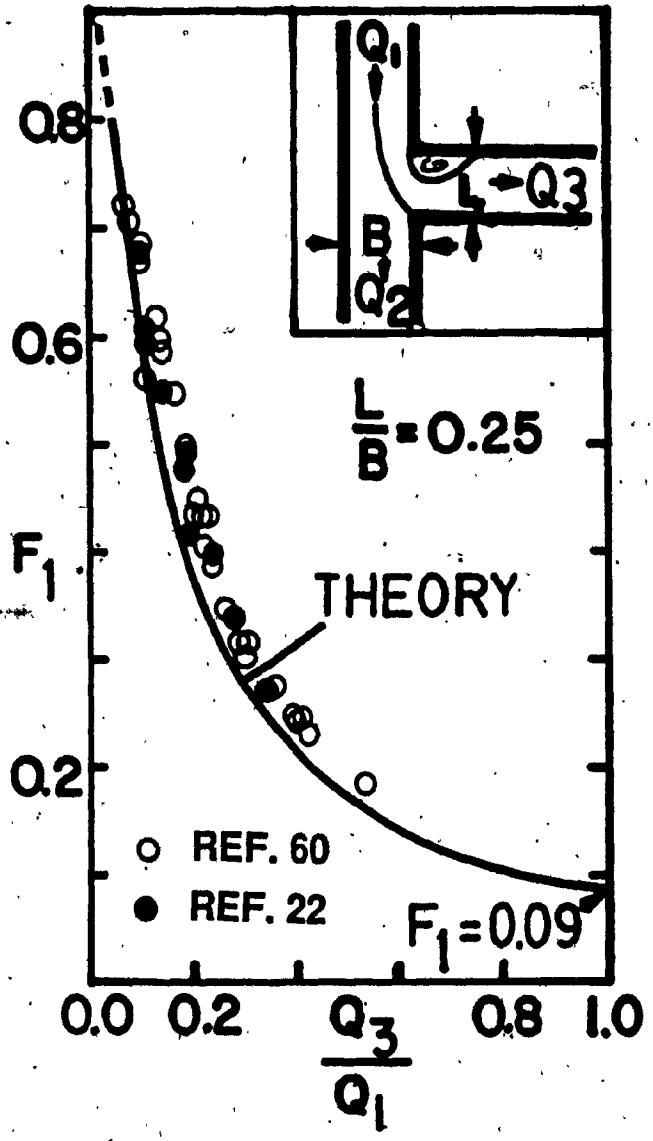

Fig.19 Analytical and experimental variation of the discharge ratio Q_3/Q_1 with the upstream Froude number F_1 for $L/B = 0.25$

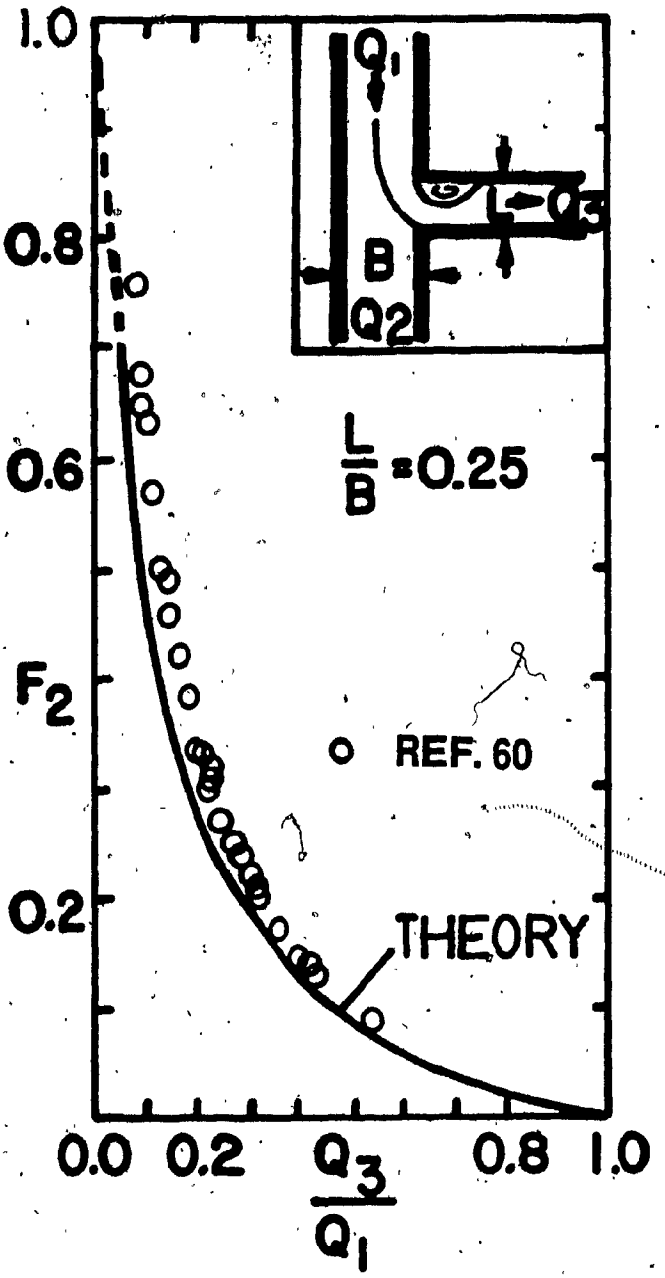

Fig.20 Analytical and experimental variation of the discharge ratio Q_3/Q_1 with the downstream Froude number F_2 for L / B = 0.25

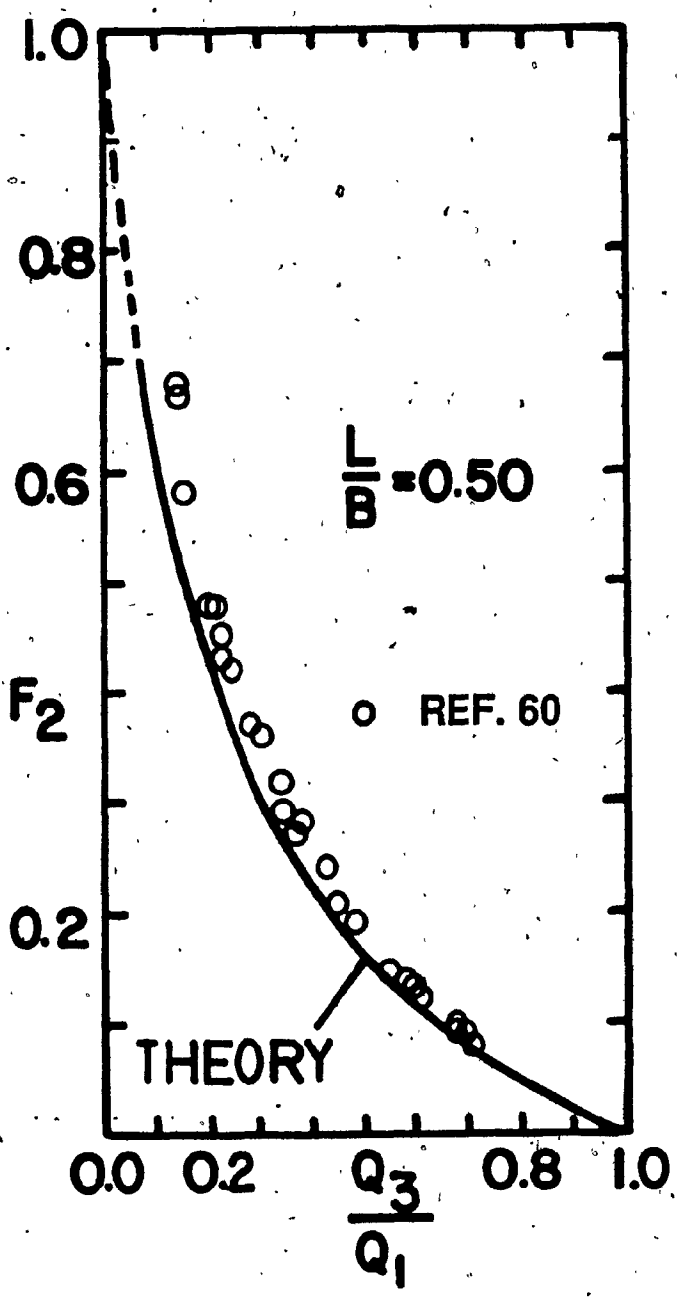

Fig.21 Analytical and experimental variation of the discharge ratio Q_3/Q_1 with the downstream Froude number F_2 for L / B = 0.50

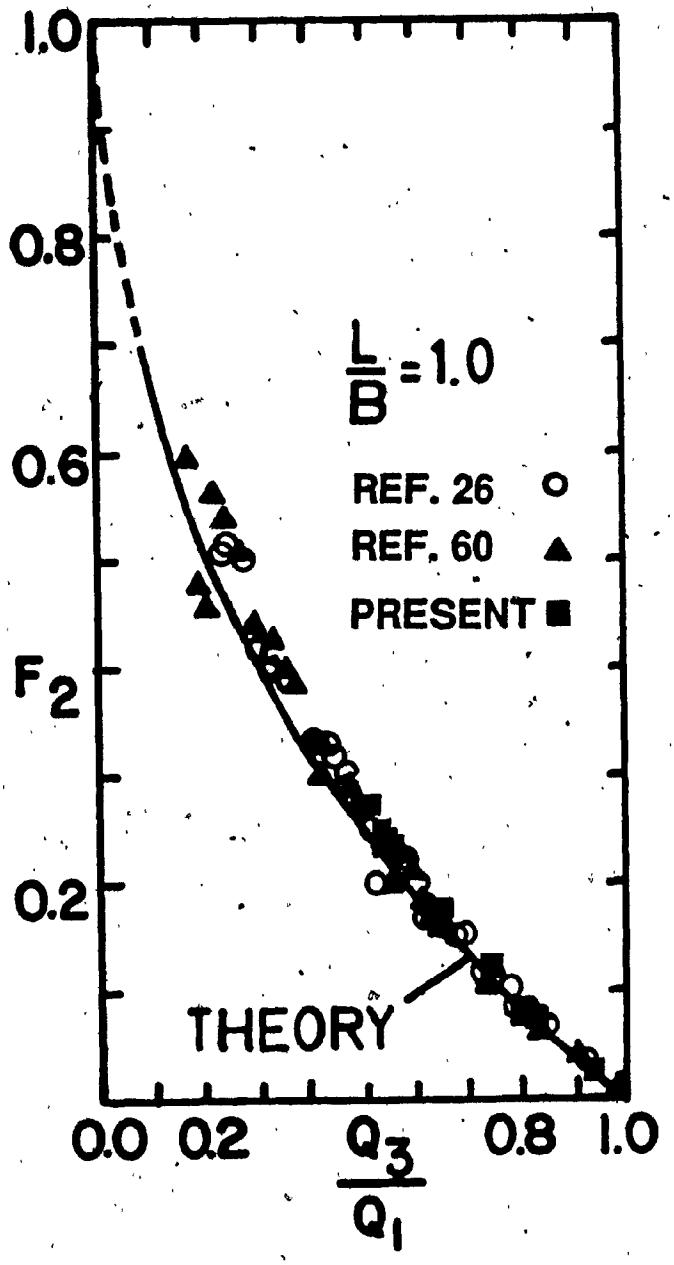

Fig.22 Analytical and experimental variation of the discharge ratio Q_3/Q_1 with the downstream Froude number F_2 for L / B = 1.0

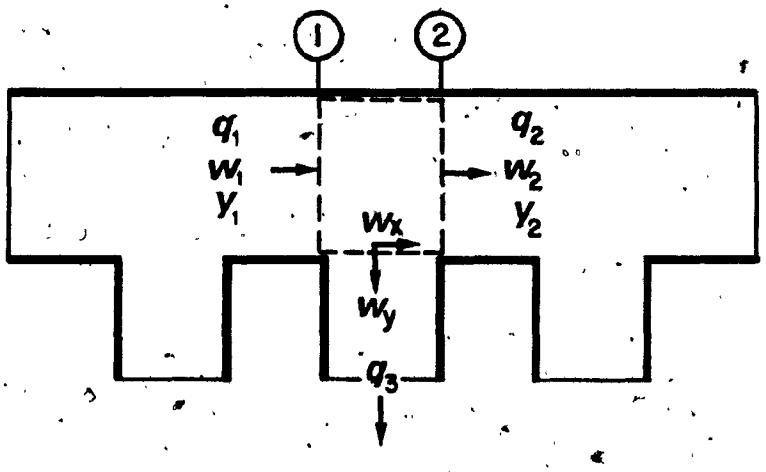

Fig.23(a) Flow in a branch channel manifold system

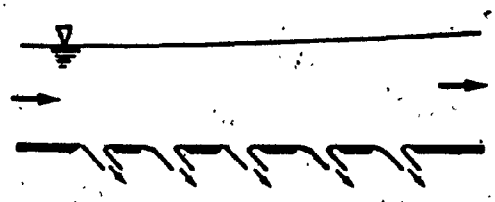

Fig.23(b) Flow past a system of floor outlets

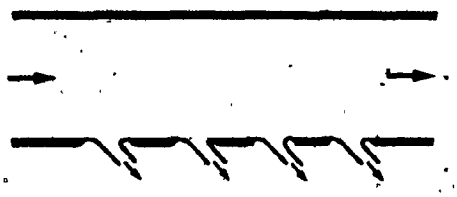

Fig.23(c) Flow past a battery of side weirs

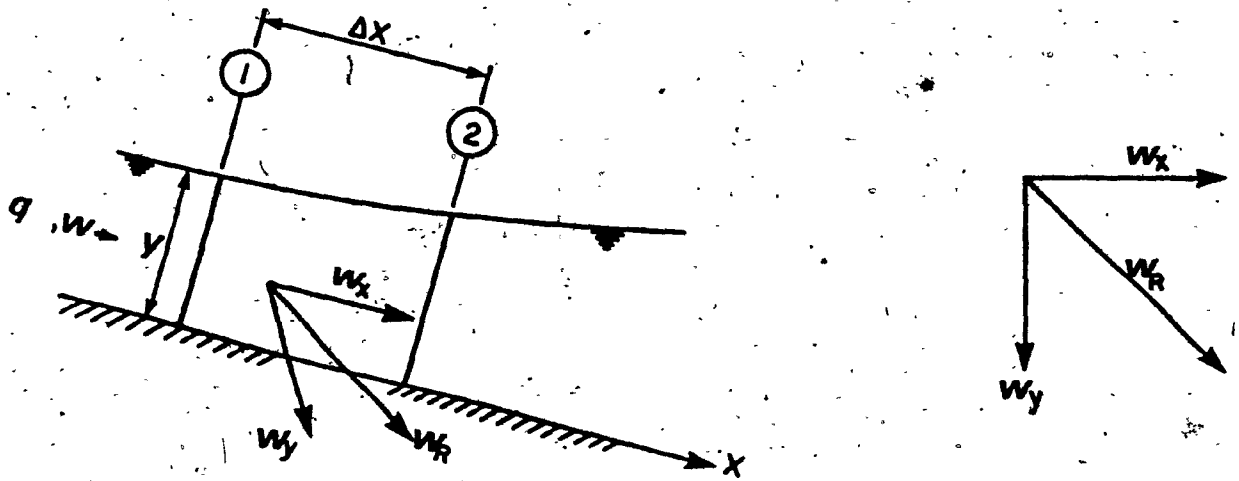

Fig.24 Definition sketch - Spatially varied diverging lateral flows

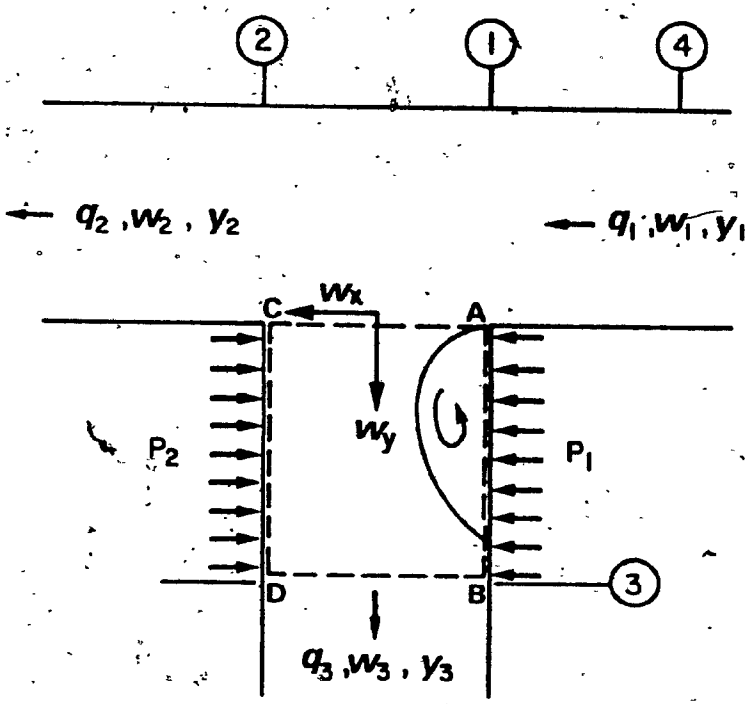

Fig.25(a) Flow past an open channel branch - Control volume in the branch

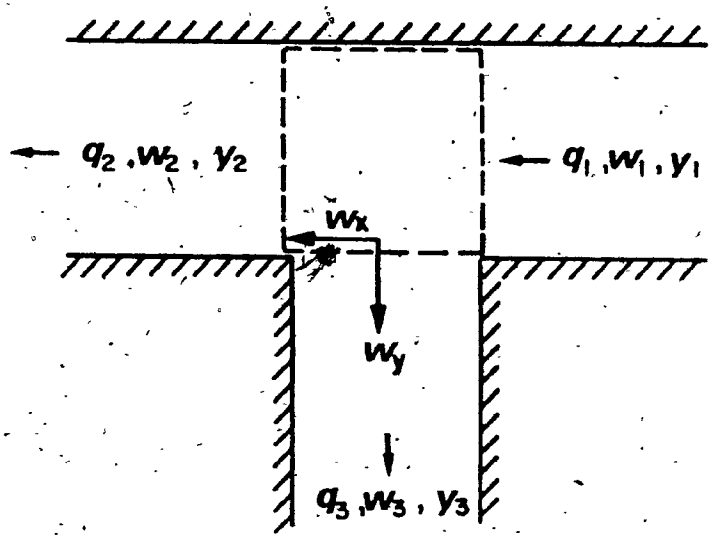

Fig.25(b) Flow past an open channel branch - Control volume in the main channel .

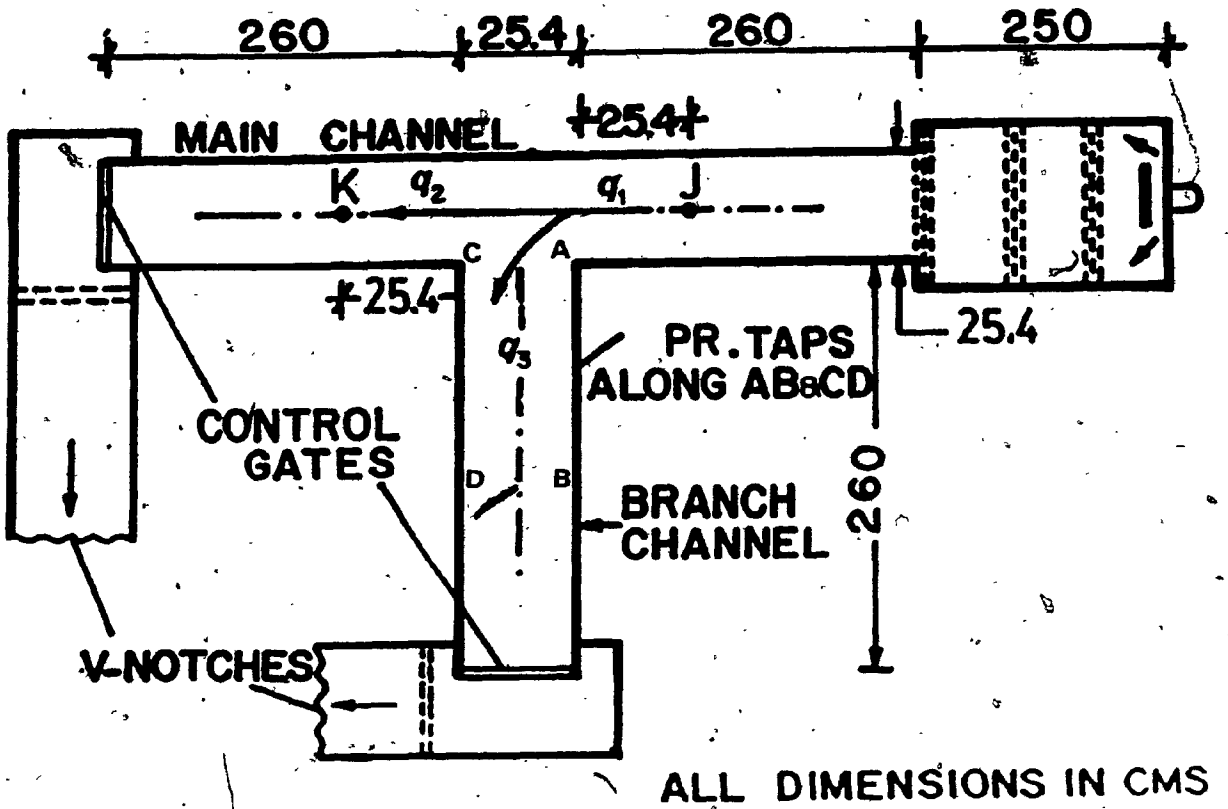

Fig.26 Experimental Set-Up : Pressure recovery in spatially varied diverging open channel flows

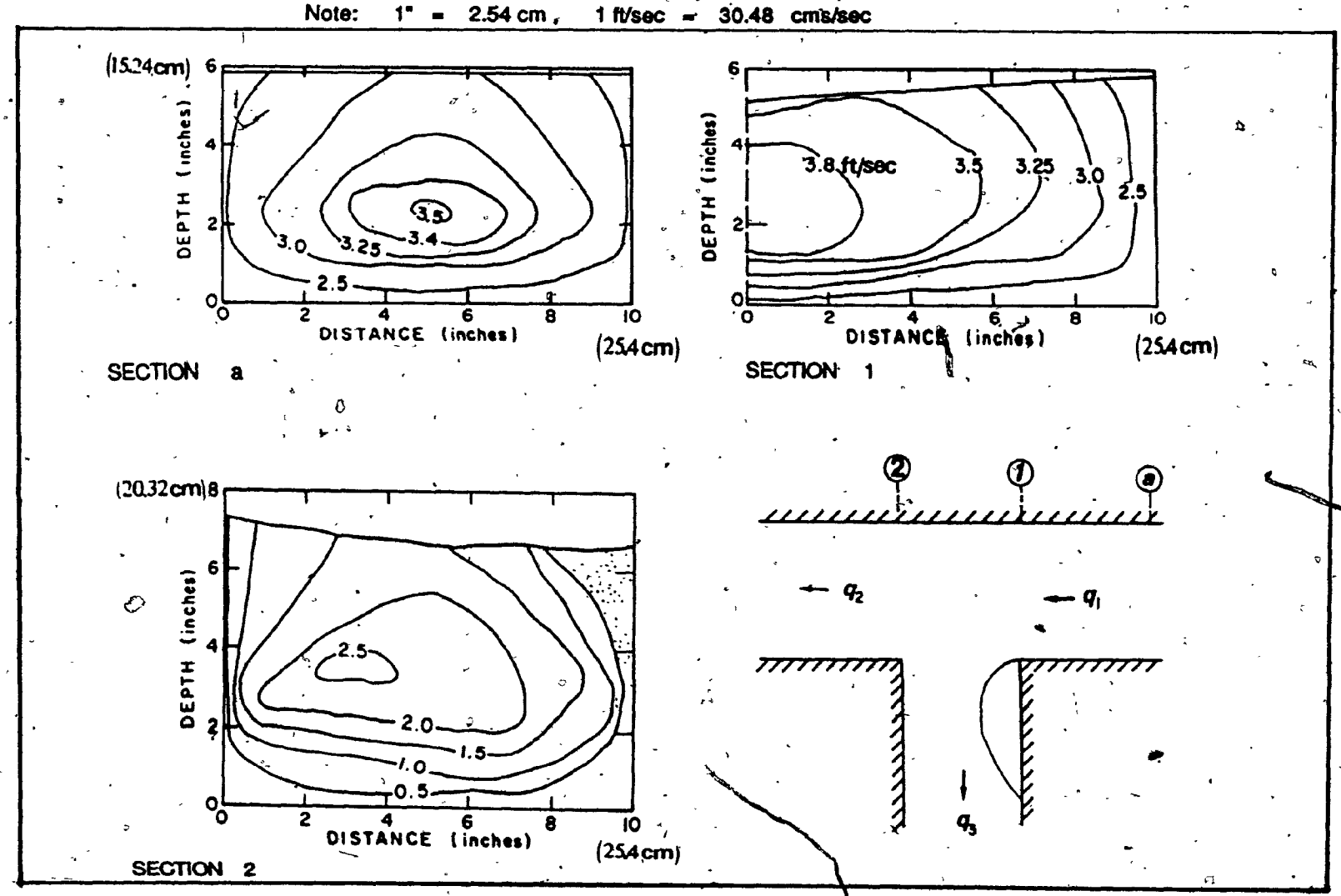

Fig.27 Typical velocity contours at various sections along the main channel

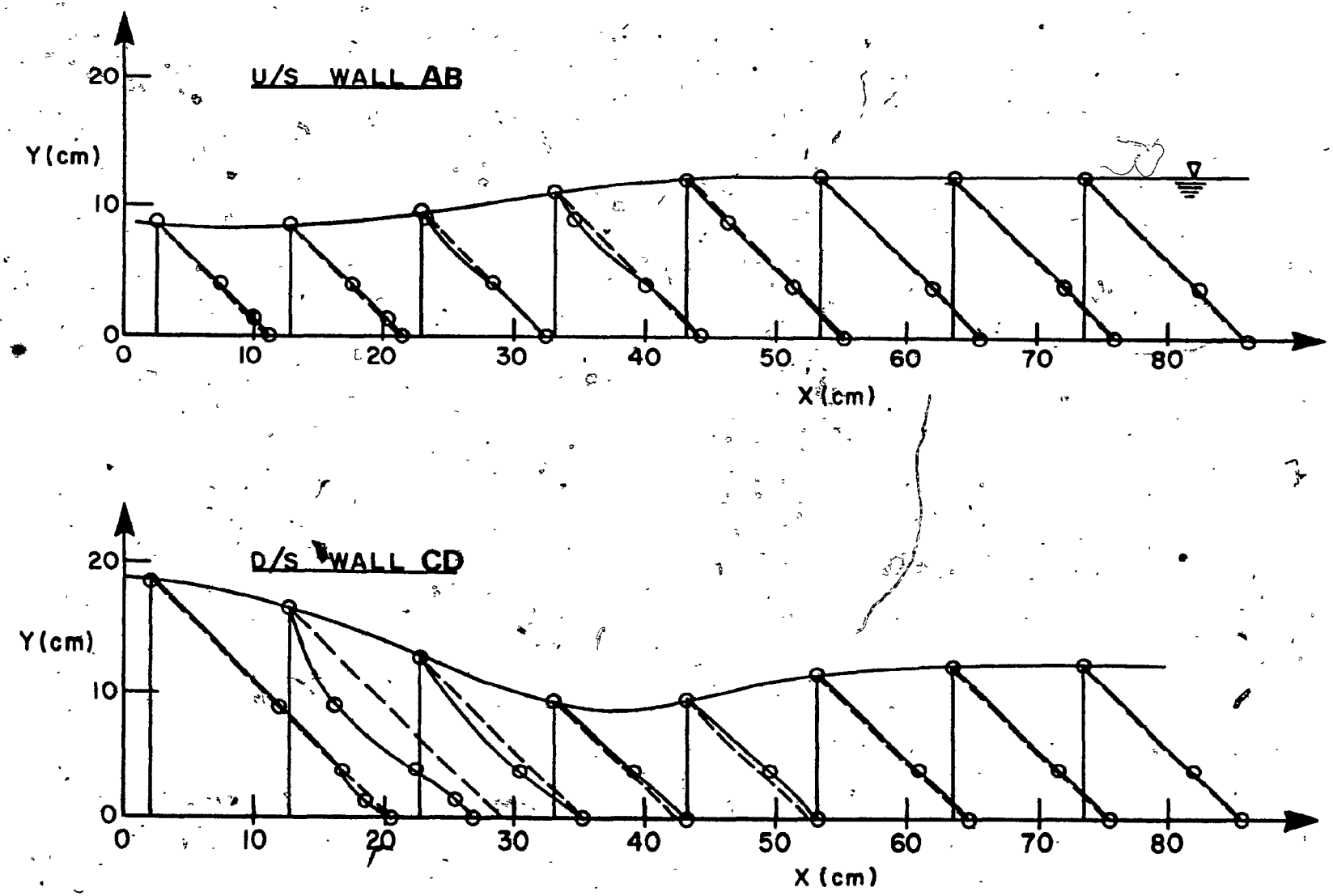

Fig.28 Typical pressure distributions on the upstream and downstream branch channel walls

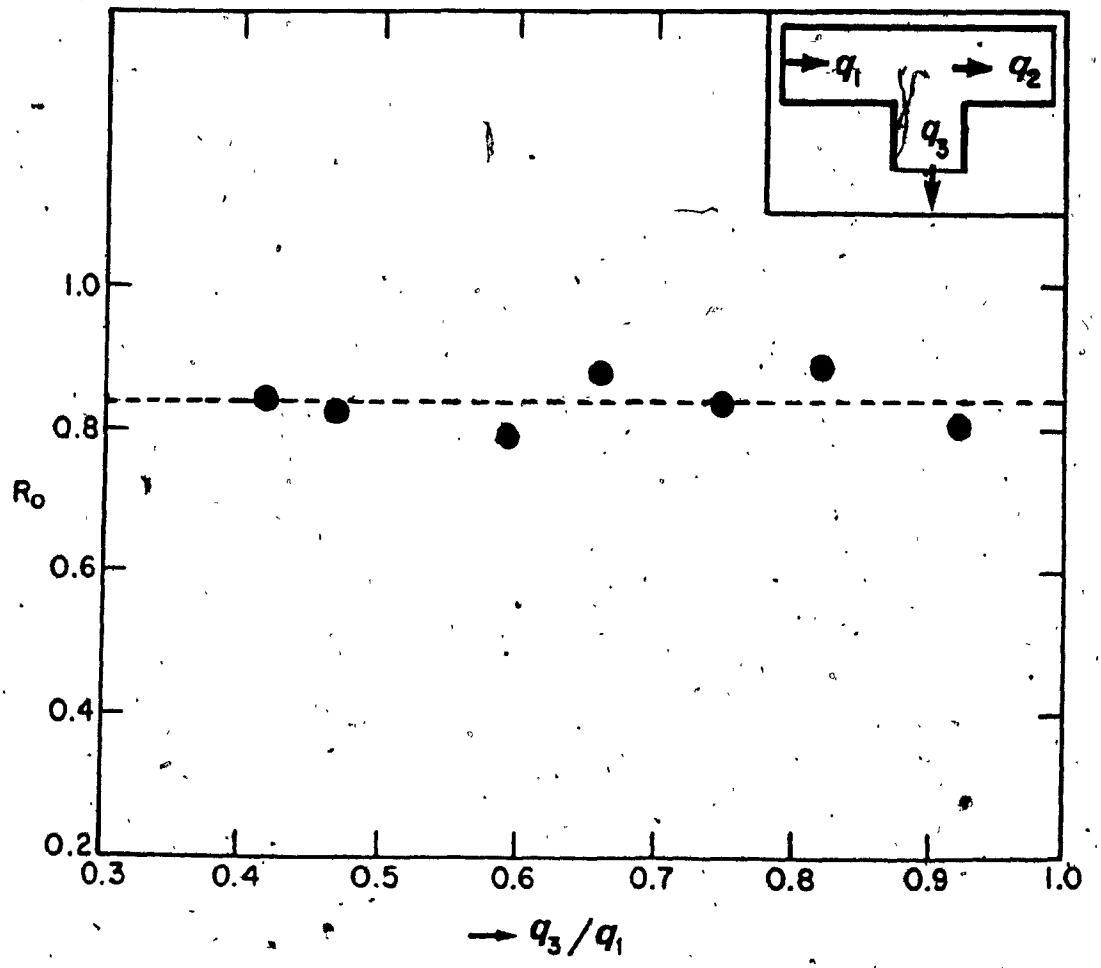

Fig.29 Experimental relationship between the pressure recovery factor R_o and the discharge ratio q_3/q_1

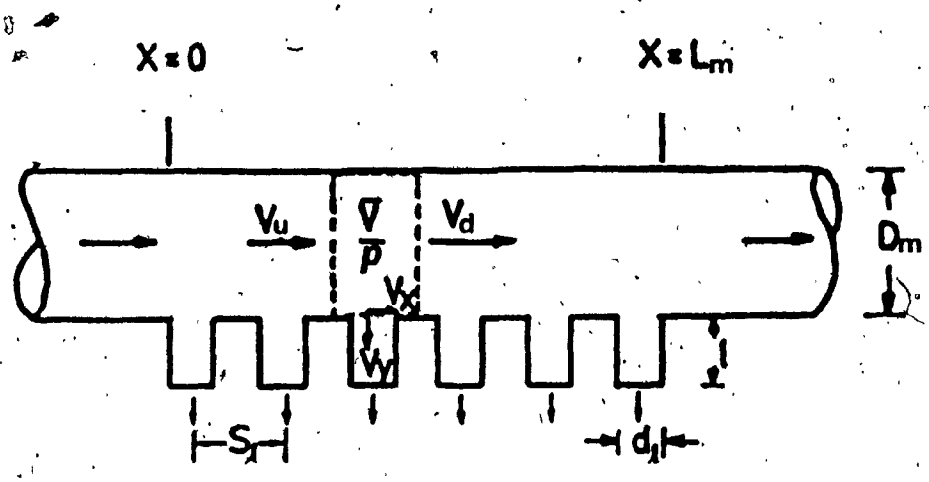

Fig.30 Definition Sketch - Multiport Diffuser .

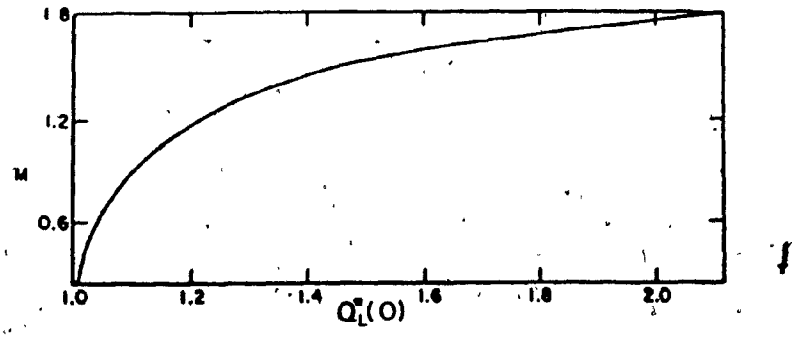

Fig.31(a) Analytical relationship between Lateral discharge at inlet $Q_L^*(0)$ and the momentum ratio M for f = 0.025 (hydraulically rough pipes)

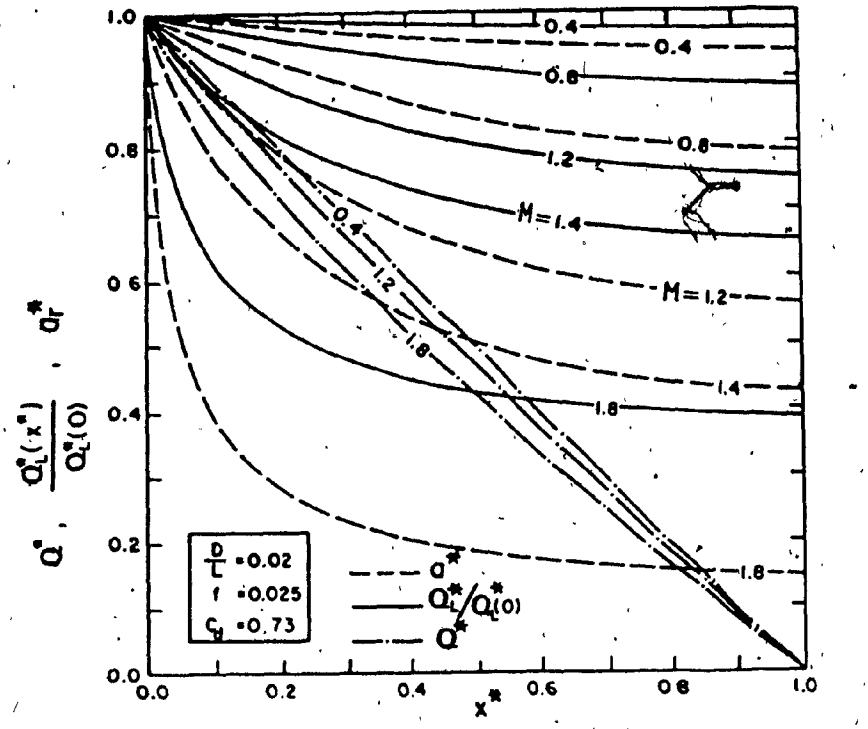

Fig.31(b) Analytical variation of the main discharge Q^*, the lateral discharge Q_L^* and the lateral area a_r^* as functions of the momentum ratio M for f =0.025 (hydraulically rough pipes)

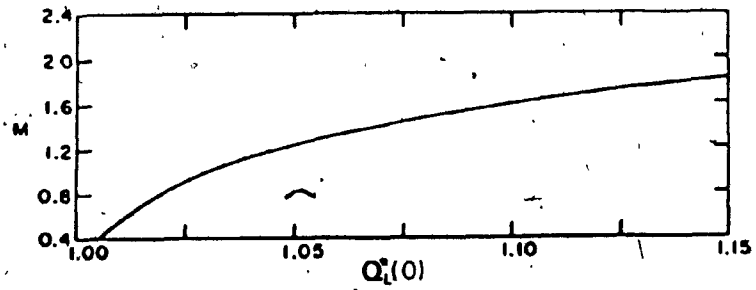

Fig.32(a) Analytical relationship between Lateral discharge at inlet $Q_L^*(0)$ and the momentum ratio M for f=0.050 (hydraulically rough pipes)

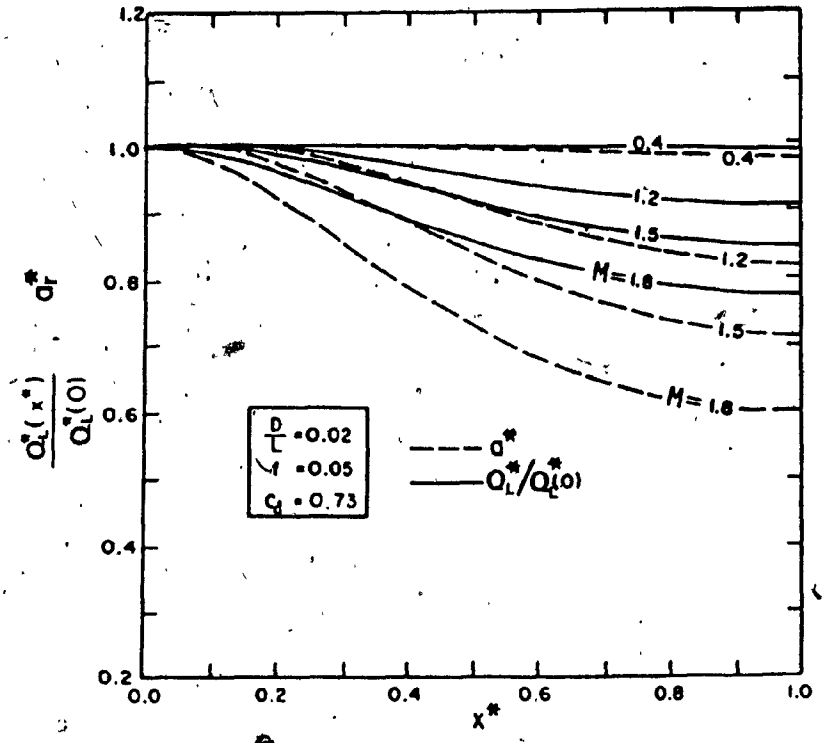

Fig.32(b) Analytical variation of the main discharge Q^*, the lateral discharge Q_L^* and the lateral area a_r^* as functions of the momentum ratio M for f = 0.050 (hydraulically rough pipes)

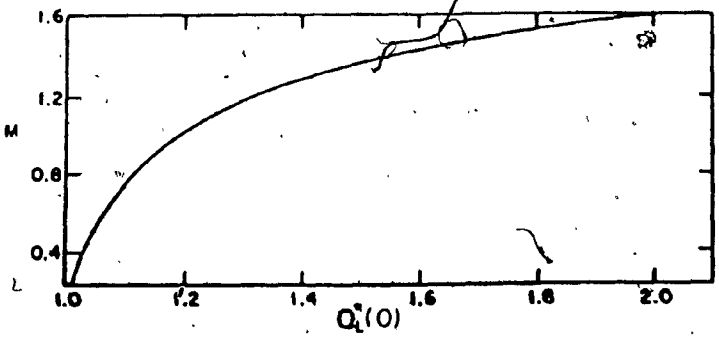

Fig.33(a) Analytical relationship between Lateral discharge at inlet $Q_L^*(0)$ and the momentum ratio M (hydraulically smooth pipes)

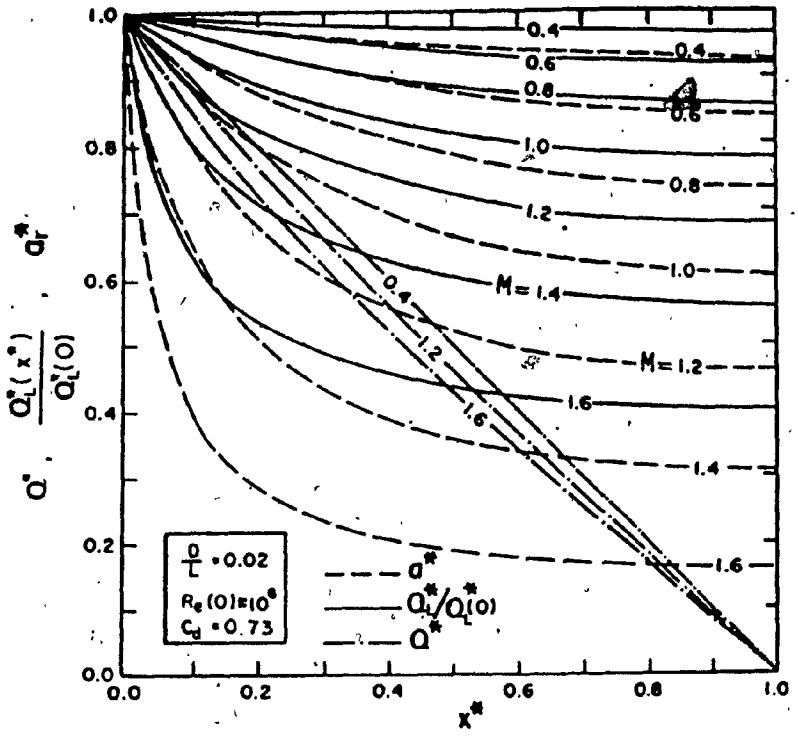

Fig.33(b) Analytical variation of the main discharge Q*, the lateral discharge Q_L^* and the lateral area a_r^* as functions of the momentum ratio M (hydraulically smooth pipes)

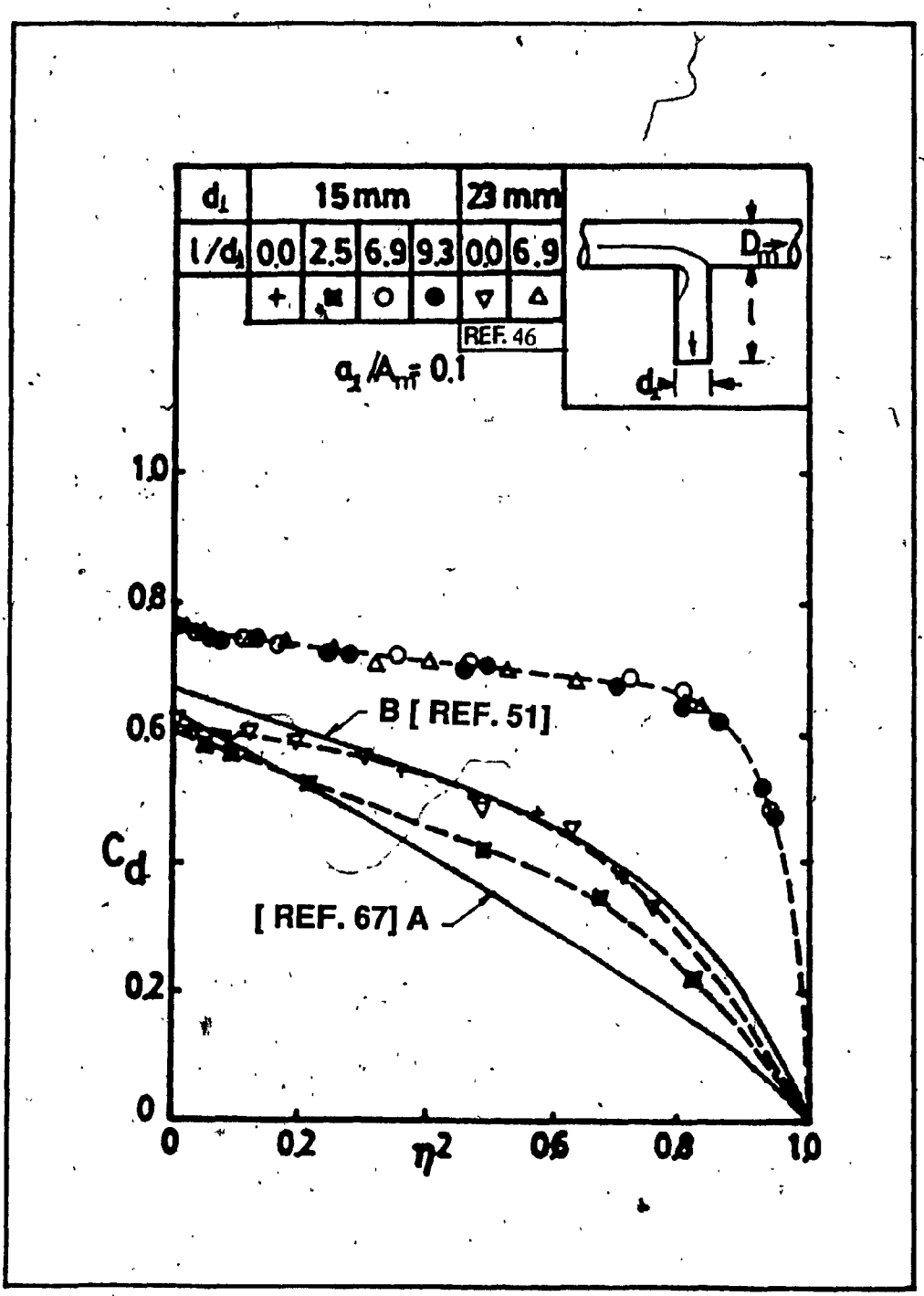

Fig.34 Variation of the discharge coefficient C_d as a function of the velocity parameter η and l/d_1

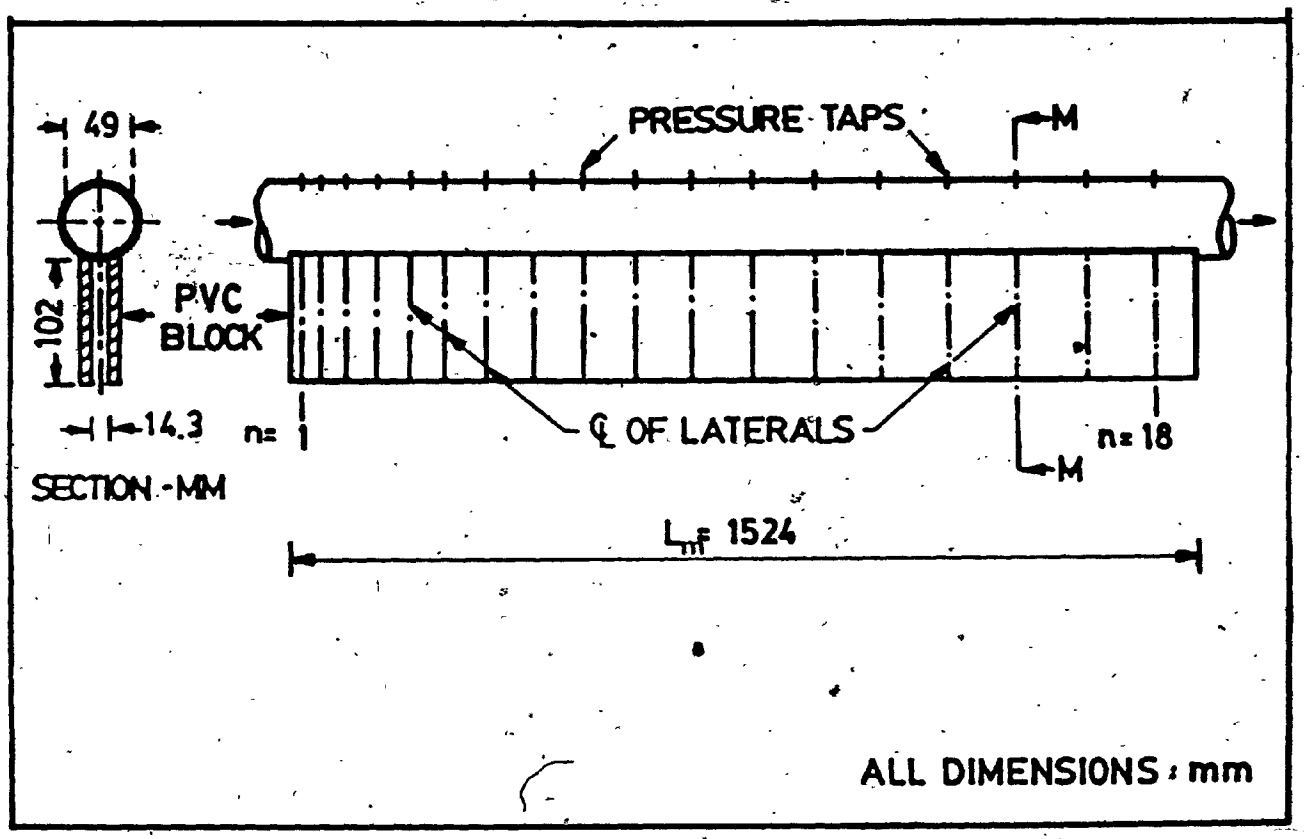

Fig.35 Experimental Set-Up : Multiport Diffuser Manifold

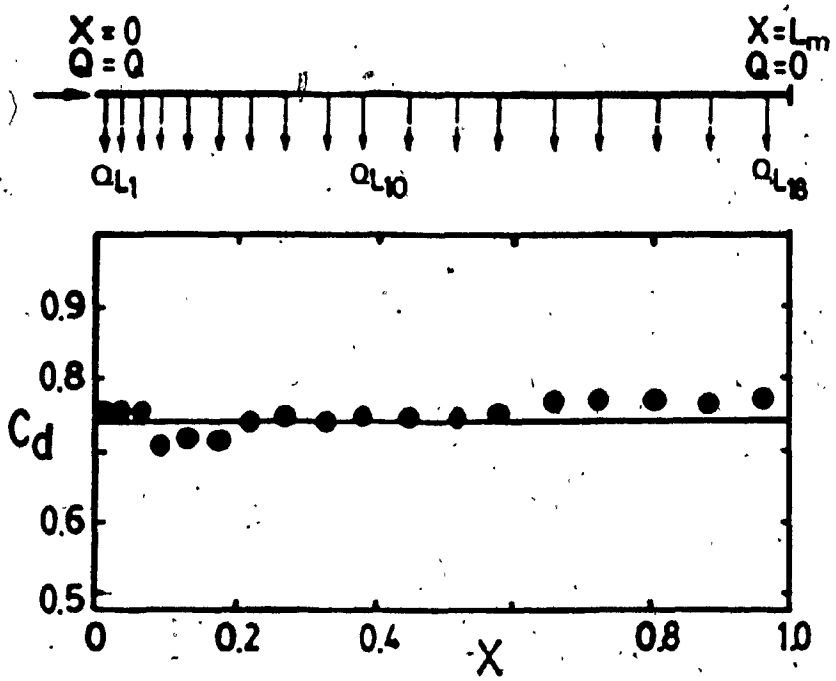

Fig.36(a) Typical distribution of the discharge coefficient C_d for individual laterals along the manifold

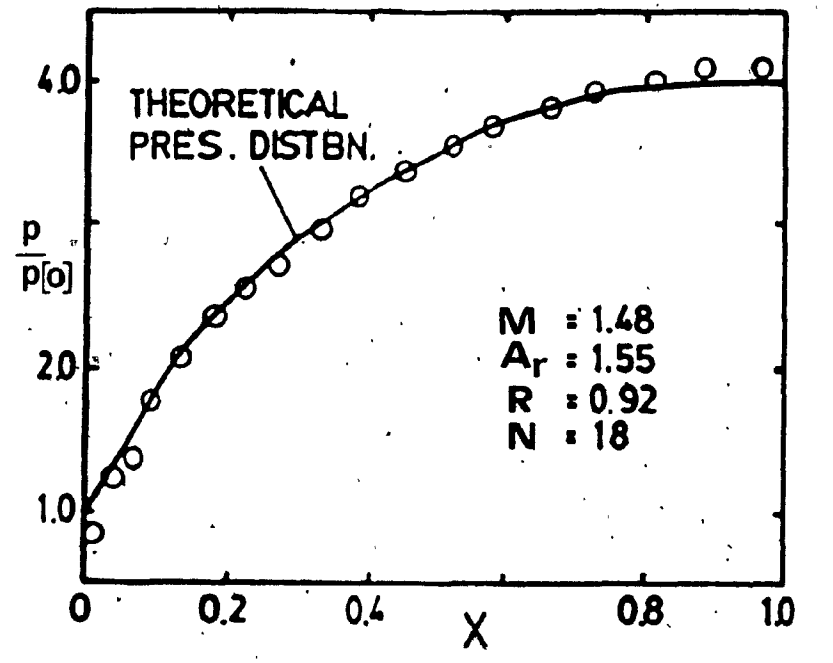

Fig.36(b) Analytical and experimental distribution of the pressure p along the manifold- a typical test run

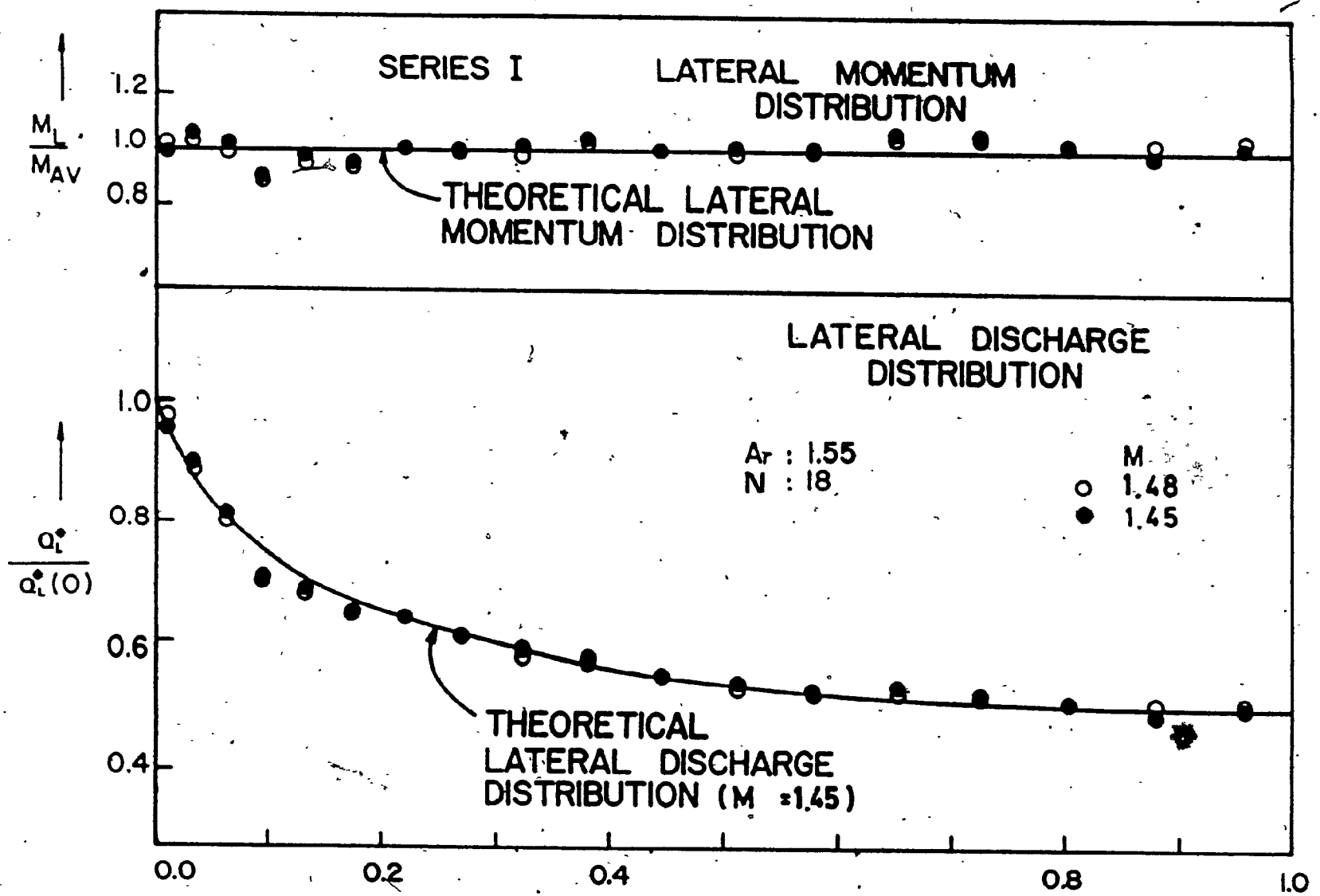

Fig.37 Analytical and experimental distribution of the lateral momentum and the lateral discharge along the manifold for the design momentum ratio M = 1.45

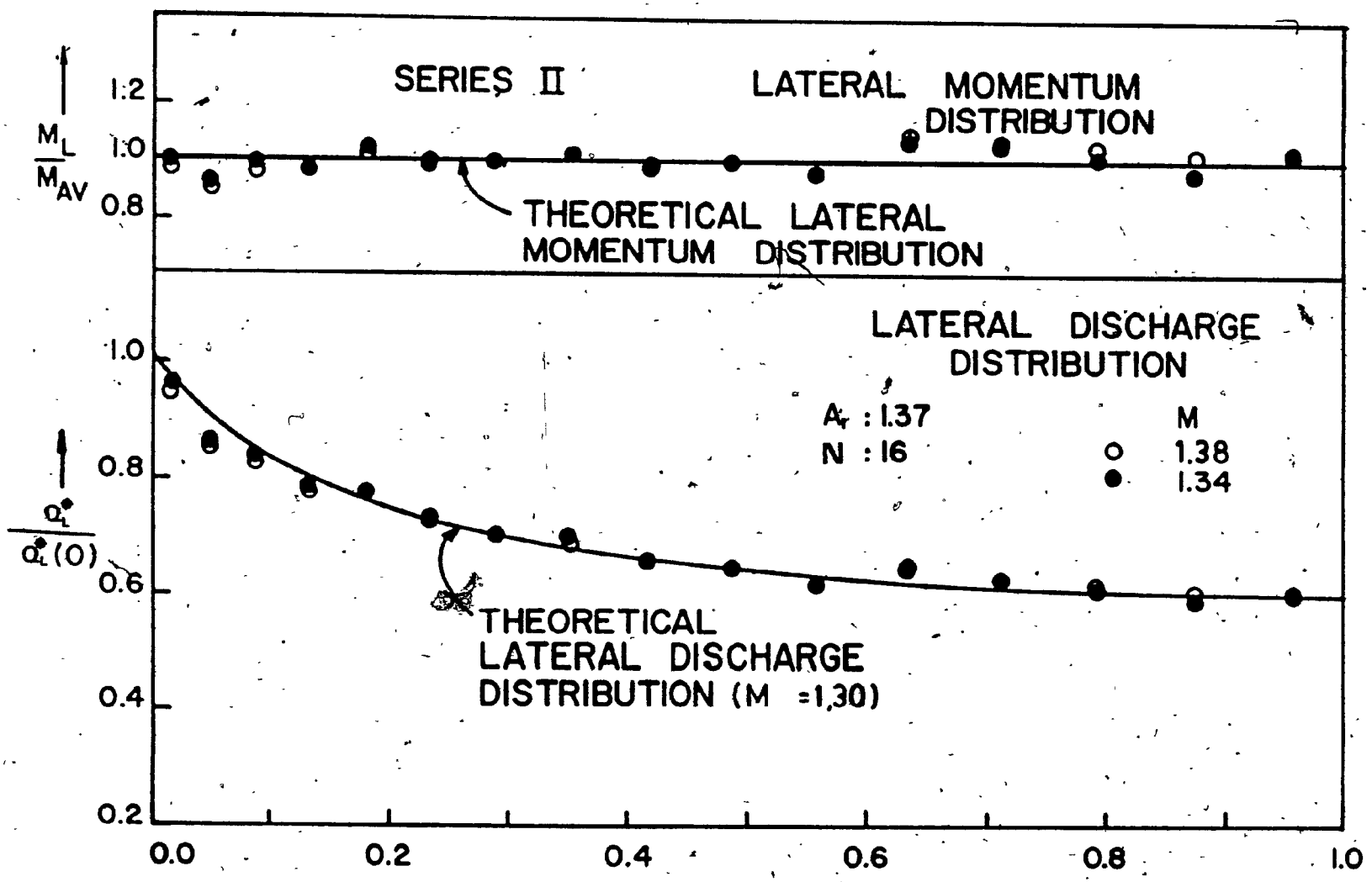

Fig.38 Analytical and experimental distribution of the lateral momentum and the lateral discharge along the manifold for the design momentum ratio M = 1.45

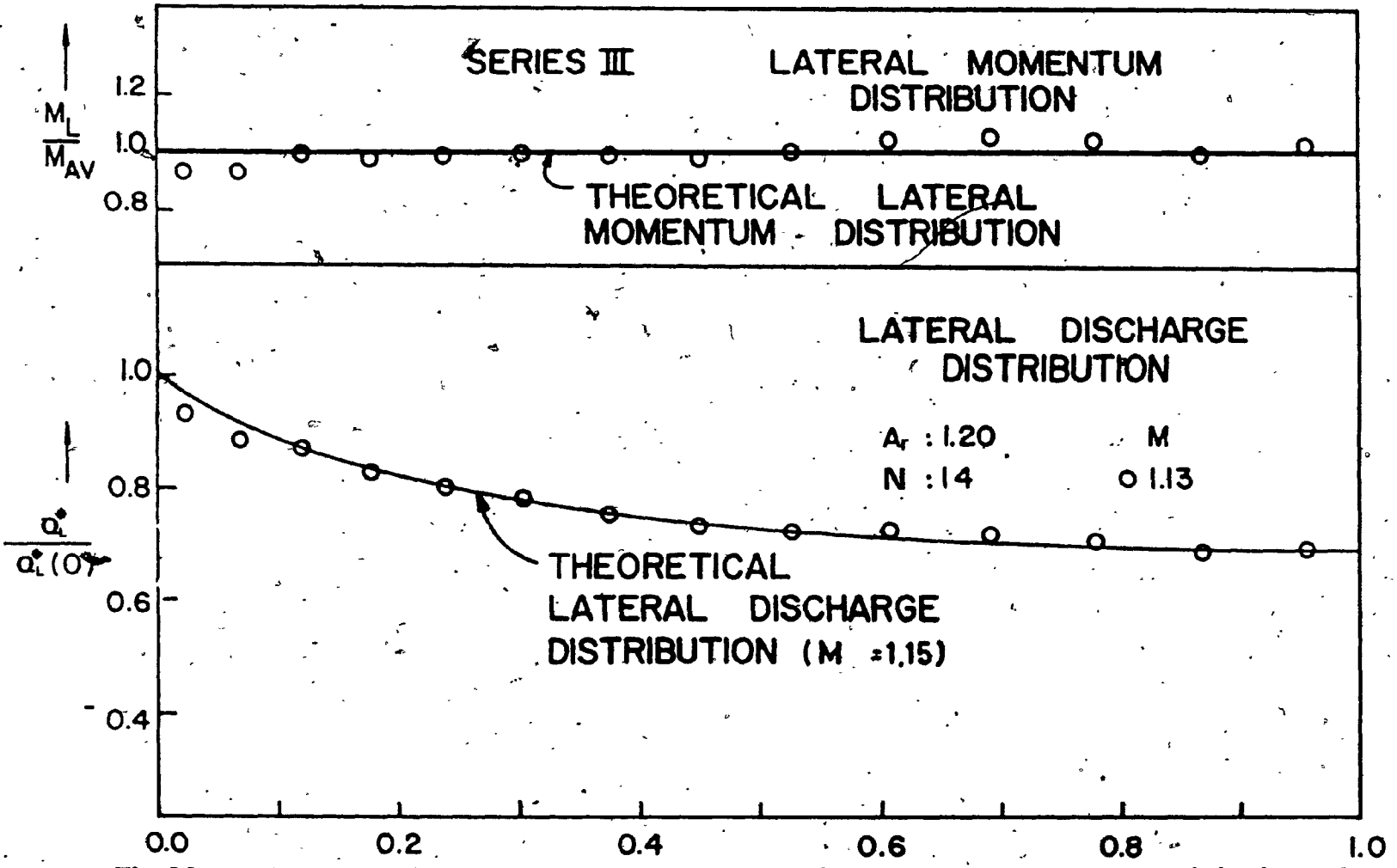

Fig.39 Analytical and experimental distribution of the lateral momentum and the lateral discharge along the manifold for the design momentum ratio M = 1.45

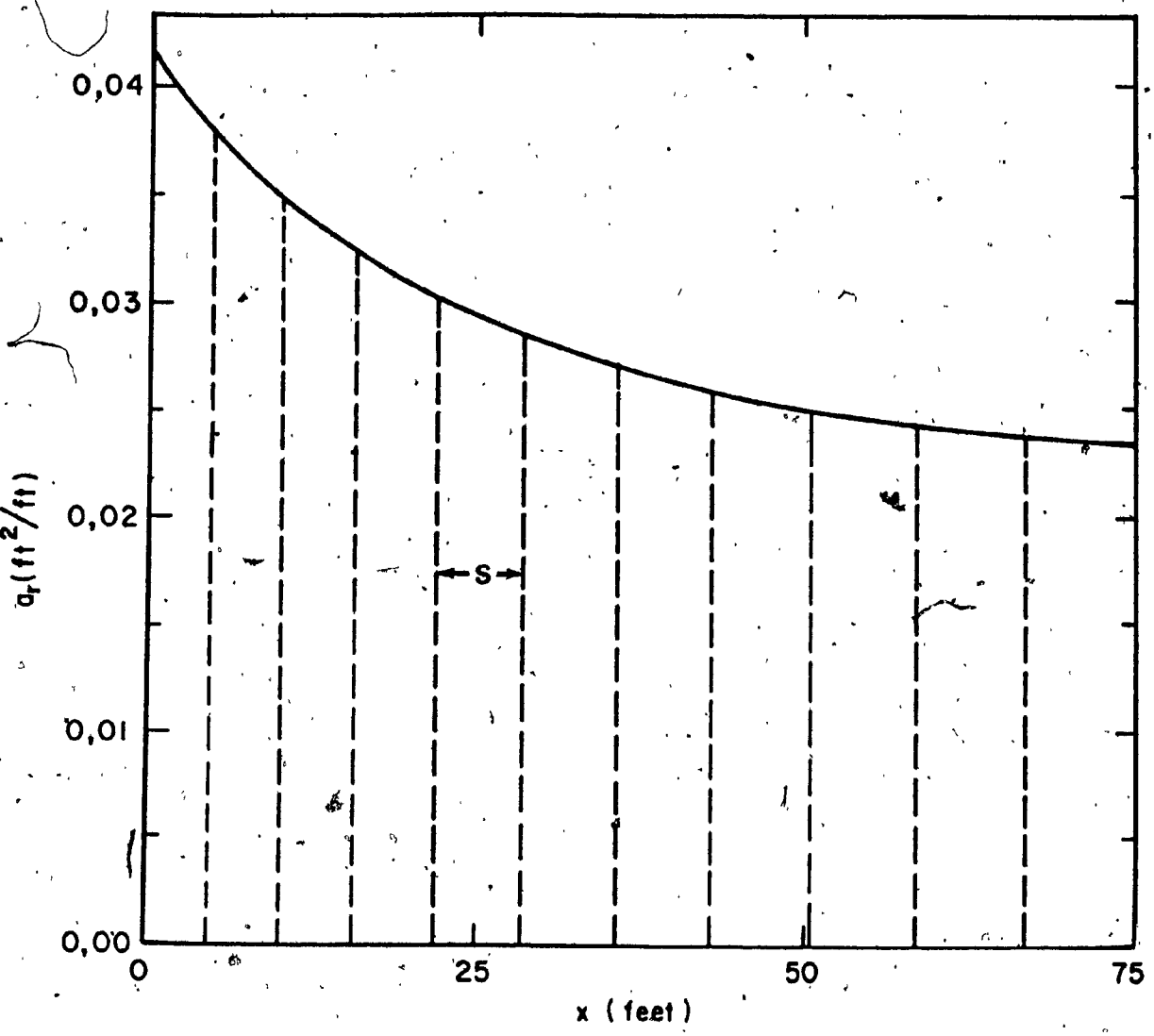

Fig.40 Distribution of the Lateral area a_r along the span of the manifold

APPENDIX III - TABLES

Table 1. Range of η_1 and C_c for various values of L/B

$\frac{L}{B}$	C_c	2-D LATERAL OUTLET MODEL η_1	BRANCH CHANNEL MODEL η_1
0.25	0.000 - 0.607	0.023 - 1.000	0.023 - 1.000
	0.607	-	0.010 - 0.023
0.50	0.000 - 0.584	0.085 - 1.000	0.085 - 1.000
	0.584	-	0.038 - 0.085
1.00	0.000 - 0.525	0.276 - 1.000	0.276 - 1.000
	0.525	-	0.134 - 0.276

TABLE 2

Lateral area distribution along the manifold

Lateral No.	1	2	3	4	5	6	7	8	9	10	11
Distance x in ft.	2.3	7.4	12.9	18.8	25.1	31.9	39.1	46.5	54.3	62.3	70.4

APPENDIX IV

EXPERIMENTAL EVALUATION OF R_O IN BRANCH CHANNELS - COMPARISON BETWEEN THE TWO SUGGESTED METHODS

APPENDIX IV EXPERIMENTAL EVALUATION OF R_O - COMPARISON BETWEEN THE TWO SUGGESTED METHODS

Data : Run No. 1 (page 147)

q_1 = 1.234 cfs (0.0349 m^3/sec) , q_2 = 0.660 cfs (0.0187 m^3/sec)

y_1 = 0.450 ft (0.137 m) , y_2 = 0.552 ft (0.168 m) , b = 0.833 ft (0.254 m)

P_{CD} = 13.296 lbs (5.99 Kg) , P_{AB} = 10.182 lbs (4.587 Kg)

β_1 = 1.03 , β_2 = 1.24 , K_1 = K_2 = 1

From the above data, one can get

$q_3 = q_1 - q_3$ = 1.234 - 0.660 = 0.574 cfs (0.0163 m^3/sec)

q_3 / q_1 = 0.5741/ 1.234 = 0.465

$w_1 = q_1 / a_1$ = 1.234 / (0.450 x 10/12) = 3.29 ft/sec (1.003 m/sec)

$w_2 = q_2 / a_2$ = 0.660/ (0.552 x 10/12) = 1.435 ft/sec (0.437 m/sec)

Estimate of R_o using Eq. 4.17:

$$R_o = \frac{P_{CD} - P_{AB}}{\rho\, q_3\, V_1} = \frac{13.296 - 10.182}{1.98 \times 0.574 \times 3.29} = 0.833$$

Estimate of R_o using Eq. 4.19:

$$R_o = \frac{b\,g\,(y_1^2 - y_2^2) + 2(\beta_1 q_1 w_1 - \beta_2 q_2 w_2)}{2\,q_3\,w_1}$$

$$\frac{0.833 \times 32.2\,(0.45 - 0.552^2) + 2(1.03 \times 1.234 \times 3.29 - 1.24 \times 1.435)}{2 \times 0.574 \times 3.29}$$

$$= 0.867$$

APPENDIX V

SPECIMEN COMPUTATIONS

APPENDIX V : SPECIMEN COMPUTATIONS

FLOOR OUTLETS:

Run No. 5 (Page 134)

Data: Q_{f1} = 0.717 cfs (0.02 m^3/sec) , Q_{f2} = 0.689 cfs (0.0195 m^3/sec)

U_1 = 4.6 ft/sec(1.4 m/sec), d_1 = 0.187 ft(0.057 m), L = 0.25 in(0.00635 m)

From the above data, one can get

$Q_f = Q_{f1} - Q_{f2}$ = 0.717 - 0.689 = 0.028 cfs (0.000793 m^3/sec)

d_c = 0.284 ft(0.0866 m) , L/d_c = 0.0734 , L/d_1 = 0.11

From Eq. 2. 12,

$$K = 1.01 - 0.35\,(0.0734) - 0.95\,(0.0734)^2 + 0.9\,(0.0734)^3$$

$$= 0.98$$

$$E = K d_1 + U_1^2 / 2g$$

$$= 0.98 \times 0.187 + 4.6/(2 \times 32.2) = 0.514 \text{ ft } (0.1567 \text{ m})$$

$$C_{df} = \frac{Q_f}{B L \sqrt{2 g E}} = \frac{0.028}{\left(\frac{10}{12}\right)\left(\frac{0.25}{12}\right)\sqrt{2 \times 32.2 \times 0.514}} = \underline{0.28}$$

$$F_f = \frac{V_1}{\sqrt{g\, d_1}} = \frac{4.6}{\sqrt{32.2 \times 0.187}} = \underline{1.875}$$

From Eq. 2.9,

$$\eta_f^2 = \frac{1}{1 + \frac{2K}{F_f^2}} = \frac{1}{1 + \frac{2 \times 0.98}{1.875^2}} = \underline{0.64}$$

Specimen computations for the analytical curve

Let $L/d_1 = 0.2$ and $\eta_f^2 = 0.6$

From Eq. 2.7,

$C_1 = -0.538 + 0.254\,(0.2) = -0.4872$

$C_2 = 0.058 + 0.234\,(0.2) = 0.1048$

$C_3 = -0.129 - 0.489\,(0.2) = -0.2268$

From Eq. 3.6,

$$C_{df} = 0.611 - 0.4872\,(0.6) + 0.1048\,(0.6)^2 - 0.2268\,(0.6)^3$$

$$= \underline{0.307}$$

BRANCH CHANNEL:

Analytical curve [Branch Channel program : Appendix vi - page 124]

For $F_1 = 0.45$ and $L/B = 1.0$

$C_c = 0.52$, $F_2 = 0.11$ and $Q_3 / Q_1 = 0.727$.

Experimental Data

Run No. 1 [Page 143]

Q_1 = 0.948 cfs(0.0268 m^3/sec), Q_2 = 0.172 cfs (0.00487 m^3/sec)

B = 10 in (0.254 m), h_1 = 0.571 ft (0.174 m), h_2 = 0.60 ft (0.183 m)

From the above data, one can get

$Q_3 = Q_1 - Q_2 = 0.948 - 0.172 = 0.776$ cfs(0.022 m^3/sec)

$Q_3 / Q_1 = 0.776 / 0.948 = 0.819$

$$F_1 = \frac{(Q_1 / A_1)}{\sqrt{g\, h_1}} = \frac{(0.948)/(0.571 \times 10/12)}{\sqrt{32.2 \times 0.571}} = 0.465$$

$$F_2 = \frac{(Q_2 / A_2)}{\sqrt{g\, h_2}} = \frac{(0.172)/(0.60 \times 10/12)}{\sqrt{32.2 \times 0.600}} = 0.078$$

MULTIPORT DIFFUSERS:

Series 1 Run No. 1 [Page 152]

Lateral No. 1

Data : $x = 0.0511$ ft (0.0156 m), $s = 0.1074$ ft (0.0372 m)

$Q_t = 0.0151$ cfs (0.0004276 m^3/sec), $a_t = 0.001726$ ft^2(0.01858 m^2)

$Q(0) = 0.42254$ cfs(0.012 m^3/sec), $M_{AV} = 2.342$ lb/sec^2(1.055 Kg/sec^2)

From the above data, one can get

$M_t = \rho Q_t (Q_t / a_t) = 1.98 (0.0151)^2 / (0.001726) = 0.261$ lb-ft/sec^2
(0.036 Kg-m/sec^2)

$Q_L = Q_t / s = 0.0151 / 0.1074 = 0.1405$ cfs/ft (0.013 m^3/sec/m)

$M_L = M_t / s = 0.2610 / 0.1074 = 2.4289$ lb/ sec^2 (1.094 Kg/sec^2)

$M_L / M_{AV} = 2.4289 / 2.342 = \underline{1.037}$

$$\frac{Q_L}{Q_L(0)} = \frac{Q_L / Q(0)}{Q_L(0) / Q(0)} = \frac{0.1405 / 0.42254}{0.341} = \underline{0.975}$$

APPENDIX VI - COMPUTER PROGRAMS

PROGRAM TO COMPUTE BRANCH CHANNEL DISCHARGE

```
      PROGRAM MCK(INPUT,OUTPUT)
C     THIS PROGRAM DETERMINES CONTRACTION COEFFICIENT BY MCKNOWN
C     METHOD AND CALCULATES THE BRANCH CHANNEL DISCHARGE BY CONDUIT
C     MODEL AND FURTHER COMPUTES DOWNSTREAM FROUDE NUMBER FROM
C     THE UPSTREAM FROUDE NUMBER
*
*
      READ*, VV,ABR
*
*
      ALHS=ABR
      PI=3.1415927
      CC=0.01
*
*
      DO 10 I=1,10000
      VR=(CC*ABR)/(1.-VV)
      A1=(1.+(VR*VR))*2./PI
      A2=(2./PI)*(1.+(VV*VV*VR*VR))
      A3=VR*(1.-VV)
      B1=0.5*ALOG((1.+VR)/(1.-VR))
      B2=VV*VR
      B3=0.5*ALOG((1.+B2)/(1.-B2))
      RHS=(A1*B1)-(A2*B3)+A3
      ERR=ABS(ALHS-RHS)
      IF(ERR.LE.0.01) GO TO 20
   10 CC=CC+0.0001
*
*
   20 ETA=(CC*ABR)/(1.-VV)
      ETAS=ETA*ETA
      ETAF=(3.0/ETAS)-1.0
      F1S=2.0/ETAF
      F1=F1S**0.5
      F1R=1.0+(2.0/F1S)
      F1RP=F1R**1.5
      C1=0.19245009
      QR=C1*ABR*F1S*F1RP*CC
      FF1=1.0+(2.0/(F1*F1))
      ANU=F1*F1*/FF1**1.5)
      AD=1.0-QR
      ARHS=ANU/AD
      F2=0.01
      DO 50 I1=1,100000
      FF2=1.0+(2.0/(F2*F2))
      AALHS=(F2*F2)*(FF2**1.5)
      AERR=ABS(AALHS-ARHS)
      IF (AERR.LE.0.05) GO TO 60
   50 F2=F2+0.0001
*
*
   60 PRINT 100,I,I1,VV,VR,ABR,CC,F1,F2,QR
  100 FORMAT(2X,2I10,/F14.3)
      STOP
      END
```

PROGRAM FOR MULTIPORT DIFFUSER DESIGN

[CONSTANT FRICTION FACTOR - HYDRAULICALLY ROUGH PIPES]

```
      DIMENSION Z(4),Q(4),F1(4),F2(4),DIST(20)
      DT=0.0001
      AR=1.545
      NN=1
      C1=1.81
      DIST(1)=0.0
      AA=1.0000/10.0
      RE=1000000.
      RO=RE**0.19
      RON=100000*0.25
      ARR=AA
      ARR1=AA/2.0
      H=1.9
      AL=5.0
      DT=0.16
      AMR=1.4
      RD=0.92
      A=(0.080*AMR*AMR)/(H*0.032*RO)
      B=(2.-RD)*(AMR*AMR/H)
      C1=1.81
      Q1=1.0
      Z1=-1.560
      QL=-Z1
      QLO=QL
      ARE1=QL*QL
      AREA0=ARE1
      SL=0.0
      DO  10 N=1,10000
      Z(1)=Z1
      Q(1)=Q1
      DO  20 N=1,4
      F1(N)=A*(Q(N)**C1)*Z(N)*Z(N)*Z(N)+
     +B*Q(N)*Z(N)*Z(N)*Z(N)*Z(N)
      F2(N)=Z(N)
      AN=0.5
      IF  (N.EQ.3)  AN=1.0
      IF  (N.EQ.4)  GO TO 30
      Z(N+1)=Z(1)+AN*DT*F1(N)
   20 Q(N+1)=Q(1)+AN*DT*F2(N)
   30 Z1=Z1+(DT*(((1./6.)*F1(1))+((1./3.)*F1(2))+
     +((1./3.)*F1(3))+((1./6.)*F1(4)))
      Q1=Q1+(DT*(((1./6.)*F2(1))+((1./3.)*F2(2))+
     +((1./3.)*F2(3))+((1./6.)*F2(4))))
      QL=-Z1
C
C
      AREA=QL*QL
      QLC=QL/QLO
      AREAC=AREA/AREA0
      ARE2=(ARE1+AREA)*0.5*DT
      ARE=ARE+ARE2
   50 IF(ARE.LT.ARR)  GO TO 60
      NN=NN+1
      DIST(NN)=SL
      SP=DIST(NN)-DIST(NN-1)
      WRITE(6,200)  SL,SP,ARE,Q1,QLC,AREAC
      ARR=ARE+AA
   60 IF(ARE.LT.ARR1)  GO TO 70
```

```
      WRITE(6,300) SL,ARE,Q1,QLC,AREAC
      ARR1=ARR+AA
   70 SL=SL+DT
      ARE1=AREA
C
C
      RN=RE*Q1
      IF(RN.GE.100000.) GO TO 10
      A=0.158*AHR*AHR/(H*0.032*RON)
      CT=1.75
   10 CONTINUE
      WRITE(6,150) Q1,QLC,AREAC,SL,ARE
  150 FORMAT(10X,5F14.3)
  200 FORMAT(25X,3F15.3)
  300 FORMAT(10X,5F10.3)
      STOP
      END
```

PROGRAM FOR MULTIPORT DIFFUSER DESIGN

[HYDRAULICALLY SMOOTH PIPES]

```
      DIMENSION Z(4),Q(4),F1(4),F2(4),DIST(20)
      DT=0.0001
      NN=1
      DIST(1)=0.0
      AA=1.0300/10.0
      PP=0.025
      ARR=AA
      ARR1=AA/2.0
      H=1.9
      AL=5.0
      D1=0.16
      ANR=1.45
      RD=0.92
      A=(PP*ANR*ANR)/(2.*H*0.032)
      B=(2.-RD)*(ANR*ANR/H)
      Q1=1.0
      Z1=-1.546
      QL=-Z1
      QLO=QL
      ARE1=QL*QL
      AREA0=ARE1
      SL=0.0
      DO 10 M=1,10000
      Z(1)=Z1
      Q(1)=Q1
C
      DO 20 N=1,4
      F1(N)=A*(Q(N)**(7./4.))*Z(N)*Z(N)*Z(N)*
     *B*Q(N)*Z(N)*Z(N)*Z(N)*Z(N)
      F2(N)=Z(N)
      AN=0.5
      IF (N.EQ.3) AN=1.0
      IF (N.EQ.4) GO TO 30
      Z(N+1)=Z(1)+AN*DT*F1(N)
   20 Q(N+1)=Q(1)+AN*DT*F2(N)
   30 Z1=Z1+(DT*(((1./6.)*F1(1))+((1./3.)*F1(2))+
     *((1./3.)*F1(3))+((1./6.)*F1(4))))
      Q1=Q1+(DT*(((1./6.)*F2(1))+((1./3.)*F2(2))+
     *((1./3.)*F2(3))+((1./6.)*F2(4))))
      QL=-Z1
C
      AREA=QL*QL
      QLC=QL/QLO
      AREAC=AREA/AREA0
      ARE2=(ARE1+AREA)*0.5*DT
      ARE=ARE+ARE2
   50 IF(ARE.LT.ARR) GO TO 60
      NN=NN+1
      DIST(NN)=SL
      SP=DIST(NN)-DIST(NN-1)
CC    WRITE(6,200) SL,SP,ARE
      ARR=ARE+AA
   60 IF(ARE.LT.ARR1) GO TO 70
CC    WRITE(6,300) SL,ARE,Q1,QLC,AREAC
      ARR1=ARE+AA
   70 SL=SL+DT
      ARE1=AREA
   10 CONTINUE
      WRITE(6,150) Q1,QLC,AREAC,SL,ARE
  150 FORMAT(10X,5F14.3)
  200 FORMAT(25X,3F15.3)
  300 FORMAT(10X,5F10.3)
      STOP
      END
```

PROGRAM FOR MULTIPORT DIFFUSER

EXPERIMENTAL SET-UP

```
      DIMENSION Z(4),Q(4),P1(4),P2(4),DIST(20)
      DT=0.000100
      AR=1.545
      NN=1
      DIST(1)=0.0
      AA=1.4990/18.0
      RO=22.175
      ARR=AA
      ARR1=AA/2.0
      H=1.9
      AL=5.0
      D1=0.16
      AMR=1.45
      RD=0.92
      A=(0.3164*0.5*AR*AMR*AMR)/(H*0.032*RO)
      B=(2.-RD)*(AR*AR*AMR*AMR/H)
      CT=AR*AMR
      Q1=1.0
      Z1=-1.1110
      QL=-Z1
      ARE1=CT*QL*QL
      SL=0.0
      DO 10 M=1,15*50
      Z(1)=Z1
      Q(1)=Q1
      DO 20 N=1,4
      P1(N)=A*(Q(N)**(7./4.))*Z(N)*Z(N)*Z(N)+
     +B*Q(N)*Z(N)*Z(N)*Z(N)*Z(N)
      P2(N)=Z(N)
      AN=0.5
      IF (N.EQ.3) AN=1.0
      IF (N.EQ.4) GO TO 30
      Z(N+1)=Z(1)+AN*DT*P1(N)
   20 Q(N+1)=Q(1)+AN*DT*P2(N)
   30 Z1=Z1+(DT*((1./6.)*P1(1))+((1./3.)*P1(2))+
     +((1./3.)*P1(3))+((1./6.)*P1(4)))
      Q1=Q1+(DT*((1./6.)*P2(1))+((1./3.)*P2(2))+
     +((1./3.)*P2(3))+((1./6.)*P2(4)))
      QL=-Z1
      AREA=CT*QL*QL
      ARE2=(ARE1+AREA)*0.5*DT
      ARE=ARE+ARE2
   50 IF(ARE.LT.ARR) GO TO 60
      NN=NN+1
      DIST(NN)=SL
      SP=DIST(NN)-DIST(NN-1)
CCCC  WRITE(6,200) SL,SP,ARE
      ARR=ARR+AA
   60 IF(ARE.LT.ARR1) GO TO 70
CCCC  WRITE(6,300) SL,ARE
      ARR1=ARR+AA
   70 SL=SL+DT
      ARE1=AREA
   10 CONTINUE
      WRITE(6,150) Z1,QL,SL,ARE
  150 FORMAT(10X,4F15.10)
  200 FORMAT(25X,3F15.6)
  300 FORMAT(10X,2F10.5)
      STOP
      END
```

APPENDIX VII - EXPERIMENTAL DATA

DATA - FLOOR OUTLETS

L = 0.25" (0.635 CM) B = 10" (25.4 CM)

RUN No.	Q_{f1} cfs	Q_{f2} cfs	Q_f cfs	d_1 ft	E ft	d_c ft	K	C_{df}	η_f^2	L in	L/d_1
1	.240	.154	.086	1.053	.991	.137	.94	.62	.00	.25	.02
2	.500	.460	.040	.225	.329	.224	.97	.50	.34	.25	.09
3	.921	.899	.022	.180	.767	.336	.99	.18	.76	.25	.12
4	.831	.807	.024	.180	.656	.314	.98	.21	.73	.25	.12
5	.717	.689	.028	.187	.514	.284	.98	.28	.64	.25	.11
6	.602	.571	.031	.186	.418	.253	.98	.34	.56	.25	.11
7	.541	.508	.033	.187	.370	.236	.97	.39	.51	.25	.11
8	.497	.460	.037	.200	.333	.223	.97	.46	.41	.25	.10

L = 0.5" (1.27 CM) B = 10" (25.4 CM)

RUN No.	Q_{f1} cfs	Q_{f2} cfs	Q_f cfs	d_1 ft	E ft	d_c ft	K	C_{df}	η_f^2	L in	L/d_1
9	1.065	1.029	.036	.184	.930	.370	.96	.13	.81	.50	.23
10	.763	.712	.051	.186	.553	.296	.94	.25	.68	.50	.22
11	.633	.575	.058	.189	.430	.262	.94	.32	.58	.50	.22
12	.541	.479	.062	.196	.354	.236	.93	.37	.48	.50	.21
13	.416	.355	.061	.187	.282	.198	.91	.41	.39	.50	.22
14	.204	.160	.044	.099	.177	.123	.82	.38	.54	.50	.42
15	.342	.280	.062	.174	.240	.174	.88	.45	.36	.50	.24
16	.507	.443	.064	.187	.337	.226	.92	.40	.49	.50	.22
17	.502	.439	.063	.180	.341	.224	.92	.39	.51	.50	.23
18	.658	.551	.107	.415	.447	.269	.94	.57	.13	.50	.10
19	.595	.499	.096	.354	.393	.251	.93	.55	.16	.50	.12
20	.738	.620	.118	.510	.527	.290	.94	.58	.09	.50	.08
21	.807	.657	.150	.804	.786	.308	.95	.61	.03	.50	.05

L = 0.76" (1.93 CM) B = 10" (25.4 CM)

RUN No.	Q_{f1} cfs	Q_{f2} cfs	Q_f cfs	d_1 ft	E ft	d_c ft	K	C_{df}	η_f^2	L in	L/d_1
22	1.235	1.106	.129	.348	.610	.409	.94	.39	.46	.76	.18
23	1.024	.904	.120	.303	.539	.361	.93	.39	.47	.76	.21
24	.838	.726	.112	.268	.464	.315	.91	.39	.47	.76	.24
25	.740	.635	.105	.239	.431	.290	.90	.38	.50	.76	.26
26	.534	.441	.093	.185	.347	.234	.86	.37	.54	.76	.34
27	.286	.213	.073	.118	.223	.154	.77	.36	.59	.76	.54
28	1.441	1.229	.212	.746	.793	.453	.95	.56	.11	.76	.08
29	1.064	1.013	.051	.178	.969	.370	.93	.12	.82	.76	.36
30	.886	.825	.061	.174	.743	.327	.92	.17	.78	.76	.36
31	.722	.648	.074	.179	.527	.286	.90	.24	.69	.76	.35
32	.548	.464	.084	.177	.370	.238	.87	.33	.58	.76	.36
33	.502	.414	.088	.172	.340	.224	.86	.36	.56	.76	.37

L = 1.5" (3.81 CM) B = 10" (25.4 CM)

RUN No.	Q_{f1} cfs	Q_{f2} cfs	Q_f cfs	d_1 ft	E ft	d_c ft	K	C_{df}	η_f^2	L in	L/d_1
34	1.099	.991	.108	.177	1.011	.378	.81	.13	.85	1.50	.71
35	.948	.825	.123	.171	.827	.343	.79	.16	.83	1.50	.73
36	.688	.537	.151	.173	.484	.277	.74	.26	.73	1.50	.72
37	.527	.361	.166	.164	.344	.232	.68	.34	.67	1.50	.76
38	.527	.361	.166	.164	.344	.232	.68	.34	.67	1.50	.76

DATA - FLOOR OUTLETS (INTERFERENCE EFFECTS)

Run No.	Q_{f1} cfs	Q_{f2} cfs	Q_{fu} cfs	Q_{fd} cfs	d_1 ft	d_2 ft	L in	K	E ft	η^2_{f1}	η^2_{f2}	C_{d2}	K_i	S_f
1	1.129	.248	.418	.463	.283	.171	3.000	.628	.534	.67	.72	.38	1.00	1.25
2	1.029	.170	.414	.445	.271	.158	3.000	.611	.488	.66	.69	.42	.90	1.25
3	1.496	.529	.437	.530	.344	.241	3.000	.687	.659	.64	.66	.38	1.02	1.25
4	1.332	.398	.430	.504	.317	.210	3.000	.662	.605	.65	.68	.38	1.02	1.25
5	1.886	1.343	.228	.315	.416	.372	1.500	.890	.830	.55	.54	.36	1.14	1.50
6	2.080	1.514	.242	.324	.450	.408	1.500	.899	.882	.54	.51	.37	1.11	1.50
7	1.348	.872	.210	.266	.331	.284	1.500	.852	.653	.57	.55	.37	1.07	1.50
8	1.304	1.060	.110	.134	.344	.323	.750	.941	.645	.50	.47	.38	1.05	2.00
9	1.547	1.302	.108	.137	.362	.345	.750	.950	.752	.54	.52	.35	1.07	2.00
10	1.272	1.016	.119	.137	.335	.315	.750	.939	.637	.51	.47	.38	1.08	2.00
11	1.056	.817	.110	.129	.292	.264	.750	.928	.563	.52	.51	.36	1.13	2.00
12	.725	.519	.098	.108	.227	.198	.750	.898	.432	.53	.52	.37	1.06	2.00

Run No.	Q_{f1} cfs	Q_{f2} cfs	Q_{fu} cfs	Q_{fd} cfs	d_1 ft	d_2 ft	L in	K	E ft	η^2_{f1}	η^2_{f2}	C_{d2}	K_i	S_f
13	1.221	.982	.112	.127	.333	.303	.750	.937	.613	.49	.49	.37	1.04	3.00
14	.879	.666	.101	.112	.265	.229	.750	.914	.488	.50	.53	.36	1.07	3.00
15	.709	.515	.094	.100	.224	.187	.750	.896	.425	.53	.57	.34	1.07	3.00
16	.642	.461	.088	.093	.217	.175	.750	.886	.388	.50	.58	.34	1.05	3.00
17	1.157	.923	.108	.126	.318	.284	.750	.934	.593	.50	.51	.36	1.09	3.00
18	1.057	.830	.106	.121	.294	.260	.750	.928	.562	.51	.53	.35	1.10	3.00
19	.514	.347	.083	.084	.176	.137	.750	.861	.342	.56	.65	.31	1.10	3.00
20	.402	.250	.079	.073	.145	.108	.750	.828	.292	.59	.69	.30	1.07	3.00
21	1.239	1.070	.073	.096	.260	.246	.750	.938	.752	.68	.67	.27	.98	3.00
22	1.018	.827	.086	.105	.263	.236	.750	.925	.578	.58	.60	.31	1.05	3.00
23	.813	.615	.093	.105	.255	.218	.750	.908	.459	.50	.53	.36	1.03	3.00
24	1.238	.996	.125	.117	.335	.292	.750	.938	.619	.49	.52	.35	1.01	5.00
25	1.190	.952	.123	.115	.328	.280	.750	.935	.601	.49	.54	.35	1.03	5.00

Run No.	Q_{f1} cfs	Q_{f2} cfs	Q_{fu} cfs	Q_{fd} cfs	d_1 ft	d_2 ft	L in	K	E ft	f_{f1}^2	f_{f2}^2	C_{d2}	K_i	S_f
26	1.166	.937	.124	.105	.330	.271	.750	.934	.587	.48	.56	.33	.98	7.00
27	.864	.661	.113	.090	.263	.203	.750	.913	.481	.50	.64	.30	1.04	7.00
28	1.382	1.153	.117	.112	.327	.292	.750	.944	.708	.56	.59	.31	1.02	7.00
29	1.428	1.171	.132	.125	.377	.320	.750	.945	.677	.47	.54	.34	1.06	7.00
30	1.144	.921	.122	.101	.316	.257	.750	.933	.588	.50	.60	.31	1.01	7.00
31	1.009	.792	.120	.097	.293	.237	.750	.924	.536	.49	.59	.32	.98	7.00
32	.706	.521	.106	.079	.223	.166	.750	.895	.424	.53	.69	.27	1.06	7.00
33	.523	.363	.094	.066	.175	.128	.750	.863	.351	.57	.72	.27	1.00	7.00
34	.398	.255	.086	.057	.147	.102	.750	.827	.285	.57	.73	.27	.95	7.00
35	.833	.628	.114	.091	.265	.199	.750	.910	.462	.48	.63	.30	1.06	10.00
36	.732	.537	.110	.085	.234	.181	.750	.899	.429	.51	.62	.32	.98	10.00
37	1.159	.968	.101	.090	.273	.243	.750	.934	.658	.61	.64	.29	.92	10.00
38	1.040	.840	.108	.092	.272	.225	.750	.927	.579	.56	.66	.28	1.04	10.00

DATA - BRANCH CHANNEL

Run No.	Q_1 cfs	Q_2 cfs	Q_3 cfs	Q_3/Q_1	h_1 ft	h_2 ft	F_1	F_2
1	1.203	.598	.605	.503	.539	.602	.643	.271
2	1.098	.198	.900	.820	.615	.638	.481	.082
3	1.096	.276	.820	.748	.578	.608	.527	.123
4	1.098	.371	.727	.662	.535	.572	.593	.181
5	.948	.172	.776	.819	.571	.600	.465	.078
6	.750	.332	.418	.557	.387	.444	.659	.237
7	.850	.407	.443	.521	.411	.468	.682	.269
8	.851	.061	.790	.928	.578	.593	.410	.028
9	.415	.177	.238	.573	.264	.289	.647	.241
10	.418	.201	.217	.519	.279	.310	.600	.246

DATA FOR FIGURE 16 [BRANCH CHANNELS]

Run No.	Q_1 cfs	Q_2 cfs	Q_3 cfs	Q_3/Q_1	h_1 ft	h_2 ft	h_b ft	h_c ft	h_c/h_2	F_1	F_2	F_b
1	.954	.789	.165	.173	.479	.582	.489	.344	1.692	.609	.376	.102
2	.955	.765	.190	.199	.473	.520	.475	.344	1.511	.621	.431	.123
3	.949	.740	.209	.220	.449	.517	.458	.343	1.508	.667	.421	.143
4	.953	.724	.229	.240	.437	.496	.444	.344	1.443	.698	.438	.164
5	.951	.702	.249	.262	.440	.496	.420	.343	1.445	.689	.425	.193
6	.950	.682	.268	.282	.390	.476	.395	.343	1.388	.825	.439	.220
7	.948	.666	.282	.297	.398	.466	.369	.343	1.360	.798	.443	.266
8	.950	.647	.303	.319	.382	.475	.359	.343	1.385	.851	.418	.298
9	.954	.639	.315	.330	.344	.450	.343	.344	1.308	1.000	.448	.332
10	.952	.630	.322	.338	.334	.448	.319	.343	1.304	1.043	.444	.378
11	.949	.624	.325	.342	.334	.445	.299	.343	1.298	1.040	.445	.420
12	.944	.615	.329	.349	.332	.446	.281	.342	1.306	1.044	.437	.467
13	.948	.617	.331	.349	.332	.438	.168	.343	1.279	1.048	.450	1.017
14	.984	.851	.133	.135	.487	.538	.495	.351	1.532	.612	.456	.081
15	.981	.843	.138	.141	.437	.502	.452	.350	1.432	.718	.501	.096
16	.977	.835	.142	.145	.422	.427	.395	.349	1.222	.754	.633	.121
17	.980	.851	.129	.132	.338	.414	.310	.350	1.182	1.055	.676	.158
18	.984	.840	.144	.146	.380	.467	.402	.351	1.330	.888	.557	.119
19	.984	.840	.144	.146	.380	.467	.402	.351	1.330	.888	.557	.119

DATA - PRESSURE RECOVERY IN A BRANCH CHANNEL JUNCTION

Run No.	q_1 cfs	q_2 cfs	q_3 cfs	y_1 ft	y_2 ft	w_1 ft/sec	P_{CD} Lbs	P_{AB} Lbs	q_3/q_1	R_o
1	1.234	.660	.574	.450	.552	3.291	13.296	10.182	.465	.833
2	1.156	.466	.690	.507	.570	2.736	15.672	12.687	.597	.799
3	1.157	.677	.480	.390	.508	3.560	12.630	9.766	.415	.846
4	.851	.061	.791	.578	.593	1.767	19.585	17.341	.929	.811
5	1.098	.198	.900	.615	.638	2.141	23.207	19.776	.820	.899
6	1.096	.276	.820	.578	.608	2.275	20.570	17.449	.748	.845
7	1.098	.371	.727	.535	.572	2.463	18.075	14.907	.662	.894

DATA - SINGLE LATERALS

Run No.	Q_u cfs	Q_d cfs	Q cfs	P/Y ft	η^2	C_d
1	.186	.181	.004	.550	.715	.376
2	.183	.174	.009	1.479	.477	.502
3	.184	.177	.007	1.000	.576	.474
4	.184	.171	.013	2.417	.359	.543
5	.178	.157	.021	5.281	.194	.582
6	.166	.136	.031	11.494	.088	.592
7	.151	.108	.044	22.220	.040	.600
8	.041	0.000	.041	19.465	.003	.605
9	.260	.258	.003	.570	.826	.215
10	.259	.253	.006	1.263	.680	.341
11	.258	.247	.011	2.734	.494	.416
12	.254	.229	.025	9.502	.214	.518
13	.246	.204	.042	23.148	.095	.567
14	.231	.176	.056	37.571	.054	.588
15	.201	.172	.029	11.139	.127	.564
16	.211	.195	.016	4.671	.276	.489
17	.014	0.000	.014	1.507	.005	.761
18	.218	.203	.015	1.915	.498	.699
19	.214	.188	.026	5.657	.245	.718

Run No.	Q_u cfs	Q_d cfs	Q cfs	p/Y ft	η^2	C_d
20	.210	.177	.034	8.965	.165	.726
21	.206	.168	.039	11.295	.131	.743
22	.197	.148	.049	18.875	.076	.736
23	.177	.108	.069	36.012	.034	.748
24	.212	.188	.024	4.773	.274	.713
25	.219	.214	.005	.330	.853	.610
26	.219	.212	.007	.457	.808	.634
27	.219	.210	.009	.803	.705	.666
28	.219	.210	.009	.748	.720	.653
29	.217	.201	.016	2.190	.463	.689
30	.216	.196	.020	3.390	.355	.712
31	.189	.133	.056	24.012	.056	.742
32	.209	.177	.032	8.253	.175	.727

DATA - MULTIPORT DIFFUSER

SERIES I RUN NO. 1 Q(0) = 0.42254 cfs(0.012 m^3/sec) , M = 1.49

Lateral No.	x	s	Q_i	Q_L	M_1	M_L	p/γ
	ft	ft	cfs	cfs/ft	Lb-ft/sec^2	Lb/Sec^2	ft
1	.051	.107	.015	.141	.201	1.420	4.021
2	.169	.129	.017	.129	.314	2.440	4.458
3	.309	.151	.017	.115	.346	2.292	4.688
4	.471	.173	.018	.102	.355	2.050	5.367
5	.655	.196	.019	.099	.430	2.196	5.833
6	.862	.218	.020	.093	.474	2.172	6.300
7	1.092	.241	.022	.093	.573	2.381	6.604
8	1.344	.262	.023	.088	.609	2.319	6.875
9	1.617	.283	.024	.084	.643	2.271	7.263
10	1.910	.303	.025	.083	.729	2.406	7.683
11	2.223	.322	.026	.080	.752	2.339	7.967
12	2.553	.339	.026	.077	.778	2.299	8.267
13	2.899	.354	.027	.076	.822	2.324	8.517
14	3.260	.367	.028	.076	.900	2.452	8.750
15	3.633	.378	.029	.076	.934	2.473	8.917
16	4.015	.386	.029	.074	.936	2.423	9.042
17	4.405	.392	.029	.073	.951	2.424	9.208
18	4.799	.395	.029	.074	.976	2.469	9.208

SERIES I RUN NO. 2 $Q(0) = 0.1885$ cfs$(0.00534\ m^3/sec)$, $M = 1.46$

Lateral No.	x	s	Q_l	Q_L	M_l	M_L
	ft	ft	cfs	cfs/ft	Lb-ft/sec^2	Lb/Sec^2
1	.051	.107	.007	.061	.049	.458
2	.169	.129	.007	.058	.063	.493
3	.309	.151	.008	.052	.072	.475
4	.471	.173	.008	.046	.071	.412
5	.655	.196	.009	.045	.087	.445
6	.862	.218	.009	.042	.095	.437
7	1.092	.241	.010	.041	.114	.473
8	1.344	.262	.010	.039	.120	.457
9	1.617	.283	.011	.038	.133	.470
10	1.910	.303	.011	.037	.146	.483
11	2.223	.322	.011	.036	.150	.467
12	2.553	.339	.012	.035	.160	.471
13	2.899	.354	.012	.034	.163	.460
14	3.260	.367	.013	.034	.182	.495
15	3.633	.378	.013	.034	.187	.494
16	4.015	.386	.013	.033	.184	.476
17	4.405	.392	.012	.032	.178	.454
18	4.799	.395	.013	.032	.188	.475

SERIES II RUN NO. 1 Q(0) = 0.2540 cfs(0.00719 m^3/sec), M = 1.40

Lateral No.	x ft	s ft	Q_ℓ cfs	Q_L cfs/ft	M_ℓ Lb-ft/sec^2	M_L Lb/Sec^2
1	.073	.151	.011	.074	.143	.949
2	.235	.173	.012	.067	.153	.886
3	.419	.196	.013	.065	.185	.943
4	.626	.218	.013	.061	.202	.927
5	.856	.241	.015	.061	.244	1.015
6	1.107	.262	.015	.057	.253	.966
7	1.380	.283	.016	.055	.277	.976
8	1.674	.303	.016	.054	.306	1.010
9	1.986	.322	.017	.051	.314	.976
10	2.317	.339	.017	.050	.333	.984
11	2.663	.354	.017	.048	.331	.936
12	3.024	.367	.019	.050	.393	1.071
13	3.396	.378	.019	.049	.396	1.047
14	3.779	.386	.019	.048	.400	1.036
15	4.168	.392	.019	.047	.395	1.006
16	4.562	.395	.019	.047	.403	1.020

SERIES II RUN NO. 2 Q(0) = 0.1636 cfs(0.00463 m^3/sec), M = 1.344

Lateral No.	x	s	Q_l	Q_L	M_l	M_L
	ft	ft	cfs	cfs/ft	Lb-ft/sec^2	Lb/Sec^2
1	.076	.151	.007	.049	.062	.409
2	.235	.173	.008	.044	.065	.378
3	.419	.196	.008	.043	.079	.406
4	.626	.218	.009	.040	.087	.396
5	.856	.241	.009	.039	.103	.42
6	1.107	.262	.010	.037	.107	.406
7	1.380	.283	.010	.036	.116	.410
8	1.674	.303	.011	.035	.130	.430
9	1.986	.322	.011	.033	.130	.406
10	2.317	.339	.011	.033	.138	.408
11	2.663	.354	.012	.034	.161	.455
12	3.024	.367	.012	.032	.161	.438
13	3.396	.378	.012	.032	.163	.431
14	3.779	.386	.012	.031	.161	.416
15	4.168	.392	.012	.029	.153	.390
16	4.562	.395	.012	.030	.163	.41

SERIES III RUN NO. 1 Q(0) = 0.1785 cfs(0.00505 m^3/sec), M = 1.13

Lateral No.	x ft	s ft	Q_l cfs	Q_L cfs/ft	M_l Lb-ft/sec^2	M_L Lb/sec^2
1	.095	.196	.010	.050	.109	.555
2	.302	.218	.010	.047	.122	.557
3	.532	.241	.011	.046	.143	.592
4	.784	.262	.012	.044	.152	.579
5	1.056	.283	.012	.043	.166	.588
6	1.350	.303	.013	.042	.182	.600
7	1.662	.322	.013	.040	.188	.583
8	1.993	.339	.013	.039	.197	.582
9	2.339	.354	.014	.038	.211	.596
10	2.700	.367	.014	.039	.228	.623
11	3.073	.378	.014	.038	.244	.628
12	3.455	.386	.014	.037	.258	.615
13	3.845	.392	.014	.036	.279	.585
14	4.239	.395	.015	.036	.311	.609